UNIVERSITAT POLITÈCNICA DE CATALUNYA
BARCELONATECH
Escola d'Enginyeria de Barcelona Est

TRABAJO DE GRADO

Grado en Ingeniería Eléctrica

ANALYSIS OF DIFFERENT PV TECHNOLOGIES AND LONG-TIME MONITORING WITH AN EMBEDDED SYSTEM

Memoria

Autor: Cristina Romero Pérez

Director: Heinrich Christoph Neitzert

Departamento I.I.

Convocatoria: Junio 2017

ABSTRACT

The present thesis focuses on photovoltaic low-power generation and on the design, realization and test of an energetically autonomous measurement system.

The conceptual phase aims to provide a better base for the study and comprehension of the structure and the electrical characteristics of two PV technologies currently in use: Amorphous Silicon and Polycrystalline Silicon based solar cells. In particular this thesis offers an analysis of questions related to the daily and seasonally related sun's influence on the photovoltaic power-generation capacity of a small complete electrical energy harvesting system.

In the experimental paragraph the monitoring and analysis of Amorphous Silicon and Polycrystalline Silicon solar cell arrays as well as the test of charge/discharge processes of different batteries and accumulators, which are based either on Ni-Cd, Alkaline or on Ni-MH technologies, used for storing the electrical energy that is generated by the investigated solar cell arrays, is presented. The final project also shows the results of the design and monitoring, of different electronic circuits energetically autonomous with the energy contribution of a PV powered rechargeable battery and an "embedded system", using the ArduinoUNO platform.

The experimental results lead to the conclusion that both solar cells are sufficient for the autonomous operation of the embedded measurement system during one morning, but, not powerful enough to allow the daily operation and recharge of the battery as the same time, because the consumption of the ArduinoUNO system is slightly too high, when combined with the mini-solar cell panels, used in the investigated system.

ACKNOWLEDGEMENTS

Until finishing the final project at the end of the degree, I don't realize the time and effort that I had used in the accomplishment of the same one, and here it is where I would want to be grateful for all people who has encouraged and helped me to finish it. It is the result of last 6 months of hard experimental and theoretical work, that would not have been possible without the collaboration and support of my tutor of final project, the colleagues of the university of destination, friends from Spain, to which I want to express my sincerer gratefulness.

First of all, I wanted to be especially grateful with Dt. Heinrich Christoph Neitzert for accepting me in order to realize this final Project of degree under his oversight. For always having facilitated to me the necessary tools to carry out the project and to allow me to know excellent people of his department and nearby. For his good ideas and advices in the interpretation of measures. His nearness, availability, help, motivation and excellent guidance of the project in this period. Also, I would like to thank his shared coffees together with Giovanni Landi to whom also I am grateful for his support, motivation and all time helping.

Later, I would like to thank to the people of the mechanical engineering department, for his help in the accomplishment of the support for the photovoltaic cells. Also to Hassan Benali and Giuseppe Quarata, colleagues from the "Università degli Studi di Salerno", who spent a lot of their valuable free time helping me in the accomplishment of the electronic and programming part of the project.

Special thanks to the "Erasmus family", who it always has showed his interest for the evolution of the project and also because they have helped me to overcome my doubts and burden moments being far from my family and friends of Spain, facilitating my work abroad. Also sincere thanks to Andrea Pollio, who has been always present and to know how to give me a strong support.

Special appreciation to my dear parents Inocencio Romero and Josefa Pérez, for their support and unconditional love at all times also when being far from them. For listening to my doubts and help me always to improve. For showing me the value of the well done work and constant efforts, and for their humble lessons. Also I want to be grateful to my dear brother Jose Maria Romero, for his support in rough times. He knows what it means to study engineering. He also knows how to overcome obstacles and help to me to reach my principal goals during these years of studies.

Finally, special thanks to the "ERASMUS+" program and to both universities: "Escuela de Ingeniería de Barcelona Este" and "Università degli Studi di Salerno" to offer me the opportunity to live this beautiful experience, finishing in this way my studies with a Degree in Electrical Engineering. My gratefulness to all is as big as the great satisfaction that I feel for having finished the degree.

GLOSSARY

- I Current [A]
- T Temp [°C]
- V Voltage [V]
- C Capacity [F]
- P Power [W]
- R Resistance [Ω]
- V_{ref} Voltage reference [V]
- E_g Excitation energy [eV]
- CB Conduction band
- VB Valence band
- PV Photovoltaics
- I_{adj} Adjust current [A]
- V_o Input voltage[V]
- p.p.m Parts per million
- Ω Ohm
- µF micro Farad
- V Volt
- A Ampere
- nm nano meters
- eV electron Volt
- W Watt
- mA mili Ampere
- Si Silicon
- pc - Si Polycrystalline Silicon
- aSi:H Amorphous Silicon
- I_{sc} Short Circuit Current[A]
- V_{oc} Open Circuit Voltage
- I_M Current at MPP [A]
- V_M Voltage at MPP [V]
- MPP Maximum Power Point
- P_v Ideal Power
- P_o Input power
- q Eletric Charge
- G Irradiance in STC
- K Boltzmann Constant 1.38× 10-23 m2 kg s-2 K-1

MEMORY

Index

1. Introduction

From the realization of this Project that follows, it is expected to realize the objectives previously established as "road map". These objectives are classified in general and particular that will lead to achieve the general.

1.1. Objectives

At a general level, it is intended to investigate within the world of photovoltaic technologies. From the most influential environmental factors on photovoltaic cells to knowing the Amorphous and Polycrystalline Silicon technologies currently developed, as well as theoretically understanding the main inequalities that exist between them. It is also intended to analyse and understand the various internal structures of each technology, as well as physical processes that take place within them.

At the specific level, it is intended to develop and describe more extensively two of the technologies. From the history of the discovery of the same, to the components and internal physical functioning, the type of semiconductor used in each case and the differences in the manufacturing process of each cell.

Once the above is understood, it is intended in a more experimental way, to contrast the previous theoretical knowledge with the data to be extracted from different electrical assemblies. These numerous assemblies have no other purpose than to physically achieve the design of an autonomous embedded system of measurement of different parameters related to the photovoltaic cells that feed the system itself. For this reason, this second part of the project is more specific since it is characterized by its appearance of continuous exploration. The well-known heuristic method known with the expression "test-error", in which different proposals are going to be presented until reaching the optimum one.

1.2. Scope

For the accomplishment of this project, first are theoretically analysed two photovoltaic cells based on diverse technologies: Amorphous and Polycrystalline Silicon. From the history of their discovery, the creation of these cells and the difference between main electrical characteristics of each one.

Later, these cells are physically analysed through the design of different electrical circuits that allow the long-time monitoring of measurements by the programming of the software VEEPro and the platform ArduinoUNO.

2. Solar Energy

2.1. Solar Geometry

The Earth rotates around the Sun once per year in a slightly elliptical orbit at a mean distance of 149,6 million km. Due to the elliptical nature of Earth's orbit, the irradiance at the outer layer of the Earth's atmosphere varies over the course of each year, reaching a maximum of 1414 W/m^2 and a minimum of 1322 W/m^2 [1].

The modelling of the geometry and the behaviour of the solar star allow to make estimates of the radiation of the radiation throughout the year.

2.1.1. Related Terms

- Latitude (φ): Angular location of a point of the Earth with respect to the line of the equator (from -90° for the South and from +90° for the North).
- Length (λ): Angular location of a point of the Earth in relation to the line of Greenwich Meridian (until +180° towards the East and until -180° towards the West of the same).
- Slope (β): angle forming the Surface of the photovoltaic module and the horizontal of the floor (0 ÷ 180) °.
- Orientation or azimuth of the surface (γ): angle between the normal projection to the Surface that forms the photovoltaic module and the South (negative towards the East, positive towards the West).
- Solar azimuth (γ_s): angle between the projection of direct radiation on the horizontal plane and the South (negative to towards the East, positive towards the West).
- Angle of incident (θ): angle between the normal of a Surface and the direct radiation of the Sun with respect to it.
- Zenith angle (θ_z): angle between the vertical and the line that describes the incidence of the Sun. Equivalent to the angle of incidence of direct radiation on the horizontal plane, and is the complementary angle of the solar height (α_s). It varies throughout the year, being lower in summer since the Sun is higher than in winter, where the Sun is lower.
- Time angle (ω): angular displacement of the Sun from East to West, with respect to the local meridian. It is equivalent to 15° per hour, with 12 of midday in daylight as reference (0°), and taking the morning as negative and the afternoon as positive.
- Angle of departure (ω_s) and sunset (ω_d): angle corresponding to the instant of sunrise and sunset respectively.

2.1.2. Method of calculation

The incidence of the sun on the photovoltaic modules that are to be tried is nor constant during all the days of the year nor during the hours of the same day. For this reason, the calculation methodology carried out to estimate the sun's trajectory for a latitude $\varphi = 40.77°N$, longitude $\lambda = 14.87°$, slope $\beta = 45º$, orientation $\gamma = -87$ °.

Thus, for each day of the year (n) the declination δ in °,

$$\boldsymbol{\delta = 26.45 \cdot sin\left(\frac{360 \cdot (284 + n)}{365}\right)} \quad \textbf{(Eq. 2.1)}$$

Also, the angle of sunrise and sunset ω_s i ω_d respectively, also measured in degrees, as well as the different angles between the exit and the sunset (hour angle):

$$\boldsymbol{\omega_s = \mathrm{acos}(-tan(\varphi) \cdot \tan(\delta))} \quad \textbf{(Eq. 2.2)}$$

$$\boldsymbol{\omega_d = -\omega_s} \quad \textbf{(Eq. 2.3)}$$

$$\boldsymbol{\omega_{inf} = 15 \cdot \left(\left(r_{sup}\left(\frac{-\omega_s}{15} + 12\right)\right) - 12\right) + 7.5} \quad \textbf{(Eq. 2.4)}$$

$$\boldsymbol{\omega_{sup} = 15 \cdot \left(\left(r_{inf}\left(\frac{-\omega_d}{15} + 12\right)\right) - 12\right) - 7.5} \quad \textbf{(Eq. 2.5)}$$

After the zenith angle θ_z measured in degrees and the solar height α_s,

$$\boldsymbol{\theta_z = \mathrm{acos}\left(\cos(\varphi) \cdot cos(\delta) \cdot cos(\omega) + sen(\varphi) \cdot sen(\delta)\right)} \quad \textbf{(Eq. 2.6)}$$

$$\boldsymbol{\alpha_s = 90º - \theta_z} \quad \textbf{(Eq. 2.7)}$$

Necessary to calculate the solar azimuth γ_s in degrees,

$$\boldsymbol{\gamma_s = signe(\omega) \cdot \left|\mathrm{acos}\left(\frac{cos(\theta_z) \cdot sin(\varphi) - sin(\delta)}{sin(\theta_z) \cdot cos(\varphi)}\right)\right|} \quad \textbf{(Eq. 2.8)}$$

And finally, the angle of incidence is obtained θ in (°)

$$\begin{aligned}\cos(\theta) = {} & sin(\delta) \cdot sen(\varphi) \cdot \cos(\beta) - sin(\delta) \cdot cos(\varphi) \cdot \sin(\beta) \cdot \cos(\gamma) + cos(\delta) \\ & \cdot cos(\varphi) \cdot \cos(\beta) \cdot cos(\omega) + cos(\delta) \cdot sin(\varphi) \cdot \sin(\beta) \cdot \cos(\gamma) \\ & \cdot cos(\omega) + cos(\delta) \cdot \sin(\beta) \cdot \sin(\gamma) \cdot sin(\omega)\end{aligned} \quad \textbf{(Eq. 2.9)}$$

$$\boldsymbol{\theta = \cos^{-1}\theta}$$

Once explained the procedure to calculate [2] the different concepts related with solar geometry of the star, it is also interesting representing the angle between the line Sun-Earth and the equatorial celestial plane (it means, the projection of the terrestrial equator).

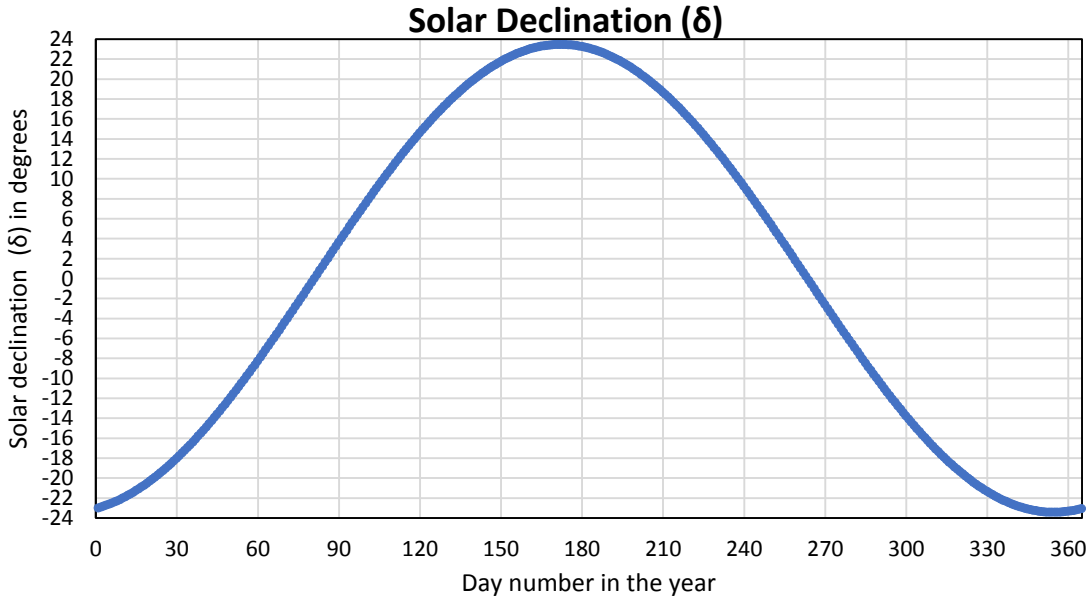

Figure 2.1. Solar declination over the course of a year as a function of day number. 1st of January = day 1; 31th of December = day 365. (Source: Own Elaboration)

As can be observed in Fig.2.2, the value of *solar decline* changes throughout the year, from 23.45° to 23.45°, passing two times for a zero in the spring and autumn equinoxes as can be observed too in the next image.

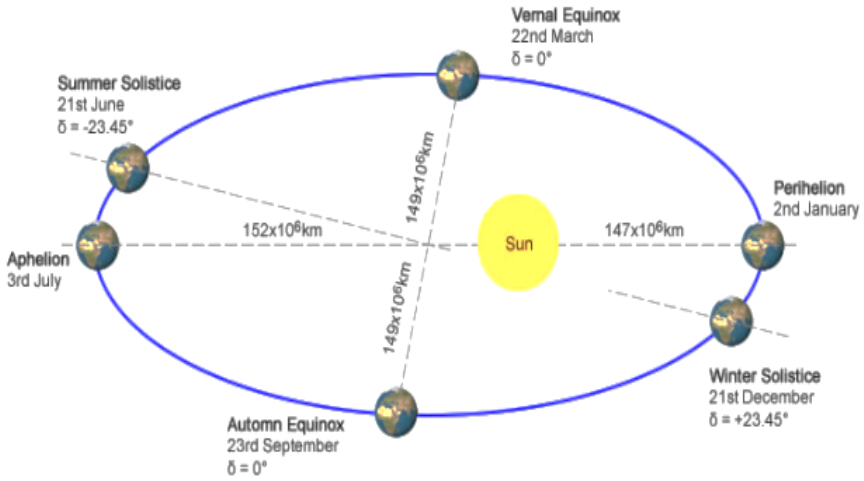

Figure 2.2. Earth's orbit around the sun with equinoxes and solstices declination angles represented. (Source: [3]**)**

Finally, with the obtained values of *solar azimuth* (γ_s) and solar altitude (α_s) the path of Sun is represented in Fig 2.3:

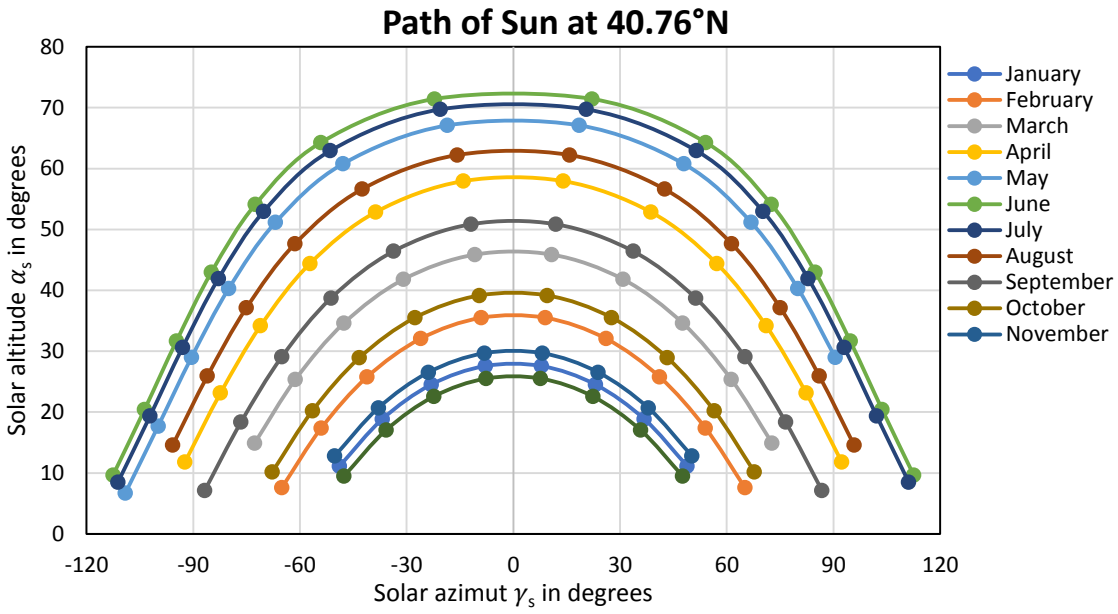

Figure 2.3. Earth's orbit around the sun with equinoxes and solstices declination angles represented. (Source: Own Elaboration)

2.2. Total Energy Incident on Surface

The total energy incident on surfaces in a generic situation is not only composed by the direct beam irradiated energy, also by diffuse radiation and ground reflection radiation that result in the general equation for the calculation of total energy incident on an inclined surface case (generic case). Then, the general equation takes the following form [1]:

$$H_{Gloval} = H_{Beam} + H_{Diffuse} + H_{Reflected} \quad \textbf{(Eq. 2.10)}$$

where,

- H_{Beam} is the direct beam energy on an inclined surface
- $H_{Diffuse}$ is the irradiation from diffuse radiation
- $H_{Reflected}$ is the irradiation from ground reflection radiation

These three components of radiation can be formulated like [2]:

$$\boldsymbol{H_{Beam} = R_B \cdot H_B} \quad \textbf{(Eq. 2.11)}$$

$$\boldsymbol{H_{Diffuse} = R_D \cdot H_D} \quad \textbf{(Eq. 2.12)}$$

$$\boldsymbol{H_{Reflected} = R_R \cdot \rho \cdot H} \quad \textbf{(Eq. 2.13)}$$

Where:

- R_B is the direct beam irradiation factor
- H_B is the difference between global and diffuse radiation on the horizontal plane
- R_D is the diffuse radiation factor
- H_D is the irradiation from diffuse radiation on the horizontal plane
- R_R is the effective portion of reflective radiation
- ρ is the reflection factor of the ground
- H is the irradiation from global radiation on the horizontal plane

2.3. Composition of Solar Radiation

In order to understand how solar cell works, it is necessary to be conscious of the fact that light and solar radiation is composed of a large mixture of varying wavelengths visible and not visible to the naked eye. It means that, light is composed of a large number of individual light particles of photons, each of which exhibits a very specific energy E directly proportional with frequency (f) and indirectly proportional to wavelength (λ), as the following equation [1] shows:

$$E = h \cdot f = h \cdot \frac{c}{\lambda} \qquad \textbf{(Eq. 2.14)}$$

Where:

- E is the photon energy (eV)
- h is Planck's constant = $6.626 \cdot 10^{-34}$ W·s^2
- f is the frequency (Hz)
- c is the speed of light = $2.998 \cdot 10^8$ km/s
- λ is the wavelength (m)

2.3.1. Solar Radiation Measurement

For all aspects previously explained in the same chapter, it is known that solar radiance is strongly dependant on location and local weather. For this reason, in PV cells design it is essential to know the amount of sunlight available at a particular location because depending on the absorption properties of the semiconductor material, it is able to absorb a more or less large part of the solar spectrum.

There are two concepts which characterise solar radiation: global and/or direct radiation measurements taken throughout the day.

In Fig. 2.4 can be observed the global irradiance on the solar cells that are tested, during the morning and evening of the same day. As can be appreciate and will be seen in the experimental part of the present project, the major density of the incident radiation takes place from 16:00 until 19:00 approximately. This fact, will be very important as for production is referred.

The appreciated irradiance depends on sun position, the altitude and latitude, the clouds and the quantity of ozone in the atmosphere. Moreover, as can be seen in Fig.3.4 the level of irradiance is changing during the day, appearing the major levels when the Sun is in his maximum elevation.

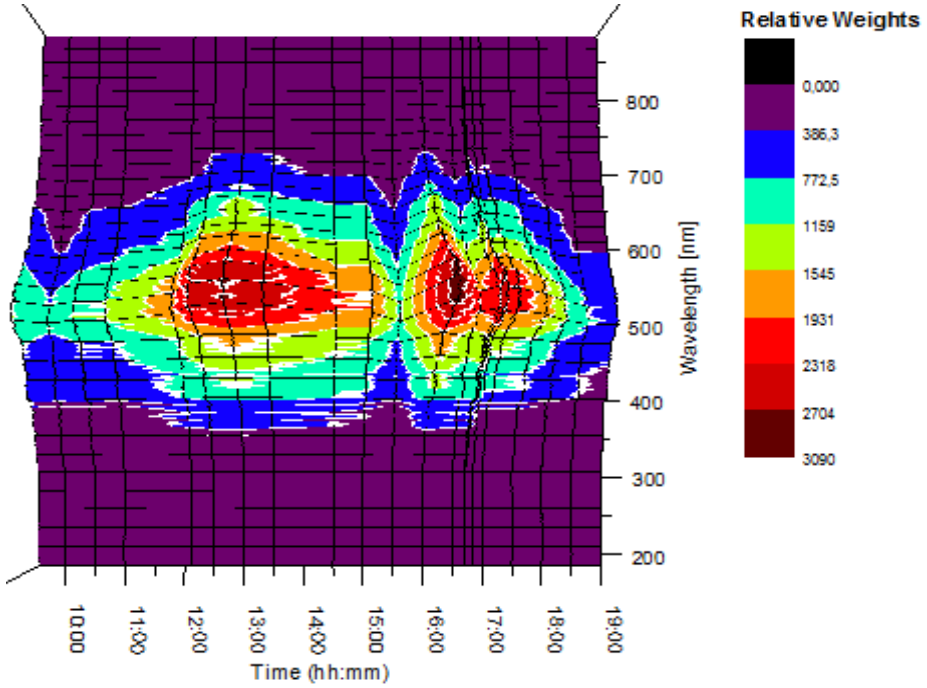

Figure 2.4. Spectral 3D distribution of Solar radiation. Date 07/06/2017 at $\varphi = 40.77°N$, length $\lambda = 17.77°$, inclination $\beta = 45º$, orientation $\gamma = -61$ º conditions. (Source: Own Elaboration)

As can be observed in Fig.2.5, the diagram displays a peak of the spectrum within the visible spectrum, but there are still significant amounts of shorter and longer wavelengths present.

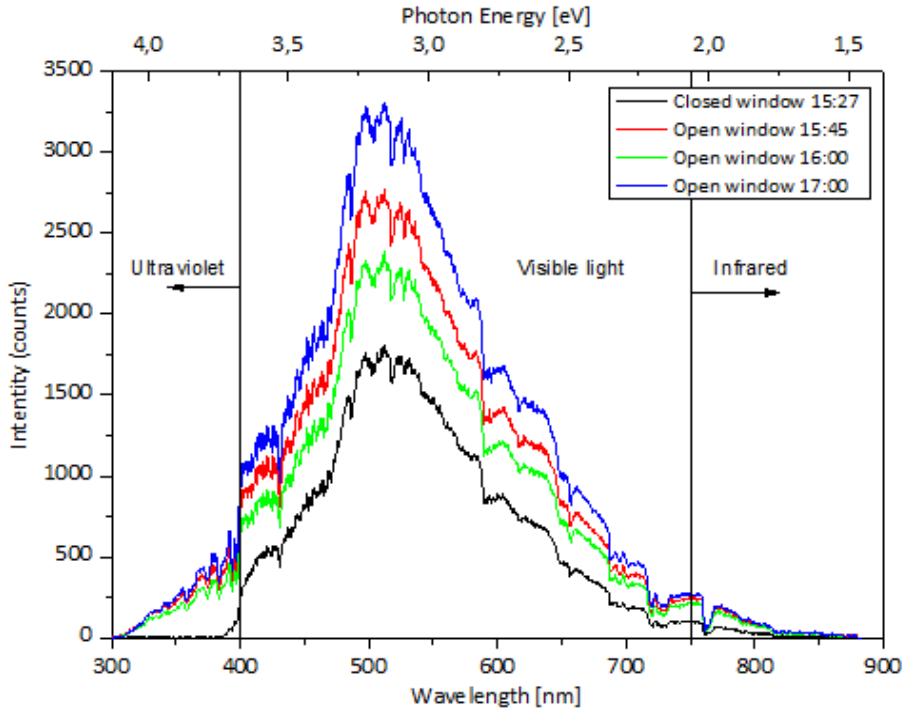

Figure 2.5. Spectral distribution of Solar radiation. Date 07/06/2017 at $\varphi = 40.77°N$, length $\lambda = 17.77°$, inclination $\beta = 45º$, orientation $\gamma = -61$ º conditions. (Source: Own Elaboration)

With this measurement, can be also shown the effect of filter that the glass of the window has on the irradiance of lower lengths than 400 nm. It means that, with opened window it is possible to capture the whole solar spectrum, but, with closed window situation it is not possible because the glass acts as a filter.

In addition, since it is possible to see in Fig.2.6, different dark lines in the solar spectrum are caused by absorption by chemical elements in the solar atmosphere. It can be appreciated by narrow regions of decreased intensity which are the result of the absorption of photons by these chemical elements.

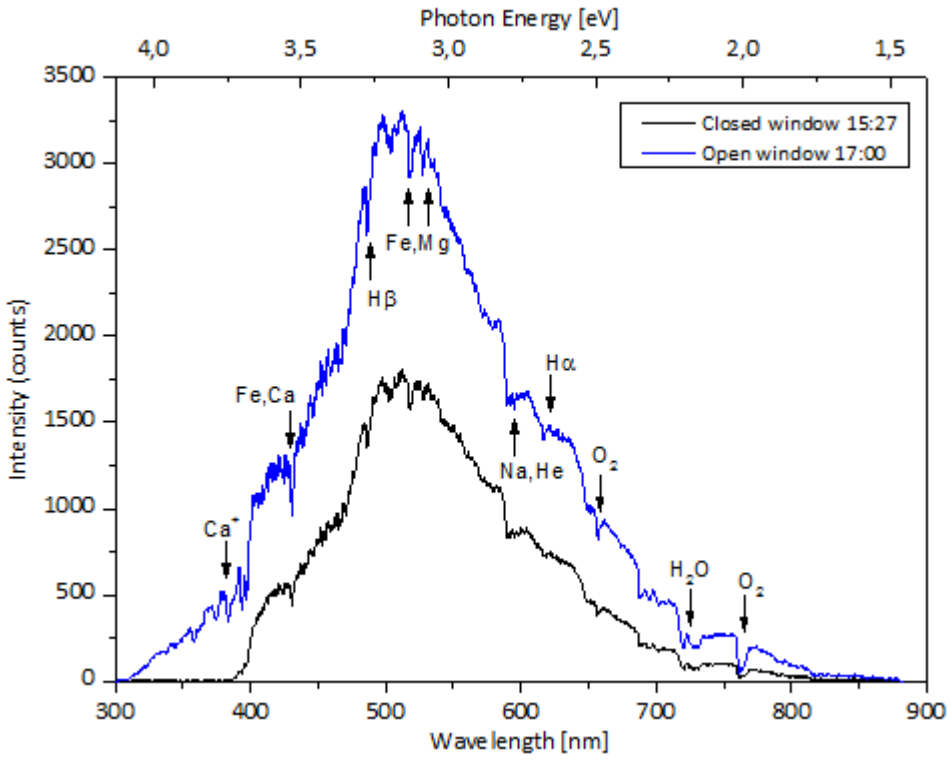

Figure 2.6. Spectral distribution of Solar radiation of blue sky. Present dips at the Fraunhofer line wavelengths. (Source: Own Elaboration based on [4] **)**

3. Photovoltaic Systems

3.1. Why PV?

The global primary energy consumption reached 14,9 TW in 2009 [5]. The increasing global demand for energy needs the demand for renewable sources because of the extreme quantity of energy consumes the humanity that has horrible consequences for the environment. These effects owed to the different processes of capture and transformation of energy that possess the diverse natural sources in other forms of energy that humans can take profit.

As is well known, the range of "solar energy conversion" includes solar thermal, solar fuels, solar-to-electricity (photovoltaic, PV) and many subcategories.

The solar energy exploitation offers many applications of PVs and it is provoking the fast growth of the electricity generation market in the last 30 years [6]. The use of PV resources falls into main different categories:

- Off-grid domestic systems, that are used to power houses not connected to the electricity network because of the remote location, population that has no access to electricity yet or power needs after disaster situations;
- Non-domestic systems, as water pumping;
- Grid-connected systems, as centralised commercial power stations.

For these purposes, to capture the flow so powerful that comes from the Sun is an important task and simultaneously intriguing because of the necessity of stimulating the development of the humanity though damaging minimally the environment.

There are many advantages of electricity production with Solar Energy, because we have to take into account that the source of Sun is:

- Not a finite resource and it is not located in only a few locations in the world, as fossil fuels, that are producing lots of political conflicts, inflated fuel prices, generating the large number of CO_2 and other greenhouse gases.
- Abundant: it means that the Earth receives 120.000 TW, 20.000 times more than the humanity needs of power [7],
- Readily available, because this resource is worldwide available,
- A clean resource far from geopolitical voltages: The utilization of the solar power generally not cause pollution. Nevertheless, there is emission to the atmosphere associated with the manufacture, transport and installation of solar power plants or panels (very low compared with conventional sources of energy),
- Cheaper, because reduces the dependence with other sources of energy not renewable which supposes a great step against the climate change,

- A very quiet resource: because there are no associate noises in the process of generation, with regard to other sources of renewable energy, as the wind power.
- Low maintenance, although the majority of plants of solar power need a minimal maintenance,

However, it's also known that today the solar cell electricity is still:

- Expensive but, there are many steps that will lead to lower cost like:
    - Implementing solar trackers where the modules follow the sun,
    - Developing concentrator solar cell systems where the sunlight is focused down to a small area,
    - Using lower-cost elements or increase the efficiency of the cells, and so on.
- Variable and intermittent, because the generation depends on cloudy or not days and also on the number of hours of light per day.
- Complicated to store it and expensive,
- Associated to greenhouse emission in the production of solar panels, like hydrochloric acid, sulphuric acid, nitric acid, acetone, gallium arsenide, nitrogen trifluoride or sulphur hexafluoride, that if they do not manage and rejected appropriately, these chemical substances can cause serious problems of contamination. Moreover, also exists the impact of transport and installation plants/ solar panels,
- Using exotic raw materials for panels based in (CdTe) or (CIGS) that are expensive because they are strange finding in nature

Then, we have always take into account advantages and disadvantages of this resource and also the past lessons learned that still require constant research, investment and political commitment that influence strongly on the rate of development.

3.2. Fundamentals of Photovoltaic Performance

The humanity has been catching solar power from the beginning in his existence. The evolution can be considered as progression in terms of the increasing efficiency of catching and converting energy.

The discovery of solids that can convert solar energy directly to produce the most flexible way of energy as the electricity is, is relatively recent, since the beginnings of photovoltaics based on a solid-liquid system.

The comprehension of the photovoltaic cells (PV) operation is not trivial, since generally it needs a physical comprehension of the internal components and also of the operation these. In addition, to make possible the interpretation of the design and the appropriate processes of creation of the above-mentioned cells is necessary to have a minimum special previous knowledge. For this reason, this chapter tries to make more accessible the physics that concerns the photovoltaic effect and, definitively, the functioning of solar cells.

Solar cells are based on semiconductors, concretely on photonic semiconductors. Then, first is necessary to define both concepts.

3.2.1. What is a Semiconductor?

The materials that could be qualified as conductor, semiconductor or insulating treats basically about a categorization of the materials according to the conductivity of these. Every material is classified under any of these three categories that appear in Fig.3.7.

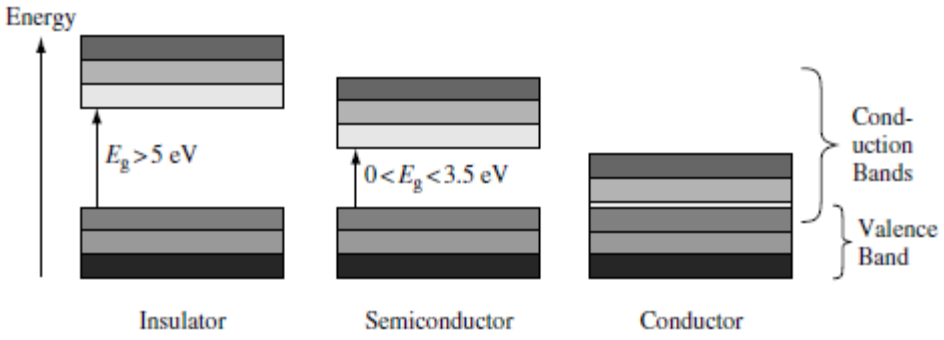

Figure 3.1. Band gap diagrams for a typical conductor, semiconductor and insulator with approximate values of excitation energy (Eg). (Source:[8])

As can be seen in the previous figure, we can talk about a solid semiconductor if the material or substance has a perceptible resistance higher than conductor material and lower than insulators.

Semiconductors have the valence band (VB) full of electrons and the conduction band (CB) empty of electrons at 0 °K. In spite of it, with the variation of the light or the variation of the magnetic field, doping it or increasing the temperature in a controlled way, could be electrons in CB because the electrons of the VB acquire sufficient heat energy to overcome the called “prohibited band”, crossing until the CB. In this case, we would be talking about the period of conduction because it needs available electrons[8].

Following with the previous image, these materials differ according to the variation of kinetic energy that electrons experience when them are having moved from a layer to the other one. Therefore, the materials with energy higher than 5 eV between CB and VB are called *insulators.* Solids with capacity of conductivity are those who have VB that are superposed by the CB creating a cloud of free electrons that generate the current when they are having been submitted to the electrical field [9]. Finally, semiconductors are those that have a variation of energy in a range of 0 – 3,5 eV.

A semiconductor, can only convert photons with the energy of the bandgap with good efficiency. Photons with lower energy can't be absorbed and those with higher energy are reduced to gap energy by thermalization of the photo generated carriers [10].

The most important requirement for a solar cell is a high light absorption coefficient, because it will make possible to use a much slighter material: for a 90% light absorption, it takes 1 µm of GaAs (a direct semiconductor) and 100 µm of Si [10]. So, light absorption is much weaker in an indirect semiconductor than in a direct semiconductor.

3.2.2. What is a Photonic Semiconductor?

Photonic semiconductors are those that can be used to convert the light into charge, and vice versa[8]. In case of photovoltaic cells, as well as photodiodes, they are only capable to convert the light in charge through the commonly known "p-n junction".

The p-n junction is the connection between two areas which are doped adequately positively (p-type semiconductor) and negatively (n-type semiconductor). Hereby, the remaining electrons that in the external orbit of the material are attracted by the positive charge of "p-type" which is characterized for having holes or deficit of electrons. These hollows are the place that electrons leave when they leave the VB turning into free or remaining electrons.

When it happens, there is generated a flow of electrons from "n-type" zone to "p-type" zone in which remaining electrons or the nearest to the layer of the union of both bands tend to occupy the holes of the other band, as can be seen in Fig.3.2.

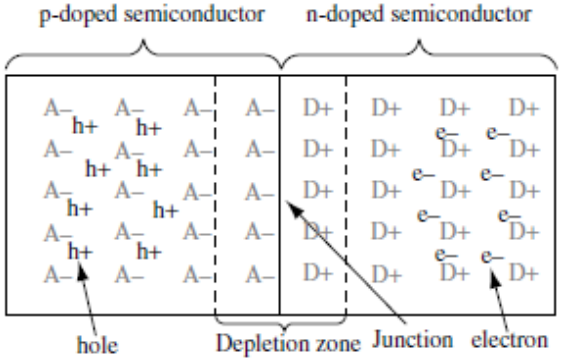

Figure 3.2. Schema of p-n junction. A^- is an ionised acceptor, D^+ is an ionised donor. (Source:[8])

Then, the electrons leave positively ionized dopants and in opposite way it happens with the holes that are occupied leaving now the atoms negatively charged (anion). Thus, in "p side" there is generated a net negative charge and a positive one in the "n side" creating an electrical field that separates the carriers, of the mobile remaining charges. This zone is commonly called "depletion zone". This zone can be overcome when a voltage is applied across the "p-n union" in forward bias, since this one decrease allowing the current flow.

3.3. Main Photovoltaic Technologies based on Silicon

Main photovoltaic devices and solar cells can be classified in many different ways: by thickness of semiconductor material, by group number in the periodic table, by specific semiconductor materials single-element or compounds or by organic polymer compounds.

In this case, the classification of the different technologies nowadays existing in the creation of photovoltaic cells based con silicon material.

3.3.1. Introduction

One of the features that more differentiate the Homo sapiens of other mammals lies in his extraordinary aptitude to design and construct instruments adapted to his intentions. The first used tools were pebbles of flint.

The Latin word to designate the flint is *Silex* from which they derive others as *silica* or *silicon* between others [11].

The non-toxic Silicon (Si) is the second element for his abundance ($2{,}57x10^{-5}$p.p.m) in the earth crust, about 20% of this. In the nature, it is found in the form of silicon dioxide (quartz sand, extremely common component of the Earth's crust) or mixed with oxygen forming Si's oxides and silicates.

This chemical element is concerned to group 14 in the periodic table [11]. This means that on each silicon atom are 14 protons (positively charged particles) in its nucleus and 14 electrons (negatively charged particles) orbiting the nucleus.

According to the organization of the electrons of Silicon, ten of the fourteen are bound to the nucleus while the remaining four electrons determine how the silicon atoms organize themselves to form the solid silicon material that is usually very hard, difficult to dilute and usually has a metallic appearance.

As for the structure of solid silicon everything works perfectly if each atom is surrounded by four other atoms equal since the four electrons of each atom always try to join with four "neighbouring" atoms.

Said that, it is logical to think that Silicon cannot be a good conductor when all the electrons are bonded, it would really be acting as an insulator since there would be no "movement" of electrons. However, it is the photons from the Sun that can release these bonds by transmitting that energy to the electron in a way that contributes to the flow of electric current. When releasing the electron, it tends to change position by generating a hole in its place and can occupy the gap left by another excited electron. As it is mentioned on previous chapter, this process results in the generation of electric current.

For this reason, the semiconductor capacity of *Si* is considered fundamental for the production of electrical energy through solar cells.

Pure silicon can be presented in crystalline or amorphous form and this depends on whether it exists and whether or not a long-range order is conserved in the arrangement of the atoms.

Currently around 90% of current PV market, are based on the silicon wafers technology and the most are manufactured in Europe and Asia. They have a thickness of approximately 300-400µm and there are two major types of crystalline silicon solar cell in current importance: monocrystalline, and multicrystalline (also called polycrystalline) silicon cells:

- Monocrystalline cells: are cut from a silicon boule that grows from a single and large crystal obtained from pure molten silicon which has grown in only one plane.
- Polycrystalline cells: are also grown from pure molten silicon, but using casting process. It is a large irregular multicrystalline silicon boule that grows from a multifaceted crystalline material which has grown in multiple directions.

The last cell technology defined have a lower efficiency compared with the monocrystalline, due to the random crystal structure and relative impurity of the silicon. That is why multicrystaline technology requires a larger area to achieve the same performance.

Other important variation of the main Silicon is:

- Amorphous silicon: is a greyish powder, more chemically active than the crystalline variety and because its structure does not keep the order in the arrangement of the atoms in a long reach, it presents electrical and optical characteristics different from those of the crystalline. This material is usually used in solar cells for low power applications, because its performance is less than crystalline, but its way of obtaining is more economical.

In terms of production, China currently is the world leader in producing c-Si-based PV cells and modules, with a capacity of over 2300 MW/year [5]. In terms of economy, the IEA[1] estimated the energy payback time of crystalline Silicon PV for the cost based on modules installed on rooftop and grid-connected of 13-14% efficiency and irradiated at 1700 kWh/m^2·year, as 1.5-2 years [5].

[1] IEA: International Energy Agency which was established in 1974 after the oil crisis in 1973 to ensure reliable and clean energy inside an economic development.

3.3.2. Brief History of Solar cells

An extraordinary discovery for the history of photovoltaic cells was in 1817 when Berzelius found the Selenium. A few years later he was the first one in preparing elementary Silicon, accidentally. Nevertheless, it was Alexandre-Edmon Becquerel, a French physicist the one that in 1839 at the age of 19 years, who observed for the first time the photovoltaic effect immersing two metal plates in a conductive fluid and analysing a small voltage across them when this system was exposed to the Sun.

Later, it was in 1941 when Russel Ohl created the first photovoltaic cell based in Silicon when he was working with a multimeter to test the electrical resistance of a silicon sample that has been cracked in the centre of it. Then, he observed that the current that was flowing across both sides of the sample increased significantly the sample was exposed to the Sun [12].

Then, was also discovered the *p-n junction* because both regions (with all their impurities or pollutants in Silicon) were isolated due to the central crack until the light transmitted energy to Silicon. One side had remaining electrons and the other one had a slight shortage of these and then both regions were called *p* and *n* type because of the respectively positive and negative type. And *p-n junction* was the name to the barrier that was separating them.

For that time, already was known the same effect of conduction on Selenium but, Silicon cell and his *p-n junction* was capable of turning more efficiently the energy of Sun's light.

Later, with other positive findings and a succession of events like "performance at any cost" culture of the industry of the space, contributed to the development of solar cell's technology to terrestrial applications. Also the petroleum crisis in 1973 [13] (known as the first crisis of the oil) in which the oil price quadrupled, was a good fact that increased the conscience of the importance of the renewable energies in general. Although, as can be seen in Fig.3.3, the real increase in PV production appears from 1995.

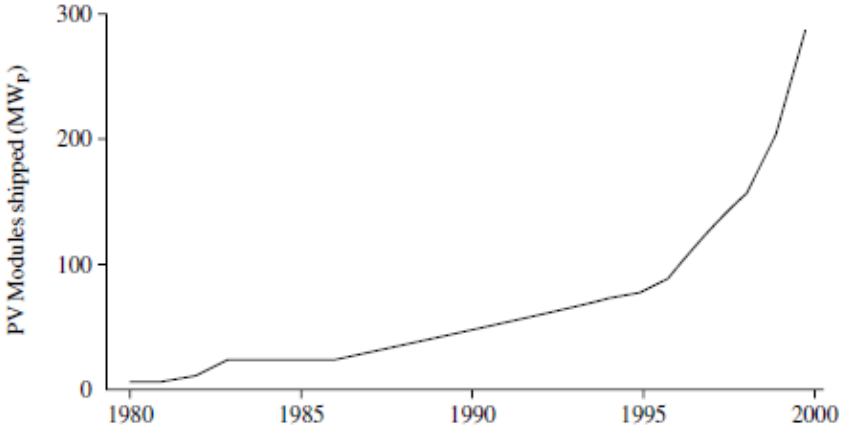

Figure 3.3. Global production of PV 1980-2000. (Source:[8])

3.3.3. Crystalline Silicon

- History

In 1954 was developed by Chapin the first silicon solar cell at Bell Laboratories which had an efficiency of 6% that increased to 10% [10]. In the first years only Czochralski (Cz) grown single crystals were used for solar cells.

In 1999 already the worldwide market of Crystalline-Silicon solar cells has increased the previous 10 years [11]. In 1998, the worldwide energy photovoltaic module production reached 152 MW/year and Crystalline-Silicon solar cells represented the 87% of the total. The market shares of the worldwide PV cells in 1998 were 39,4% for mono-crystal, 43,7% for polycrystalline, 2,6% for ribbon, and 0,7% for silicon film [11]. It was the first time ever that polycrystalline silicon has overtaken single-crystal silicon.

Currently crystalline silicon is one of the most common semiconductors for the production of large scale energy because due to its semiconductor properties is the base material of the microelectronic and photovoltaic industry, to the point that the region of California where a large number of companies in the electronics and computer industry are called "Silicon Valley".

The market is dominated by crystalline silicon in multicrystalline and monocrystalline form. It is true that crystalline silicon is not the optimal material from a solid-state point of view but for reasons of cost multicrystalline and monocrystalline silicon crystals are dominating the market and will continue to do this for next 5-10 years [10].

- Creation of Polycrystalline Silicon cell

Polycrystalline material in the form of fragments is obtained from highly purified polysilicon that is founded in a quartz crucible which itself is located in a graphite crucible and melted by induction heating.

The process of creation of polycrystalline silicon depends on small steps that have to be realized meticulously. Initially there submerges a seed crystal that has to be withdrawn very slowly with movements of rotation. With each dipping of the seed crystal into the melt, dislocations are generated in the seed crystal even if it was dislocation free before. To obtain a dislocation in a free state, a slim crystal neck of about 3mm diameter must be grown with a growth velocity of several millimetres per minute.

Fig. 3.4 shows the basic principle pc-Si solar panel structure in which the n-type Si anode is doped with elements called “electron-donor”, that are principally in the Group 15 of the periodic table and

the p-type Si cathode is doped with called "electron-acceptor" elements. Polycrystalline Silicon is a material with a bandgap of 1,1 eV [5].

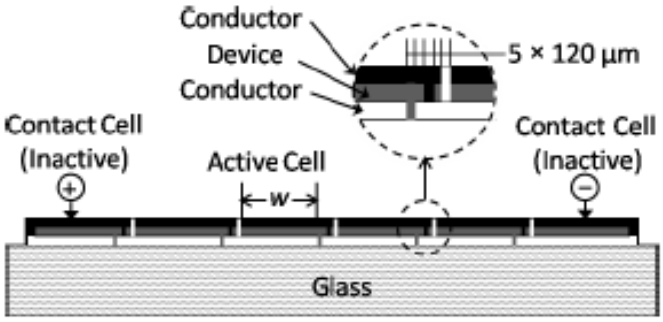

Figure 3.4. Typical diagram of a pc-Si solar panel (Source: [5]**)**

Between the anode and cathode separated by the electric field due to the absorption of a photon at the junction that generates an electron-hole pair, there is a difference in potential that results in a current *I* that follows the next expression [5]:

$$I = \sigma \cdot E \qquad \textbf{(Eq. 3.1)}$$

Where σ is the conductivity (directly proportional to the elementary charge) and *E* is the electric field.

3.3.4. Amorphous Silicon

The Amorphous Silicon typical solar cell has the structure that can be seen in next figure:

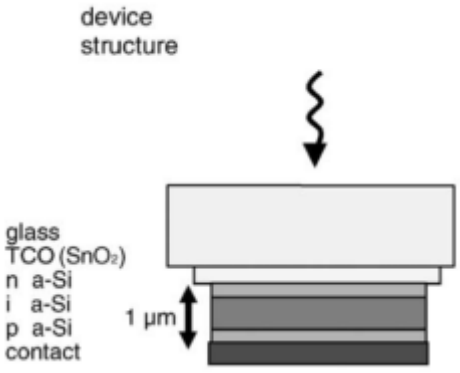

Figure 3.5. Typical structure of an amorphous Silicon solar cell (Source:[10])

- Internal Structure

The silicon atoms in the amorphous silicon, largely preserve the same basic structure that the silicon of crystal. Each atom of silicon is joined by covalent bonds to other four atoms arranged as a tetrahedron. In an understandable way, if a not crystalline structure of silicon is constructed by sticks to represent covalent bonds and balls with four small holes to represent the silicon atoms and we try to represent a not crystalline structure with these materials, it will be really difficult.

To avoid a crystalline structure, will be necessary to fold the sticks or to leave the fourth stick without connection. It means, the problem of a tetrahedral distribution is the difficulty of supporting the position of the atoms, the angles and the lengths of the bonds near the values of the chemistry of the silicon in a crystalline structure. Rapidly not crystalline crystals are formed.

Amorphous silicon is an alloy of Silicon with hydrogen [10] because for the amorphous silicon hydrogenated (aSi:H) the bonds of hydrogen solve this structural problem. A high percentage of silicon atoms form covalent bonds with only three “neighbours”. The fourth electron of silicon link itself to an atom of hydrogen. This hydrogen is crucial and invisible to the X-rays (measuring the dispersion of X-rays in the material it can be understood), but it is observed in infrared spectroscopy and the evolution of the hydrogen during the temper.

Exist enough atomic different configurations for the hydrogen in aSi:H that determines the optical and electronic general properties of the material. The optical gap, Eg, of aSi:H cell is 1,7 eV [8].

The two main phases of hydrogen that can be observed by “photon magnetic resonance” are the so called *dilute* and *clustered* phases. In *dilute phase,* any atom of hydrogen is approximately 1nm far from any other atom of hydrogen and in *clustered phase* there are two or more atoms of hydrogen in the proximities.

Some of this properties of the aSi:H are strongly affected by the faults of chemical bond and these defects of the bond can be studied through the *electron spin resonance* method. The fault that prevails more is the *D-centre* defect and it is the *silicon dangling bond*. It means that, the hydrogen atom is eliminated of the dilute-phase leaving one electron without linked, *dangling bond* [13a].

However, the most intense effect found in aSi:H is the *light-soaking effects* because, as can be observed in figure 3.6, the soaking degrades the efficiency of the solar conversion. This fact does that for engineers it is very important to obtain a stable condition after an extensive light soaking on aSi:H cell.

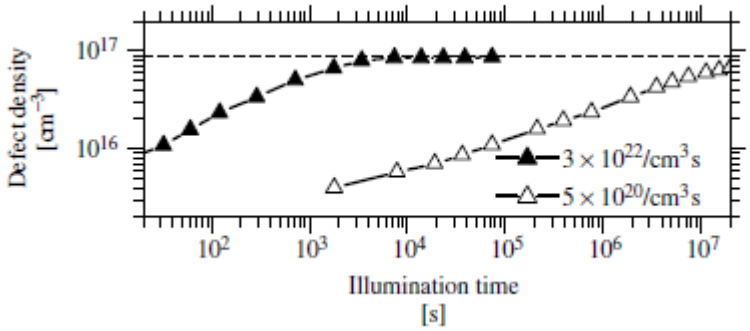

Figure 3.6. Defect (dangling bond) density representation during extended illumination of an a-Si:H film for high- and low- intensity illumination. The legend shows the photocarrier generation rate of each intensity. (Source:[13])

3.4. Electrical Characteristics of Photovoltaic Technology

Solar cells can be characterized by a great number of common and simultaneously specific parameters of every especial material. Then, to understand the following experimental sections of this project is necessary to define the most essential electrical parameters that distinguish the different solar cells.

The most common way to compare PV devices is by their current-voltage (I-V) characteristics. Since already it has explained previously, the majority of photovoltaic cells work under p-n junction. Then, is the I-V curve which shows an exponential relation known as "diode equation" [5]:

$$Dark\ current = I_{dark}\ (V) = I_0 \cdot \left(e^{\frac{qV}{kT}} - 1\right) \quad \textbf{(Eq. 3.2)}$$

Where I_0 is a constant, q is the electric charge, k is Boltzmann constant and T is Temperature in Kelvin.

3.4.1. Net current of Solar cell

The net current of the solar cell is the difference between the dark current that means the consequence of the applied potential difference and the photocurrent, both in the opposite direction [5].

$$Net\ current = I(V) = I_{sc} - I_{dark}(V) = I_{sc} - I_0 \cdot \left(e^{\frac{qV}{kT}} - 1\right) \quad \textbf{(Eq. 3.3)}$$

Where I_{sc} is the photocurrent at short-circuit, and is given by [5],

$$I_{sc} = q \int J_s(E)\, \Phi(E) dE \quad \textbf{(Eq. 3.4)}$$

Where $J_s(E)$ is solar photon flux, *E* is photon energy, and $\Phi(E)$ is quantum yield[1] in function of photon energy.

3.4.2. Photovoltage at Open Circuit

The voltage at open circuit (V_{OC}) occurs when the current in function of the voltage turns out a null value, $[I(V) = 0]$ and it comes given by the following expression [5]:

$$V_{OC} = \frac{k \cdot T}{q} \cdot ln\left(\frac{I_{sc}}{I_0} + 1\right) \qquad \textbf{(Eq. 3.5)}$$

Where,

[1] Quantum yield: Amount of current that cell can produce when this is irradiated by protons of a particular wavelength.

- *k* is the Boltzmann's constant
- *T* is the temperature
- *q* is the electronic charge
- I_L is the light generated current
- I_S is the dark current

3.4.3. Maximum Power Point

The Maximum Power Point value, MPP, of a cell corresponds to the product of maximum voltage and current $(V_M\ y\ I_M)$ at maximum power. On the typical I-V characteristic of solar cells it is possible to notice that with the intersection of both maximum values, the major ideally possible rectangle is shown under the I-V curve, corresponding to the ideal working point of the cell.

In Fig.3.7 can be observed the curve and the most characteristic points explained before, as well as a simple dark IV measurement that produces the exponential curve so characteristic of diode, where the current is flowing in the opposite direction and also change the current path, causing a lower series resistance in the dark.

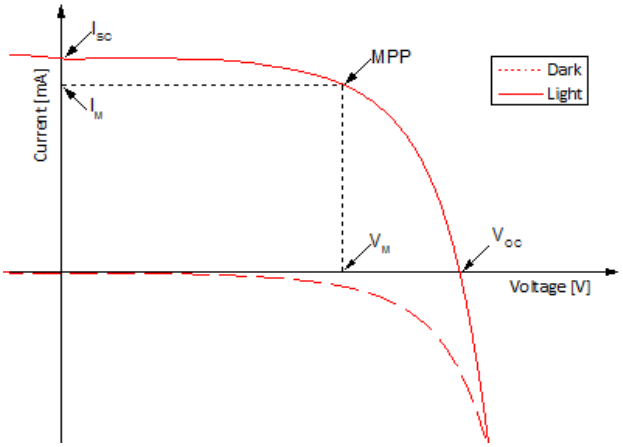

Figure 3.7. Typical I-V characteristics for a PV cell in the dark and under illumination. (Source: Own Elaboration)

3.4.4. Fill Factor

Graphically, the ratio *Fill Factor* is understood as the difference between the ideal rectangle formed by the intersection of the points $(V_{OC}\ y\ I_{SC})$ and coordination axis, and the major possible rectangle experimentally formed by $(V_{max}\ y\ I_{max})$ and coordination axis.

When $V_{max} = V_{OC}$ and $I_{max} = I_{SC}$, then, $FF = 1$ and it is calculated by the following way:

$$FF = \left(\frac{I_{max} \cdot V_{max}}{I_{SC} \cdot V_{OC}}\right) \qquad \textbf{(Eq. 3.6)}$$

The above-mentioned ratio or deviation is due to many factors, which do that FF's value is commercially concerning around 0,7-0,8. The factors that provoke this fact are always due to the resistance that materials, which form the photovoltaic systems, put between others:

- Series resistance of the cell
- Shunt resistance
- Substratum resistance
- Resistance of transfer through electrodes
- Resistance due to the charge transport through the semiconductor

3.4.5. Electrical Efficiency

The efficiency of a solar cell is one of the parameters more usually used to compare the cells between them. This parameter can be calculated by the proportion of the output Power P_{OUT} with regard to the input Power P_{IN}, as it is defined in the following equation

$$\eta = \frac{P_{out}}{P_{in}} = \frac{P_{max}}{I \cdot A} = \frac{I_{sc} \cdot V_{oc} \cdot FF}{I \cdot A} \qquad \textbf{(Eq. 3.7)}$$

Where P_{max} is Maximum Power, I is irradiance (=100mW/cm^2 for an air mass coefficient AM1.5) and A in cell area (cm^2).

Another way of differentiating PV technologies is an economical way. It concerns the comparison in function of *cost per rated power* $\left(\frac{€}{W}\right)$, the cost of generated energy along the life cycle of the system $\left(\frac{€}{kWh}\right)$, the *economic payback time* in years of the produced energy in function of the necessary energy for create the PV system.

4. Objectives

The experimental phase of the project takes as a principal aim the monitoring of photovoltaic cells for the comparison of different technologies nowadays existing, as well as the design and accomplishment of an autonomous embedder system for measurements, supplied by an electric photovoltaic system.

For it, the present experimental phase of the project is formed by different principal parts to analyse in order to be able to obtain the principal aims.

In the first part, there are analysed two different types of photovoltaic cells: Polycrystalline and Amorphous Silicon) in order to choose the suitable one. For it, there are generated the respective I-V curves in darkness and also in lighting by the previous monitoring system of voltage and current data, based in the programmed ArduinoUNO platform. Also, are generated voltage, current and power curves in function of time.

In the second part, there is analysed in different ways the consumption of ArduinoUNO system throughout a whole day to determine the current that this one needs while executes the previous written programme in it.

In the third part will be analysed different possible technologies for each necessary component for the accomplishment of the autonomous monitoring system, in order to choose the most suitable and to see the advantages and disadvantages that each of these can contribute.

Thus, are summarized the principal aims of the following below:

- Study and characterization of photovoltaic cells by an electrical experimental model,
- Monitoring of different types of solar cells for the comparison between the different ones,
- Design and accomplishment of an autonomous system of measure with photovoltaic electric power as principal source of energy,
- Comparison of different existing technologies of each necessary component for the autonomous system circuit,
- Appropriate selection of all components that form the autonomous system according to their characteristics and functioning. This means the selection of the photovoltaic generator, the rectifying diode, the regulator voltage, the accumulator of energy and the embedded system of measure,

Finally, with all chosen components will be executed the previous circuit to accomplish the completely photovoltaic autonomous system to validate the results experimentally obtained comparing it with the before obtained ones by the grid powered system of measure.

5. Electrical characteristics of both solar cells

The principal aim of this test is the knowledge of the power variation that different solar cells are capable to generate, the importance of the inclination of each cell in relation with their own capacity of energy conversion, as well as the influence of the variation of incidental radiation throughout the same day with regard to the fix position in which are they installed.

5.1. Materials

To know the power that generate the photovoltaic cell of polycrystalline Silicon as well as the amorphous silicon cell, are necessary the following components:

- Polycrystalline solar cell and Amorphous solar cell

Technology	**Amorphous Silicon**	**Polycrystalline Silicon**
Model	SOLAREX SA-1	MSX-01F
Peak Watts [W]	1,40	1,01
Min. output current at Vld [A]	0,08	0,135
Typ. Output current at Vld [A]	0,1	0,15
Voltage under load, Vld [V]	17,5	7,5
Active area size (LxWxD) [cm]	30,48 x 11,00x 0,23	11,53 x 10,62 x 0,3
V_{OC} [V]	24,0	10,3
I_{SC} [A]	0,11	0,16
Series fuse [A]	1	
Maximum Temperature		+85 °C
Minimum Temperature		-40 °C
Temperature coefficient of voltage	-65 mV per °C	-37 mV per °C
Temperature coefficient of current	0,01 mA per °C	0,15 mA per °C

Table 5.1. Electrical characteristics of both Solar Cells (Source: Own Elaboration based on cell's data sheet)

- Source Meter Series 2400
- Red and Black set of wires
- Programmed VEEPro Software

5.2. Procedure description

VEEPro software is configured in order to make it run as a regulated voltage source with the following parameters.

	Polycrystalline Silicon case	Amorphous Silicon case
Current Limit [A]	0,1	0,1
Start Voltage [V]	-2	-2
Stop Voltage [V]	10	23
Step Voltage [mV]	25	25

Table 5.2. Parameters of designed VEEPro software (Source: Own Elaboration)

Then, once configured it, the program is executed in order to measure the generated current by the cell for each value of simulated voltage by VEEPro software. This programme is executed for both solar cells and also for different inclinations: horizontal, vertical and at 45 degrees respect of horizontal plane. In addition, it is decided to realize these measurements in two principal times of the day. At 12 a.m. when due to the position of the cells the Sun's radiation arrive indirectly to them, and also at 5 p.m. when higher Sun's radiation is impinging.

It is logical to think that the interval of time between each test could influence in the results due to the variation of clockwise angle depending on time, but this fact is despicable considered taking in account that the total wasted time has been minor than one hour and the angular displacement of the Sun at every hour only changes 15 degrees.

Due to the position and orientation of the cells, the generation of power at 5 p.m. is higher than in the morning, which generation is practically void.

5.3. Results

5.3.1. Maximum Generated Power

In this section, generated power in function of time is represented in both moments of the day and to different inclinations of both solar cells: Polycrystalline Silicon and with Amorphous Silicon solar cell.

As can be seen in Fig.5.1 and Fig.5.2, one important aspect and in which depends the generation of power is the inclination of the cell. In both moments of the day and according to generated power values, is observed that, the least effective position is the horizontal one. In the morning, the most effective position is the vertical one but the most effective position in the evening is at 45 degrees.

Every any point of intersection of Intensity and Voltage on the same curve represents the power that geometrically coincides with the area of the rectangle which top vertex corresponds with every

represented point. If this point is moved towards the right (coming down over the curve) or towards the left side (coming closer the current axis), in any case the rectangle would become smaller for the side of current or the side of voltage. It means that in any both cases, generated power would be minor.

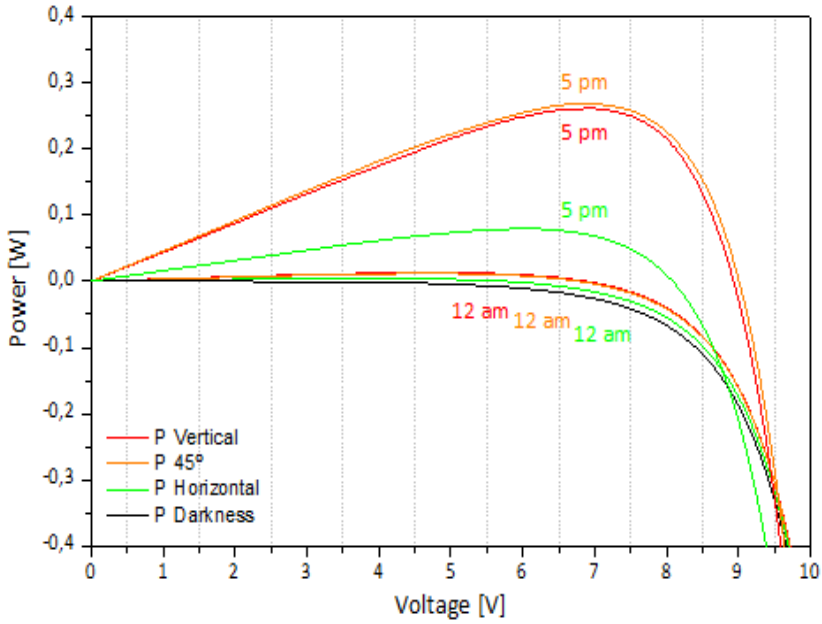

Figure 5.1. Power VS time representation of Polycrystalline Silicon at 12 AM and at 5 PM (Source: Author's measurements)

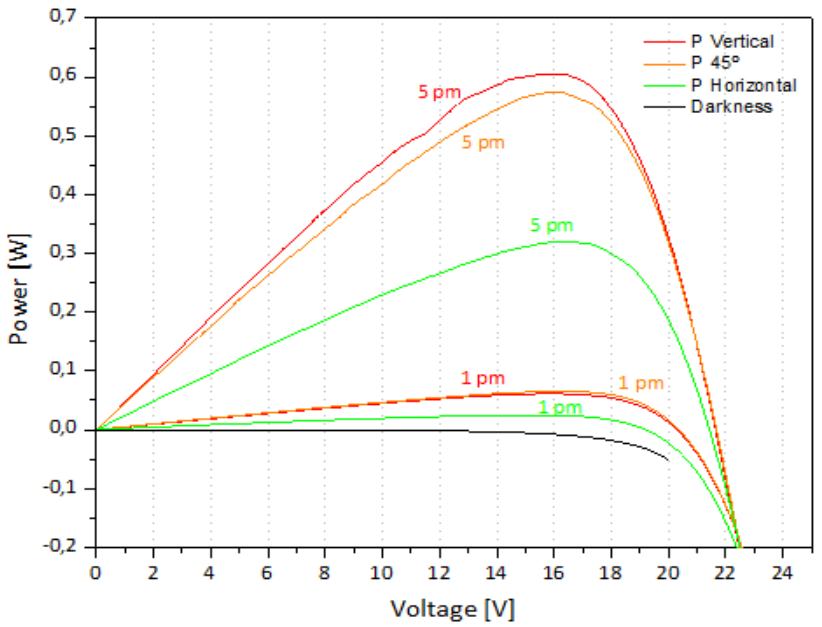

Figure 5.2. Power VS time representation of Amorphous Silicon at 1 PM and at 5 PM (Source: Author's measurements)

Due to the form of the curve, there exists an intermediate point which makes that the area of the rectangle is the major possible one. The above-mentioned point is the point of maximum power.

In both following tables appears a summary of the maximum developed power determined by the product of the respective current and voltage for the mentioned power, as well as the ideal resistance for every position and moment of the day according to the value of maximum power.

Crystalline Silicon Solar Cell						
Position	**Vertical**		**45 degrees**		**Horizontal**	
Time	**12am**	**5pm**	**12am**	**5pm**	**12am**	**5pm**
I_M (A)	0,003	0,003	0,002	**0,039**	0,001	0,013
V_M (V)	4,80	4,80	5,03	**6,90**	3,83	6,08
Maximum power (W)	0,012	0,012	0,012	**0,269**	0,004	0,079
Optimum resistance (Ω)	1794,39	1794,39	2182,42	**177,00**	3516,98	464,39

Table 5.3. Measured parameters of Crystalline Silicon Solar cell (Source: Author's measurements)

As it is observed in Table 5.3 and in the Fig.5.1, the maximum current is at 39 mA and maximum voltage is at 6,9 V for a development of maximum power of 269 mW. Whereas in the following table is observed that the cell of Amorphous Silicon is capable of working with a range of higher voltage values for almost the same value of generated current, offering a major maximum power (MPP).

Amorphous Silicon Solar Cell						
Position	**Vertical**		**45 degrees**		**Horizontal**	
Time	**12am**	**5pm**	**12am**	**5pm**	**12am**	**5pm**
I_M (A)	0,004	**0,038**	0,003	0,036	0,002	0,019
V_M (V)	16,13	**15,9**	17,93	15,95	15,18	16,38
Maximum power (W)	0,061	**0,606**	0,060	0,575	0,025	0,319
Optimum resistance (Ω)	4262	**417,28**	5347	442,7	9270	839,86

Table 5.4. Measured parameters of Amorphous Silicon Solar cell (Source: Author's measurements)

In addition, in the tests of both cells the same phenomenon is observed. In the morning, the value of the ideal resistance acquires values in the order of the kΩ, whereas in the evening they acquire values of the order of Ω.

5.3.2. I-V Curve

The typical curve of a solar cell is commonly called curve of intensity - voltage curve (I-V curve). From it curve, can be known some of the key parameters that define the quality of the photovoltaic module.

The representation of this type of curves initiates from the point of short circuit current (where the resistance is zero), that increasing the resistance above the impedance of the solar cell, the voltage increases rapidly whereas the current decreases very slowly up to coming to the "knee" of the curve. In this point, a maximum value of power (MPP) takes place by the voltage-current product, called VM and IM respectively.

Later, in figures 5.3 and 5.4 is represented the I-V curve of the photovoltaic cell of Crystalline Silicon also with the corresponding P-V curve, by the previous experimentally measured values of voltage and current in the morning and in the evening.

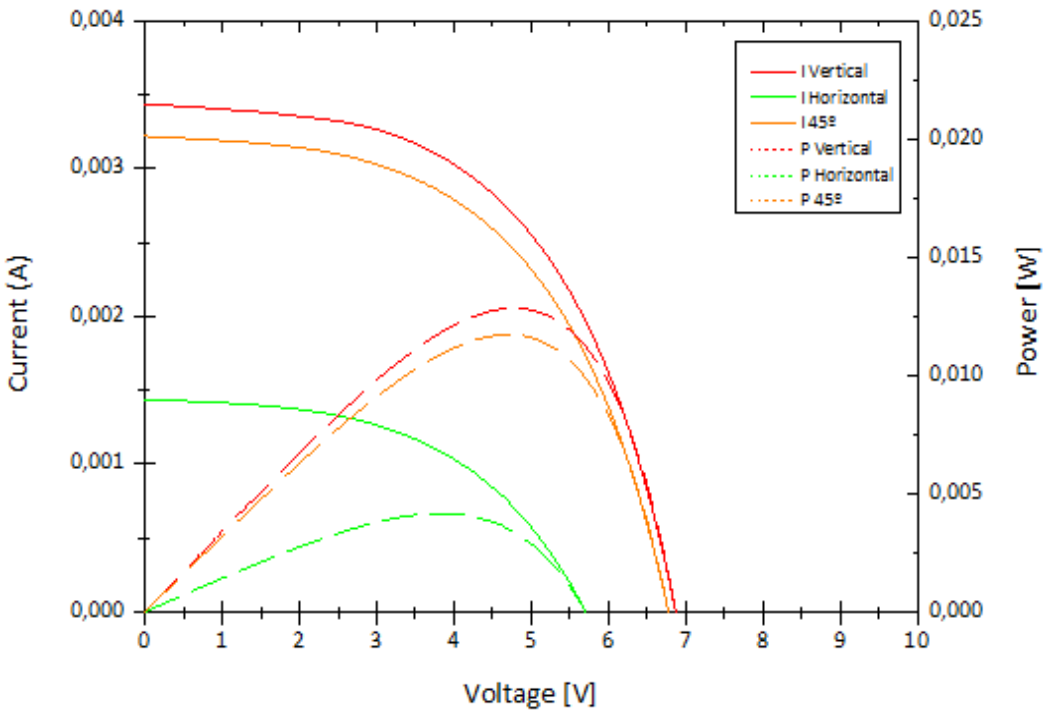

Figure 5.3. Current and Power representation in function of Voltage of Polycrystalline Silicon at 12 AM (Source: Author's measurements)

The principal difference between both slots is the current and voltage to which the cell works and in consequence the power that this one generates. The range of current generated in the evening represents 10 times the current generated in the morning.

While it is true that the position and orientation of the cell is the same, it is the clockwise angle that provokes the fact that in the morning is only generated the half power that is generated in the evening.

The clockwise angle is the one that influences the perpendicularity of the sunbeams with regard to the cell.

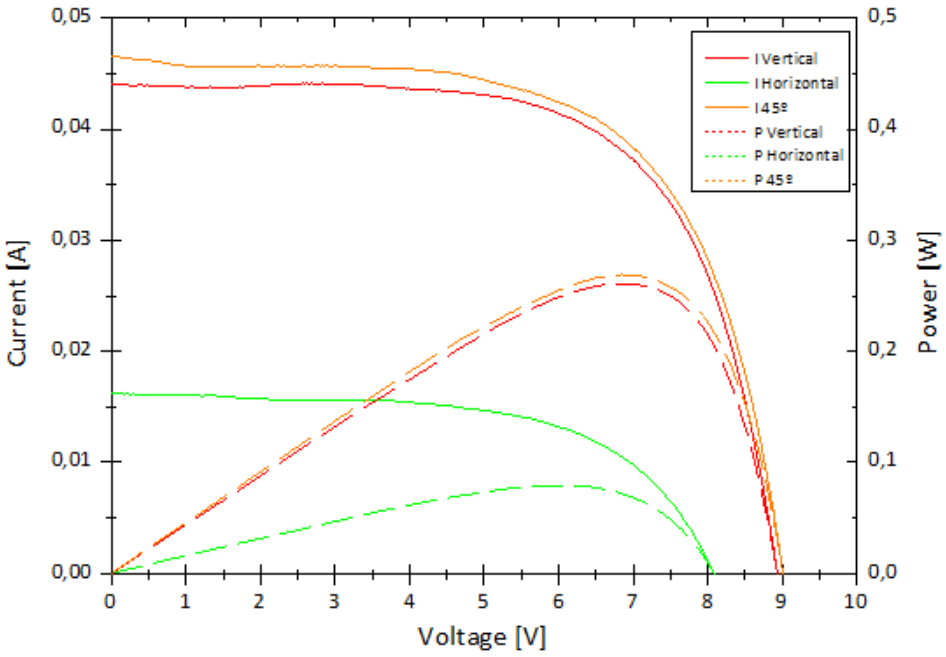

Figure 5.4. Current and Power representation in function of Voltage of Polycrystalline Silicon at 5 PM (Source: Author's measurements)

Later, the I-V curve of Amorphous Silicon cell is represented in Fig. 5.5 and 5.6 also with the corresponding P-V curve, by the previous experimentally measured values of voltage and current in the morning and in the evening.

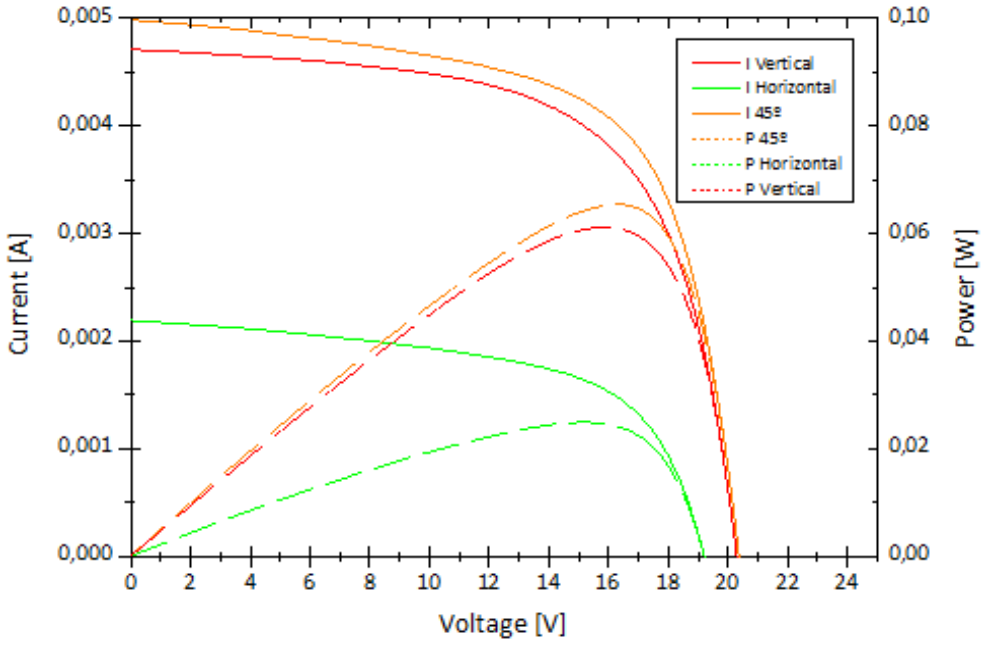

Figure 5.5. Current and Power representation in function of Voltage of aSi:H at 12 AM (Source: Author's measurements)

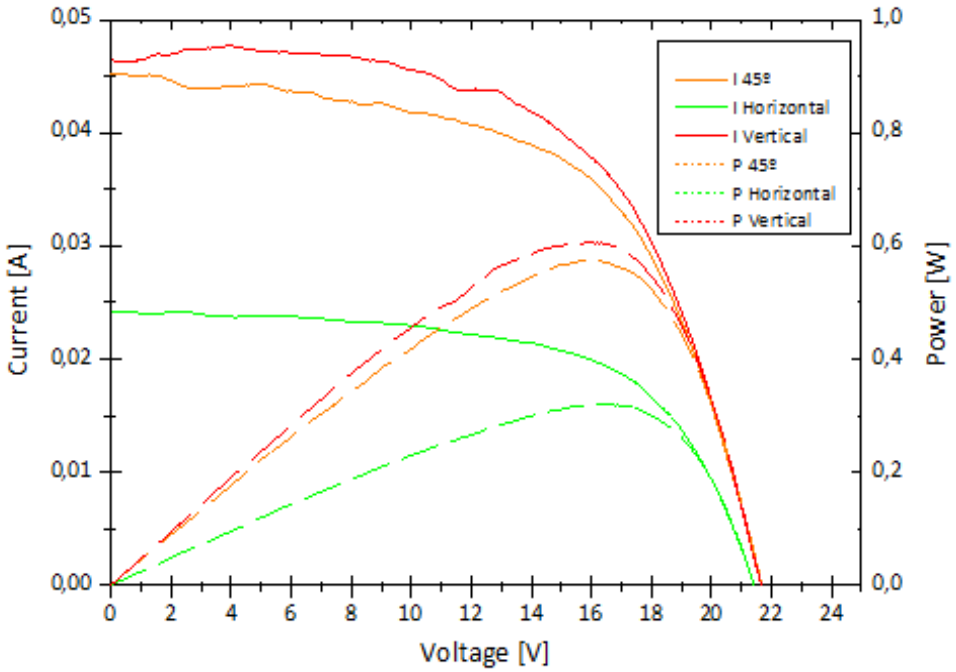

Figure 5.6. Current and Power representation in function of Voltage of aSi:H at 5 PM (Source: Author's measurements)

In the same way as in case of Polycrystalline Silicon cell, the principal difference between both slots is the current and the voltage to which the cell works and in consequence the power that this one generates. In this case, the range of current generated in the evening also represents 10 times the current generated in the morning, while the variation of the voltage does not change so much in comparison with the variation of the current. This is due to the difference of sun lighting on the cells. The major intensity of sun lighting, the highest is the I_{SC} in the I-V curve, and the same happens with V_{OC} value though in minor way.

As well as the responsible in the variation of I_{SC} values is the intensity of the incident light, in the following figure can be seen that the responsible of the variation in V_{OC} values is the room temperature:

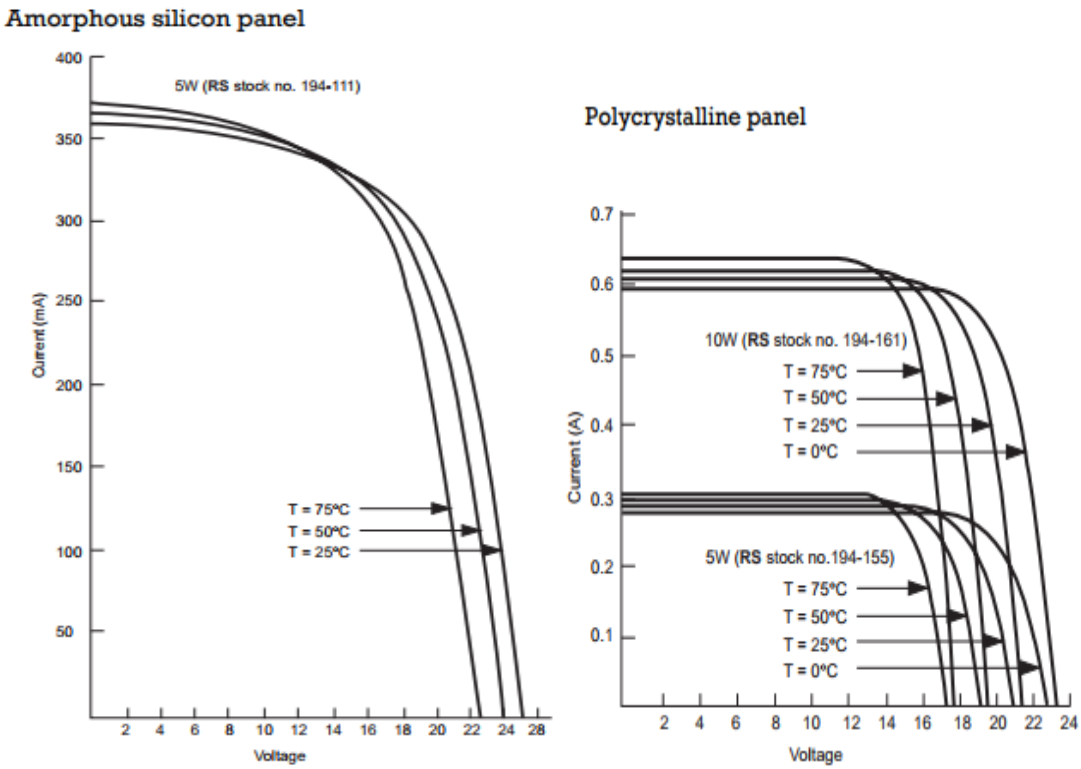

Figure 5.7. I-V curves in function of Temperature for aSi:H and polycrystalline Si (Source: Solarex datasheet added in annexes)

5.3.3. Short Circuit Current

The current across the solar cell when the voltage through the system is zero, receives the name of short-circuit current. It is the major possible value of current and is due to the generation and capture of carriers generated by the light when the resistance value is null. Normally it is write as I_{SC} (as it is also explained in section 4.4.1. It is also possible to determine it graphically because it is the intersection point between I-V curve and vertical axis, which can be seen in Fig.5.3, Fig.5.4, Fig.5.5 and Fig.5.6.

Only in case of an ideal solar cell, the I_{SC} and the current generated by the solar cell are identic. This means that, the I_{SC} is the biggest generated current that can be shown for these photovoltaic systems. Nevertheless, at practice case it is not possible to achieve that both currents coincide due to the great number of factors that influence the current of short circuit, that are defined below:

- Area of the solar cell
- Power of the incident light source
- The spectrum of the incident light
- Optical properties of the solar cell, as absorption and reflection
- Collection probability of the solar cell

The last cited factor is also a term of the equation which make possible the approximation of I_{SC}:

$$I_{SC} = q \cdot G \cdot \left(L_n + L_p\right) \qquad \textbf{(Eq. 5.1)}$$

where:

- q is the electronic charge
- G is the generation rate
- L_n and L_p are the electron and hole diffusion lengths

In table 5.5, a summary of the measured values of the open circuit voltage from both solar cells appears, for every position and moment of the day.

Crystalline Silicon Solar Cell						
Position	**Vertical**		**45 degrees**		**Horizontal**	
Time	**12am**	**5pm**	**12am**	**5pm**	**12am**	**5pm**
I_{sc} (A)	0,003	0,044	0,003	**0,047**	0,001	0,016
Amorphous Silicon Solar Cell						
Time	12am	5pm	12am	5pm	12am	5pm
I_{sc} (A)	0,005	**0,047**	0,005	0,045	0,002	0,024

Table 5.5. Measured parameters of Short-circuit Current for both solar cells (Source: Author's measurements)

5.3.4. Open Circuit Voltage

The maximum voltage available from a solar cell, receives the name of open circuit voltage, V_{OC}, and it occurs when the current through the solar cell is zero. This voltage can also be determined on the I-V curve of the solar cell, when the curve crosses with the axis of abscissas, and can be calculated with (Eq.3.5).

The open circuit value is an indirect measure of the amount of recombination in the device because V_{OC} depends on dark saturation current and this current depends on recombination in the solar cell. This is why the principal influencer on the dark current I_S is the material band gap, because it represents the minimum energy required by and incoming photon to produce an electron-hole pair. Then, the result of the experimental measurements of the above-mentioned current for the crystalline Silicon and Amorphous Silicon cells appears in the next two figures:

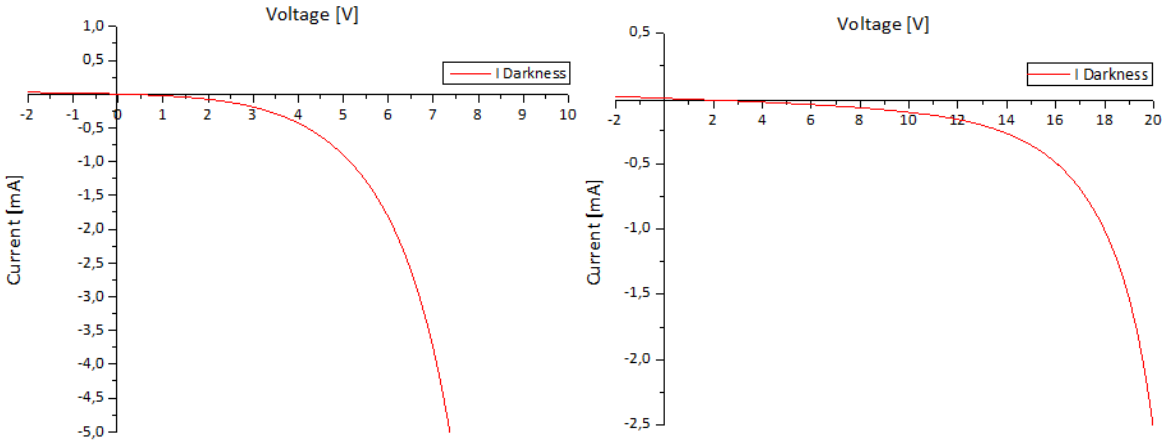

Figure 5.8. I–V characteristics of a solar cell in the dark (Source: Author's measurements)

In table 5.6, a summary of the measured values of the open circuit voltage from both solar cells appears, for every position and moment of the day.

Crystalline Silicon Solar Cell						
Position	**Vertical**		**45 degrees**		**Horizontal**	
Time	**12am**	**5pm**	**12am**	**5pm**	**12am**	**5pm**
V_{oc} (V)	6,87	8,93	6,78	**8,98**	12,73	8,075
Amorphous Silicon Solar Cell						
Time	12am	5pm	12am	5pm	12am	5pm
V_{oc} (V)	20,275	21,65	20,37	**21,68**	19,2	21,43

Table 5.6. Measured parameters of Open Circuit Voltage for both solar cells (Source: Author's measurements)

5.3.5. Fill Factor

As well as in the points of operation I_{SC} and V_{OC} the power of solar cell is zero, these points are two of the vertexes of a rectangle that is completed by other two vertexes that are, the intersection of the projection of I_{SC} and V_{OC} and the centre of coordinates. The area of this rectangle determines the maximum power that the solar cell might be capable of generate.

If the value of voltage when power is maximum is projected on I-V curve, there are obtained on the axes of coordinates the maximum voltage values (V_M) and maximum current values (I_M) that the cell can develop in these circumstances. The product of these two values is equivalent to the major quadrangular area that I-V curve can support. Nevertheless, this second rectangle always will be minor that is explained before due to the "knee" of I-V curve.

From the difference between both areas arises the fill factor concept, which is defined as the quotient that relates of the maximum possible generated power for the cell divided by the maximum "ideal" power, which would be the product of I_M (if it could be I_{SC}) and V_M (if it could be V_{OC}). Then, this value is fundamentally a measure of quality of the solar cell.

As it was explained in 4.4.4 section, FF value can also be calculated as the division of both rectangles represented in Fig.5.9. As can be observed in Eq.3.6 and in the following figures, as higher should be the difference between both areas (grey and orange areas) lower will be FF's value. It means that minor it will be the efficiency of the cell.

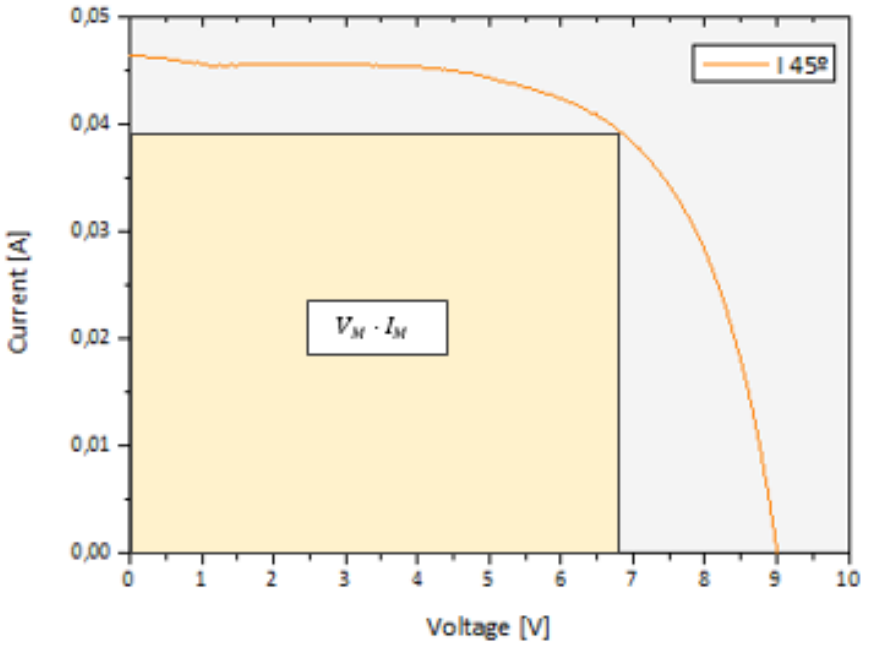

Figure 5.9. Graphical representation of both areas for the calculation of polycrystalline Silicon FF (Source: Author's measurements)

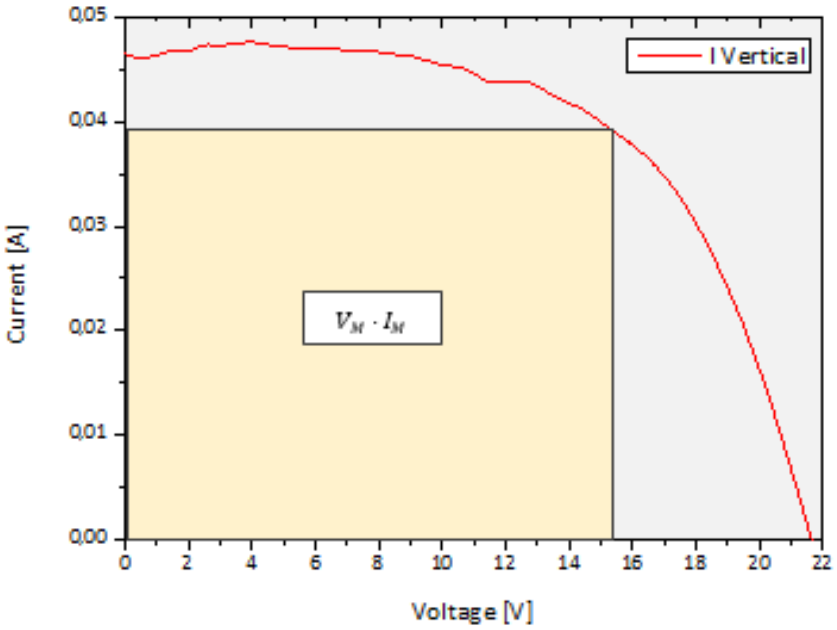

Figure 5.10. Graphical representation of both areas for the calculation of aSi:H FF

(Source: Author's measurements)

Later, the Table 5.7 shows a summary of the current and voltage values determined experimentally (I_M, V_M, I_{SC}, V_{OC}) calculating the "virtual" or ideal and generated power, for each position of both solar cells in both moments of the day.

Crystalline Silicon Solar Cell						
Position	**Vertical**		**45 degrees**		**Horizontal**	
Time	**12am**	**5pm**	**12am**	**5pm**	**12am**	**5pm**
I_M (A)	0,003	0,037	0,002	**0,039**	0,001	0,013
V_M (V)	4,80	7,00	5,03	**6,85**	3,83	6,08
Output Power, P_O (W)	0,013	0,261	0,012	**0,269**	0,004	0,079
I_{sc} (A)	0,003	0,044	0,003	**0,047**	0,001	0,016
V_{oc} (V)	6,87	8,93	6,78	**8,98**	12,73	8,075
Virtual Power, P_V (W)	0,021	0,393	0,020	**0,422**	0,013	0,129
Amorphous Silicon Solar Cell						
Position	**Vertical**		**45 degrees**		**Horizontal**	
Time	**12am**	**5pm**	**12am**	**5pm**	**12am**	**5pm**
I_M (A)	0,004	**0,038**	0,003	0,036	0,002	0,019
V_M (V)	16,13	**15,9**	17,93	15,95	15,18	16,38
Output Power, P_O (W)	0,061	**0,606**	0,060	0,575	0,025	0,319
I_{sc} (A)	0,005	**0,047**	0,005	0,045	0,002	0,024
V_{oc} (V)	20,275	**21,65**	20,37	21,68	19,2	21,43
Virtual Power, P_V (W)	0,101	**1,018**	0,102	0,976	0,038	0,514

Table 5.7. I_M, V_M, I_{SC}, V_{OC} measures and P_O, P_V calculated values for both solar cell

(Source: Author's measurements)

Then, with Eq.3.6 is possible to calculate the Fill Factor that appear in the following table:

Crystalline Silicon Solar Cell						
Position	**Vertical**		**45 degrees**		**Horizontal**	
Time	**12am**	**12am**	**12am**	**5pm**	**12am**	**5pm**
FF	**0,699**	0,659	0,495	0,633	0,301	0,612

Table 5.8. FF calculated values for Polycrystalline Silicon Solar Cell (Source: Author's measurements)

In the previous table 5.8 is observed that the highest Fill Factor and therefore the ideal one with regard to other calculated values turns out to be for a vertical position at 12 a.m. Hereby there is demonstrated that the value FF does not depend on the power that the solar panels can develop, but it depends on the relation that exists between the maximum power that can developed and the maximum "ideal" power of it.

Later, Fill Factor's values appear for the cell of Amorphous Silicon.

Amorphous Silicon Solar Cell						
Position	**Vertical**		**45 degrees**		**Horizontal**	
Time	**12am**	**12am**	**12am**	**5pm**	**12am**	**5pm**
FF	0,604	0,595	0,588	0,589	0,658	0,621

Table 5.9. FF calculated values for aSi:H Solar Cell (Source: Author's measurements)

Another way of measuring the electrical efficiency could be possible by the relation between input power P_I and output power P_O. It appears in the following equation:

$$\eta = \frac{V_M \cdot I_M}{G \cdot Area} \qquad \textbf{(Eq. 5.2)}$$

Where *G* is the irradiance in STC considered conditions 1000W/m2.

That substituting Eq. 3.6 in Eq.5.2:

$$\eta = \frac{V_{OC} \cdot I_{SC} \cdot FF}{G \cdot Area} \qquad \textbf{(Eq. 5.3)}$$

In this way, though initially according to the power generated by both cells there could seem to be better the Amorphous Silicon cell, but it is necessary to bear in mind that the surface of capture of the Amorphous Silicon cell is almost the double of the Polycrystalline Silicon cell and even this, valuating the FF and the efficiency of both solar cells, the most efficient cell of both is the Polycrystalline Silicon cell.

Since it is possible to observe in the previous table, the experimental values differ from the theoretically known ones.

Largely, this is due to the fact that normally the typical parameters of the cells that are shown in the technical specifications sheets of the manufacturers come defined in Standard Test conditions (STC). These conditions come defined by:

- Irradiance 1000 W/m2

- Spectral distribution AM 1.5
- Incidence Normal
- Temperature of the cell 25 °C

Then, taking in account that the measurement takes place inside and the temperature is more or less constant, the relatively low efficiency of solar cells is because of the not optimum position or orientation of the solar cell, optical influences or effects of lack of homogeneity (FF) and the real irradiance. It means, averaged over the year of the mean energy current density (shown Table 5.10) in the place where solar cells are tested is largely far from the 1000 W/m2. Much less than the maximum energy current density of the AM1.5 spectrum.

Time	*G*	Time	*G*	Time	*G*	Time	*G*	Time	*G*	Time	*G*	Time	*G*
4:52	36	7:07	598	9:22	722	11:37	599	13:52	341	16:07	162	18:22	78
5:07	51	7:22	627	9:37	718	11:52	575	14:07	309	16:22	156	18:37	65
5:22	65	7:37	652	9:52	712	12:07	549	14:22	276	16:37	149	18:52	51
5:37	332	7:52	673	10:07	702	12:22	523	14:37	243	16:52	142	19:07	36
5:52	388	8:07	690	10:22	691	12:37	495	14:52	210	17:07	134	19:22	21
6:07	439	8:22	704	10:37	676	12:52	466	15:07	177	17:22	124		
6:22	485	8:37	713	10:52	660	13:07	436	15:22	174	17:37	114		
6:37	527	8:52	719	11:07	641	13:22	405	15:37	171	17:52	103		

Table 5.10. Global irradiance on a fixed plane (W/m2) with an inclination of 45 degrees and an azimuth of plane -87 degrees. (Source: PVGIS-Solar radiation database)

Also, can be the degradation and derivations of the solar cell, the resistance in series and in parallel with which it is possible to model the photovoltaic cell and his losses that are represented below:

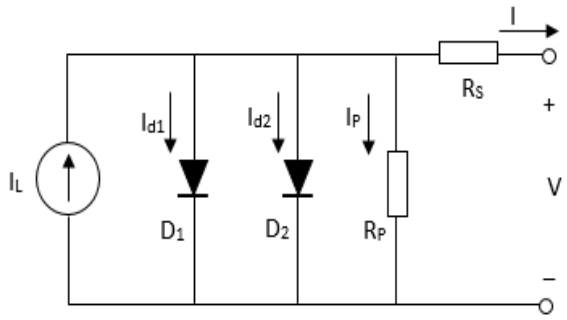

Figure 5.11. Equivalent circuit of solar cells (Source:[2]**)**

Where the diodes D1 and D2 represent respectively the diffusion in neutral zones and the effect of recombination in zones of load of the semiconductor material that constitutes the cell, the R_p resistance represents the losses of the semi conductive unions and the R_s is the loss due to the material.

6. Monitoring and analysis of both Solar Cell

The principal aims this section is the long-time monitoring of both cells through the programming of an ArduinoUNO platform initially powered by grid energy, so that it allows to measure values of temperature and voltage of both cells for the later representation of these values that allow the experimental comparison of both cells and their theoretical values.

6.1. Materials

To know the voltage, current and the power that polycrystalline and Amorphous Silicon cells are able to generate, as well as the influence of the Sun's incident radiation, the effect of clouds on the electrical generation or the relation of the temperature with the cell and Sun's incident radiation, the following components are necessary:

- Polycrystalline Silicon Solar Cell / Amorphous Silicon Solar Cell
- Resistance of real value R1= 560 Ω
- Resistance of real value R2= 99,5 Ω
- 2 sensors of temperature LM35CZ
- Grid power supply at 5V
- ArduinoUNO
- MicroSD card
- Plug wires of Arduino or protoboard with jack connector at both sides

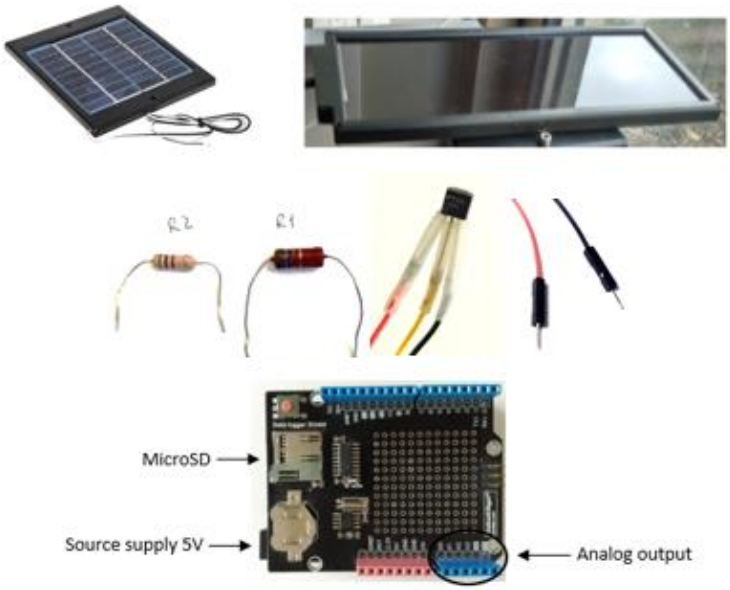

Figure 6.1. Necessary elements for V, T1, T2 measurement of both solar cells with grid power supply (Source: Own Elaboration)

6.2. Procedure description

The electrical circuit that in this case is applied for the monitoring of both cells separately is the following one:

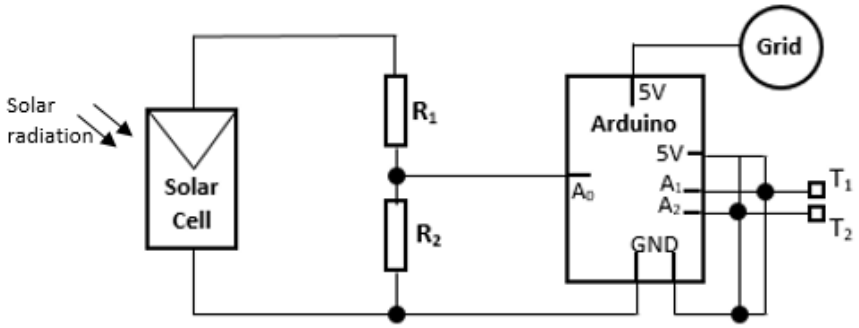

Figure 6.2. Designed and implemented circuit for data monitorization of V, T1, T2 with input power from the grid (Source: Own Elaboration)

After the photovoltaic cell that is wanted to test in each case placed in horizontal position like in Fig.7.1, the incorporation of a voltage divider is necessary in terminals of this one to contribute a minor or equal voltage of 1 V to the pin A0, because in other case there would be burned the platform ArduinoUNO. For it, are decided the values of R1 and R2 that are specified previously.

Of 5 available Pin in this platform, 3 of them will be used:

- Pin A0: it is used for the measurement of voltage which is specified in Fig.7.1 because ArduinoUNO is configured to calculate the voltage in terminals of each solar cell
- Pin A1: it is used for the measurement of room temperature just in front of the cell by LM35CZ sensors directly calibrated in degree Celsius with linear scale factor of + 10,0 mV/°C [16].
- Pin A2: it is used for the measurement of the room temperature behind solar cell through the same type of sensor that in Pin A1.

These Pin are powered supply by the 5V that supplies the platform and also is needed the connection of these to the mass of the same platform.

Later, the program execution is written in ArduinoUNO software, which allows the realization of the previously explained measures and finally, the electric circuit is verified, the microSD card is inserted in the platform. It takes 5 days of program execution.

6.3. Results

Once the measured data is registered in the microSD, the voltage in terminals of the cells and the generated power corresponding to each cell, is represented in Fig.6.3 and Fig.6.5 by OriginPro 8.6

software. In addition, the variation of the temperature T1 and T2 of both solar measurements are also analysed in Fig.6.4 and Fig.6.6.

6.3.1. Measurement of Voltage and Power Generated by the aSi:H Cell

The fluctuation of the voltage in terminals that can be notice in the following curve is due to the shades produced by clouds over the cell. Moreover, in every daily cycle is observed a period of growth of voltage values followed by a peak of production and finally can also observed a period of decrease of voltage values. This cycle is repeated every day and it corresponds with variation of Sunlight incidence over the day. It means that, according to the position of the cells in the morning until 2 or 3 PM, power generation does not reach the maximum production that corresponds with the Sun's direct radiation on the cell and over the time, when Sun's radiation comes indirect again, this period of decrease of generation appears.

In this period of 5 days of testing, remains reflected the dependence of the electric power generation on climatological changes. First and third day of measures reflect the typical characteristic in a clear day without clouds. Nevertheless, the electricity generation of the following days is practically null due to the overcast sky turns in clear sky only in two concrete moments of the day, taking place both peaks that can be appreciated.

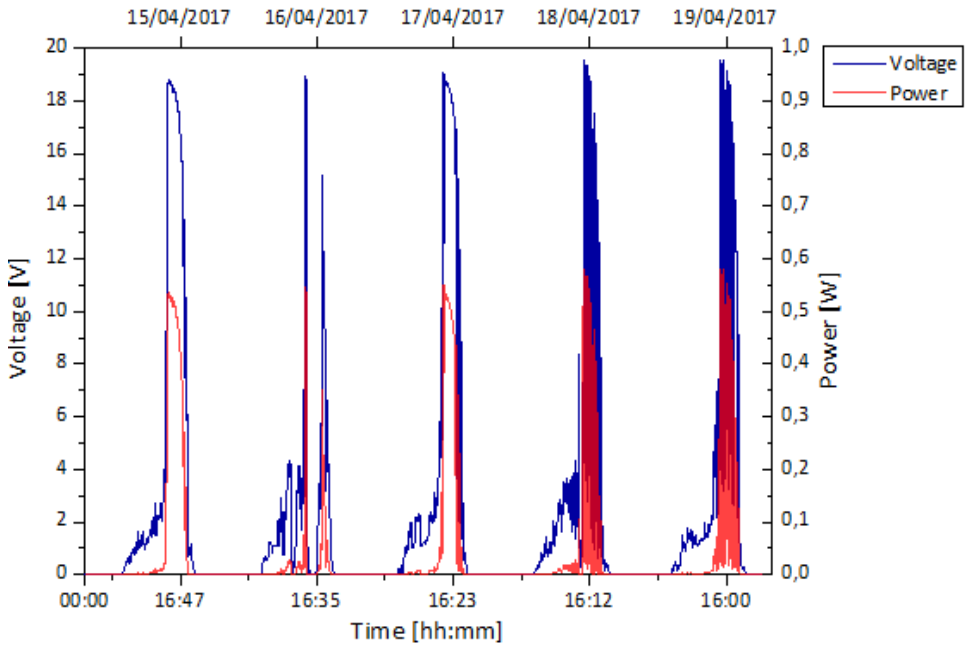

Figure 6.3. Generated power and voltage in function of time of aSi:H solar cell (Source: Own Elaboration)

According to the type of curve of last two days of measurement, a great variation of the "Sun - cloud" climatological conditions is appreciated. In spite of, a major generated power is appreciated in these two days.

Another important aspect is the fact that the cell is able to produce energy from 14:30h until 17:30h, with a maximum of almost 0,6 W at 15:30h in the evening.

6.3.2. Influence of sensor position ahead and behind aSi:H Cell

As can be seen in the following image, the shape of the function that describe both temperatures follow approximately the form of the function that represents voltage depending on the time. The temperature decreases slower than the voltage coming to a minimum of 18 °C and a maximum of 33°C in the period of time in which the measurement is realized.

There exists a visible difference between both temperatures. Though the distance that separates both sensors does not come to 30 cm, it is the difference between being in the surface of the cell and to be in the shade of this one. This makes think the fact that any element that could do shade on the cell would make diminish the generated power, due to the fact that the temperature is related to the incidental radiation on the cell and generation of electric power depends on this radiation.

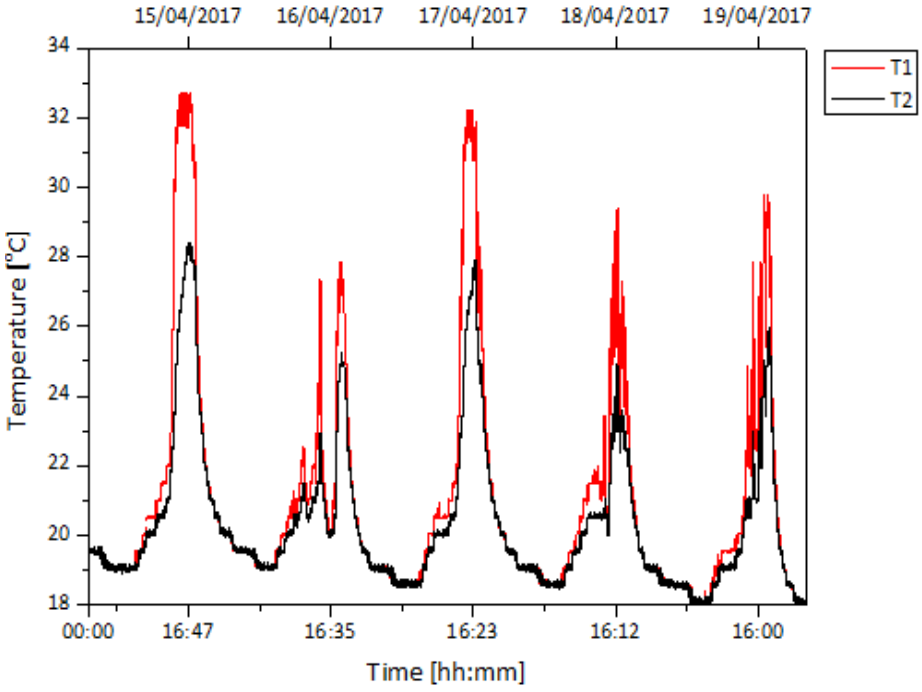

Figure 6.4. Representation of both temperatures in function of time for aSi:H solar cell (Source: Own Elaboration)

Curiously, on the first and third day of test there are registered values of temperature higher than the other days. If we observe this fact also with defined analysing the previous graph, it is possible to corroborate the fact that they have been clear-sky days where there has been major incidental radiation without presence of clouds. Nevertheless, it does not happen the other days. The presence of clouds can be seen in the Fig.6.4 and also with the variation that can be observed in V-t and P-t functions.

6.3.3. Measurement of Voltage and Power Generated by the polycrystalline Si Cell

In the case of Polycrystalline Silicon solar cell, the first thing that is notice is a seemingly lower capacity of power production than in the case of Amorphous Silicon, but it is necessary to take in account that the aSi:H solar cell is approximately two times bigger than polycrystalline Silicon solar cell.

Another observation is the difference between operating voltage of both solar cells. This cell works for the half of voltage, that through Ohm's Law does that power generation is also low.

The period of time in which both solar cells are able to generate electricity in a same day, is practically the same. Analysing the data, can be appreciated that Polycrystalline solar cell is able to generate electricity 40 minutes more than the other solar cell. It could not be due to the difference between both band gap values because in this case would be the Amorphous one which would be able to catch more sunlight spectrum, but could be due to the fact that polycrystalline Silicon measure takes place days after Amorphous Silicon test. It could mean that Polycrystalline solar cell is exposed to the Sun over major time. The fluctuation that can be seen in working voltage curve and also in generated power by the cell is necessary to emphasize the fact that in case of polycrystalline Si cell it is almost null, except for 23/04/2017 measure.

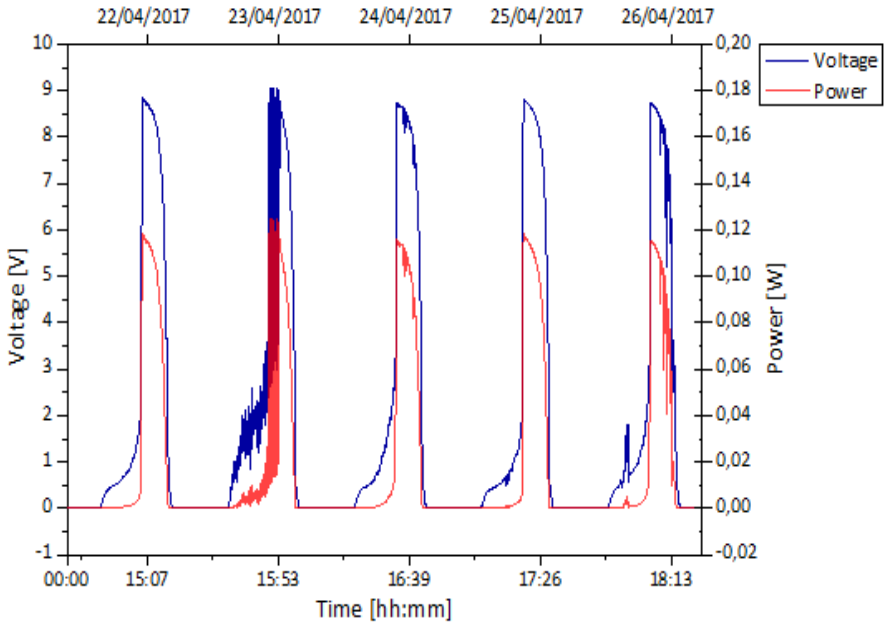

Figure 6.5. Representation of both temperatures in function of time for a polycrystalline Si solar cell (Source: Own Elaboration)

6.3.4. Influence of sensor position ahead and behind polycrystalline Si Cell

In this period of measures there is a difference of two degrees of temperature in relation to the previous measure.

As in the previous case, the existing relation between room temperature, the shades caused by the clouds and the influence of them on the radiation that arrive to the cell are demonstrated by the following figure:

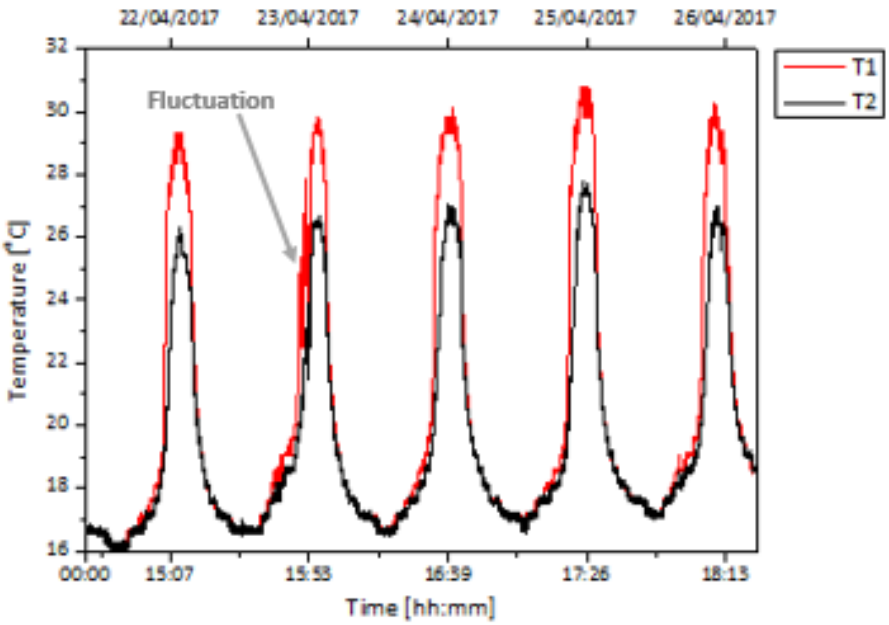

Figure 6.6. Representation of both temperatures in function of time a polycrystalline Si solar cell (Source: Own Elaboration)

The consequence, fluctuation especially in the temperature measured in front of the cell, fluctuation in working voltage of the cell and in the power that this cell is able to generate.

7. Measurement of Arduino Power Supply Requirements

To know the current that has to supply the battery of the autonomous system is necessary to know the flow of load for unit of time that crosses the compact system of measure *Arduino*. Though the technical specifications of this system report of a necessary DC Current per I/O Pin of 40mA, it is necessary to check the maximum, minimum and an average real consumption of the device in this specific situation.

7.1. Materials

To know the current that ArduinoUNO platform consumes at real time, the following components are necessary:

- SourceMeter 2400 oscilloscope
- Connector BNC with crocodile clips for mass and "positive" measuring probe
- 9V battery
- Connector for 9V battery, as can be seen in Fig.7.1
- ArduinoUNO platform

Figure 7.1. Necessary elements for measure of instantaneous Arduino power needs
(Source: Own Elaboration)

7.2. Procedure description

For it, with Ni-MH battery there is supplied a 9V voltage connected in series to a R = 10 Ω and also to the computing platform, so that connecting the oscilloscope in terminals of resistance it is possible to know the drop voltage in this one. Later, Ohm's Law allows to calculate the necessary current.

7.3. Results

After oscilloscope measurements, the generated data is represented by OriginPro 8.6.

To main peaks are observed in Fig. which correspond with closing and opening program respectively, because each time is the program executes the order of reading and writing the file is needed to open and close it in order to guarantee the record of information.

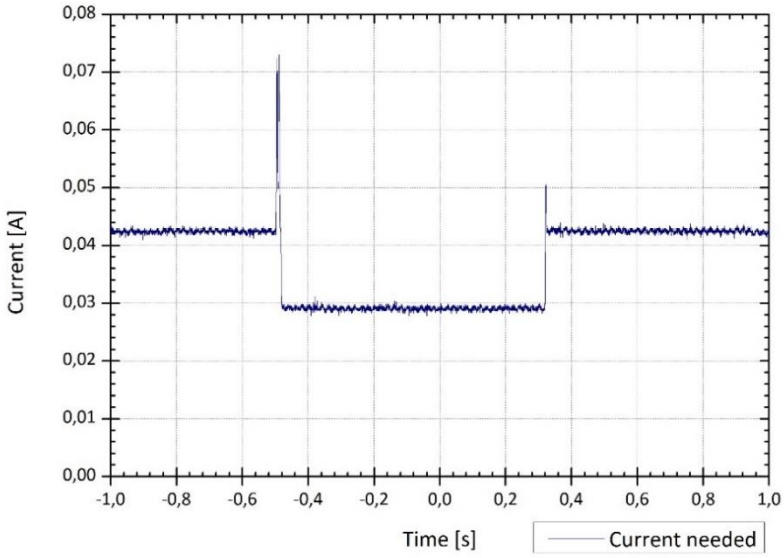

Figure 7.2. Necessary input current by ArduinoUNO system to close and open the program after 800ms of delay (Source: Own Elaboration)

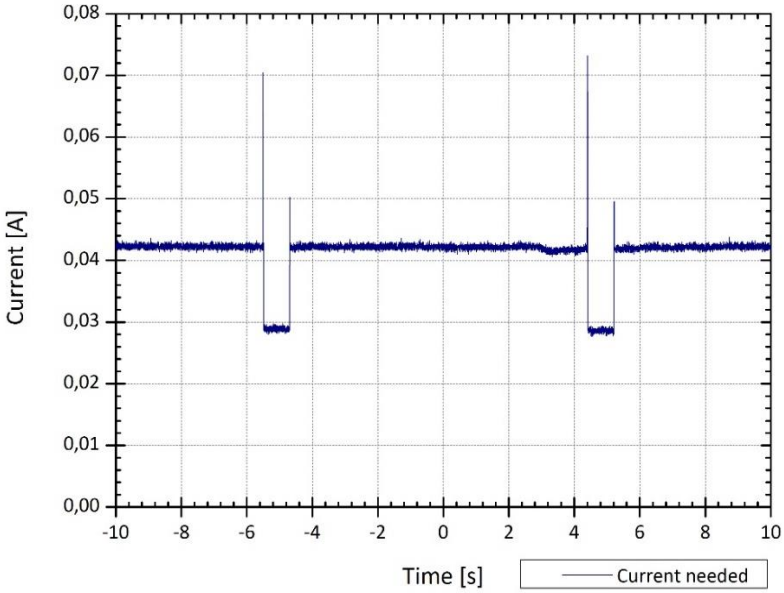

Figure 7.3. Necessary input current by ArduinoUNO system while it runs, between two closing and opening processes (Source: Own Elaboration)

The peak of maximum current of 70mA approximately happens because the program needs to be closed to write the measured and read data.
It means that the quantity of electricity fluxes decreases between the cycles of measure (that consists of the measure of voltage in terminals of the corresponding solar cell, the temperature just in front of solar cell and rom temperature), due to the previous delay Later, there returns to be restarted the curl of each measure which own average consume is about 42 mA and finally, a 50 mA peak of starting program.

In Fig.7.3 can be seen three periods of measure separated by two periods of pause. The total operation time of measure and the writing three measures (voltage and both temperatures) also is formed by some times of delay between them. Then, the total period of each measurement corresponds to 10s that can be seen in the image, between both periods of delay.

8. Energy storage system test with different battery technologies

In the previous sections are observed that, capacity of production by solar cells is dependent of: bandgap value of each semiconductor material, cells orientation, hours of direct sunshine, shadows caused by the clouds, the few exploitable hours of sunshine a day, the long hours without generation from dusk and the influence of dust, is necessary extra energy to achieve the autonomous functioning of the measurement system. For it, the study of some different technologies today known is necessary.

Later, the supply of the following rechargeable batteries is always realized by the cells above analysed. With it, one tries to know the functioning of each one in a "clean" way in order to make ArduinoUNO platform runs.

8.1. 16V Super Capacitor

In this first case, a 16V supercapacitor is analysed because of their capacity of storage major density of energy in comparison with other capacitors. It is decided to analyse the functioning of the charge and discharge capacity of a 470 000 µF connected (as can be seen in Fig.8.1) to a resistance in series as a current limiter and also connected to a blocking diode in order to block the current in direction to the cell when at night it acts as a passive element.

Figure 8.1. 16V and 470 000 µF capacity of Super Capacitor to be tested (Source: Own Elaboration)

For it, the following circuit in Fig.8.2 is realized for two different values of resistance of load. In this concrete case, the measurement is executed for one day by a resistance of load R_{L1} and later for two days by a resistance of load R_{L2}, of specific values shown respectively in the same figure:

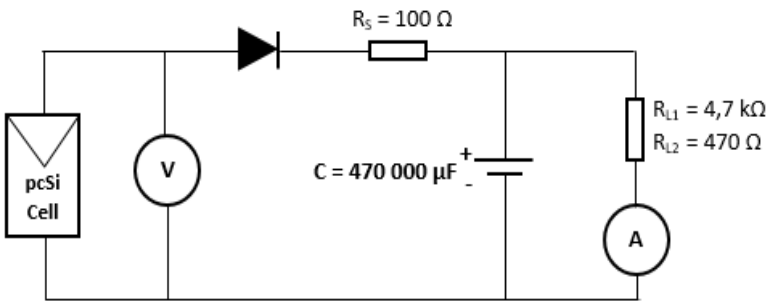

Figure 8.2. Tested circuit with 16V Super Capacitor battery and both values of resistance load. (Source: Own Elaboration)

Later there are monitored the measurement of values of voltage and current by Fluke45 multimeter. According to the position of the ammeter, across Ohm's Law it is possible to know also the voltage in terminals of the super capacitor. Then, with both following figures are represented: working voltage of Polycrystalline Silicon cell, voltage in terminals of the super capacitor after the voltage drop of 0,5V in the diode, the respective voltage drops in load resistance and the current across the load resistor in each case.

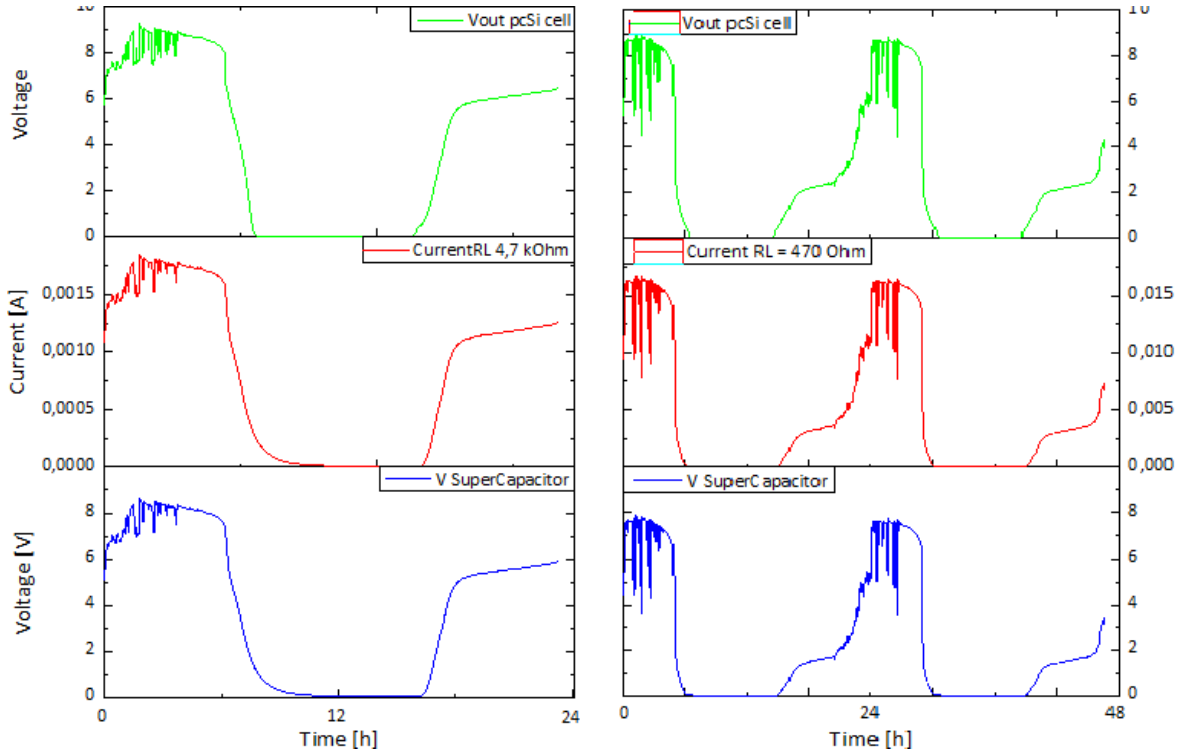

Figure 8.3. Representation of voltage in terminals of polycrystalline Silicon solar cell, current through R_{L1} and R_{L2}, and voltage in terminals of the 16V Super Capacitor. (Source: Own Elaboration)

As can be seen in Fig.8.3, several conclusions can be exposed:

- Though the circuit is also powered by Super capacitor battery, can be seen that the battery is not able to supply energy during the whole night because the super capacitor is discharging at the same time as solar cell stops to generate electrical energy in both experiments. It means that, the capacity of charging also depends on the quantity of energy that the solar cell can generate over a day.

- The load resistor value influences in energy consumption of the battery and therefore the discharge of this one. Nevertheless, the effect of the load is also better analysed in 9.3 section.
- The presence of the resistor in series provokes a limitation of current and the diode provokes a little voltage drop of 0,5V approximately. Also, can be seen the drop voltage difference between both experiments due to the supplied current to the resistor. The lower is the resistor value, the higher is the supplied current to the resistor and the difference between generated voltage and voltage in terminals of the capacitor.
- The load current between both experiments is ten times smaller in case of R_{L1} than in case of R_{L2} load.

8.2. Ni-Cd 4,8V Battery

Once demonstrated that the process of load of a battery depends directly on the working voltage of the cell, in this second case one decides to analyse a micro battery of Ni-Cd of 4,8V to 50mA.

Figure 8.4. Image of the 4,8V and 50mA battery to be tested (Source: Own Elaboration)

In the same way as in the previous case is monitored the testing data of: the voltage in terminals of load resistance as well as the current that flows across it, by Ohm's law), and the current across the battery to see concretely the periods of charge and discharge. Also in this case shall be inserted a limiting-current resistor and the same diode of blockade, for the reason previously exposed.

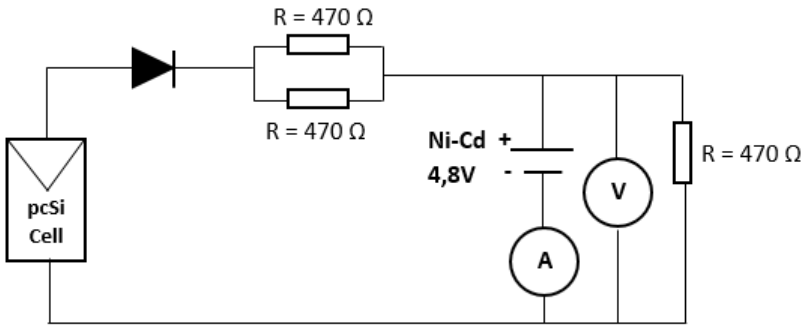

Figure 8.5. Tested circuit with Ni-Cd 4,8V battery with 470Ω value of resistance load. (Source: Own Elaboration)

The experimented data is represented in the following Fig.8.6, where can be seen the cycle of discharge and posterior charge of the battery of 4,8 V also with the proportional curve of current across the load resistor.

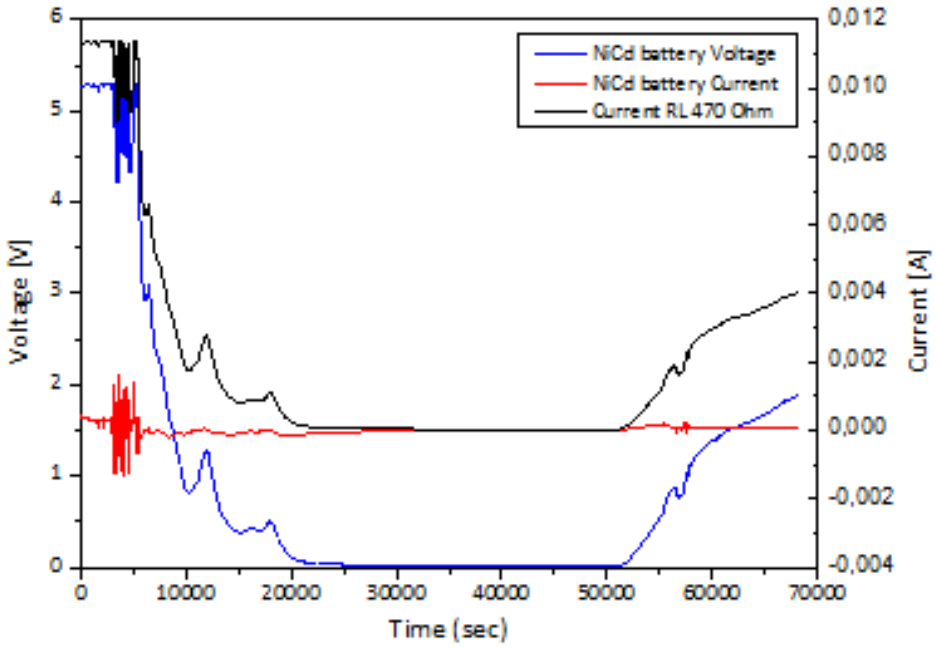

Figure 8.6. Representation of generated voltage by pc-Si solar cell, current through the 4,8V Ni-Cd battery and current through RL=470Ω (Source: Own Elaboration)

The discharge is produced in approximately 5 hours and 15 minutes, whereas the time of load needs almost the double of time due to the fact that the charging period only can happen when the voltage in terminals of the cell is higher than the voltage in terminals of the battery. In addition, is observed that the maximum current in the whole cycle is of 10 mA, which represents a quarter of the necessary direct current to feed of the input pins of the ArduinoUNO platform.

Moreover in Fig.8.7, which is an extension of charge-discharge period of the Ni-Cd battery, can be notice a constant variation between charge and discharge functions. This seems to be a characteristic of this technology or a defect of this battery because in next sections and technologies it is not appreciated.

Then, there is demonstrated once again that this second design would not also be valid for the supply of the platform because of the V_{in} of pins has to be between 7 and 12 V, fact that does not take place in the whole measurement on the part of the cell and of the battery either.

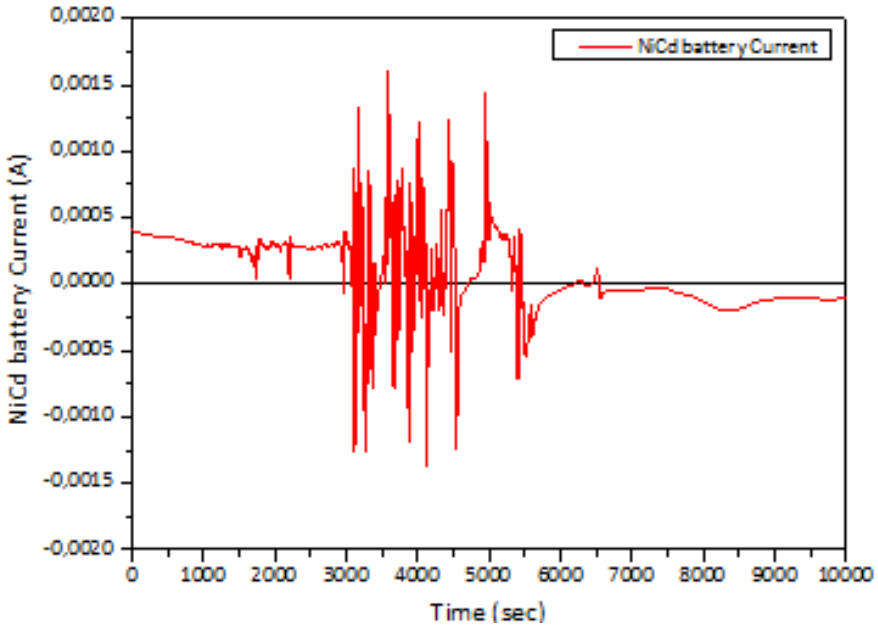

Figure 8.7. Charge-discharge current flow through the 4,8V Ni-Cd battery (Source: Own Elaboration)

8.3. Ni-MH Rechargeable 5V Battery

Due to the fluctuation of the input and output current of the battery of Ni-Cd of 4,8V previously analysed, in this point there is analysed another battery of 5V based on technology Ni-MH. It is a type of rechargeable battery formed by four sinks placed in series. These are of nickel - metal hydride, supplying a voltage of 1,25 V each one.

This type of technology presents an advantage with regard to the battery of Ni-Cd previously analysed. It is that the technology Ni-MH uses NiOOH's anode as in the previous battery, but whose cathode is of alloy of metallic hydride, allowing to eliminate the Cadmium. It is known that the Cadmium is expensive and represents a danger for the environment, beside possessing minor capacity of charge in comparison with the battery that now is analysed.

Beside changing the technology of the battery, it is decided to implement a voltage regulator. It is true that for adding a regulator is not going to obtain the same effect that a constant voltage source due to the fact that the real source in this case is a photovoltaic cell and the production of this one depends on the technology on which it is based, the hours of the Sun and many other aspects, but is added the 5V regulator LP2953 to regulate the charge of Ni-MH's battery allowing that should not be overloaded, which would concern the useful life of the battery.

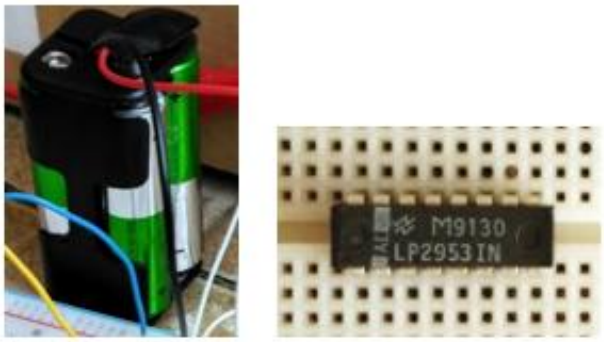

Figure 8.8. 5V battery and LM2953IN regulator (Source: Own Elaboration)

Then, for this purpose there is designed the following electrical circuit in which, since it is possible to observe in the image, there is changed the value of the load to be able to see the charge-discharge effect of the 5V battery.

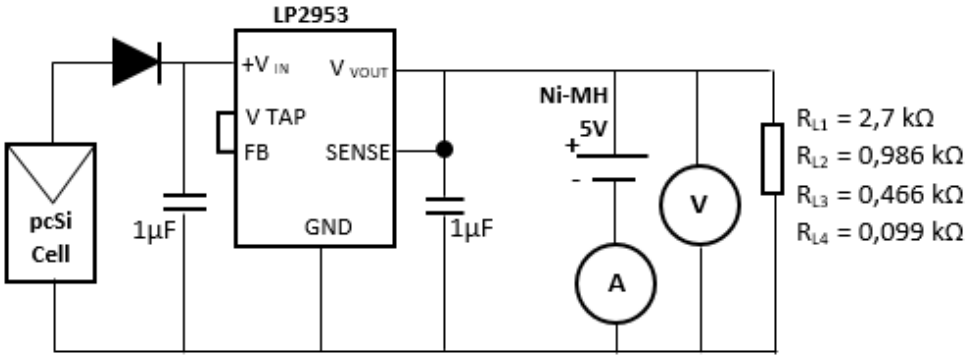

Figure 8.9. Tested circuit with Ni-MH 5V battery with different of resistance load. (Source: Own Elaboration)

Then, in Fig. 8.10 that corresponds to the information extracted with the assembly of the previous circuit it is possible to understand the influence of R_L's value on charge-discharge of the rechargeable battery.

When higher is the value of the load resistor, the voltage of the battery scarcely changes, surely due to the high opposition that the resistance presents to the current flow and to the presence of the voltage regulator. For this reason, for R_{L1} and R_{L2} the current of discharge is practically null, linear and constant, as well as the function of the voltage presents a linear discharge. This means that the battery is discharging, but very slowly and constantly.

Nevertheless, if the value of the resistance diminishes up to R_{L3} = 0,466 kΩ. The charge of the battery does not overcome the 5V, though the function of the current seems to be current of charging. Later there comes the process of discharge of the battery functioning as generator, since is observed that the current acquires negative values.

In the same way as it happens in previous cases, when there is no the Sun the battery is discharged, though not completely at these 22 hours of test. In the following morning (towards the end of the test) it returns to start a cycle that might manage to produce the second charge of the battery, because the voltage in terminals of the battery starts growing, but it is not sufficient to recharge the battery because the current presents a growth, but it does not manage to assume positive values.

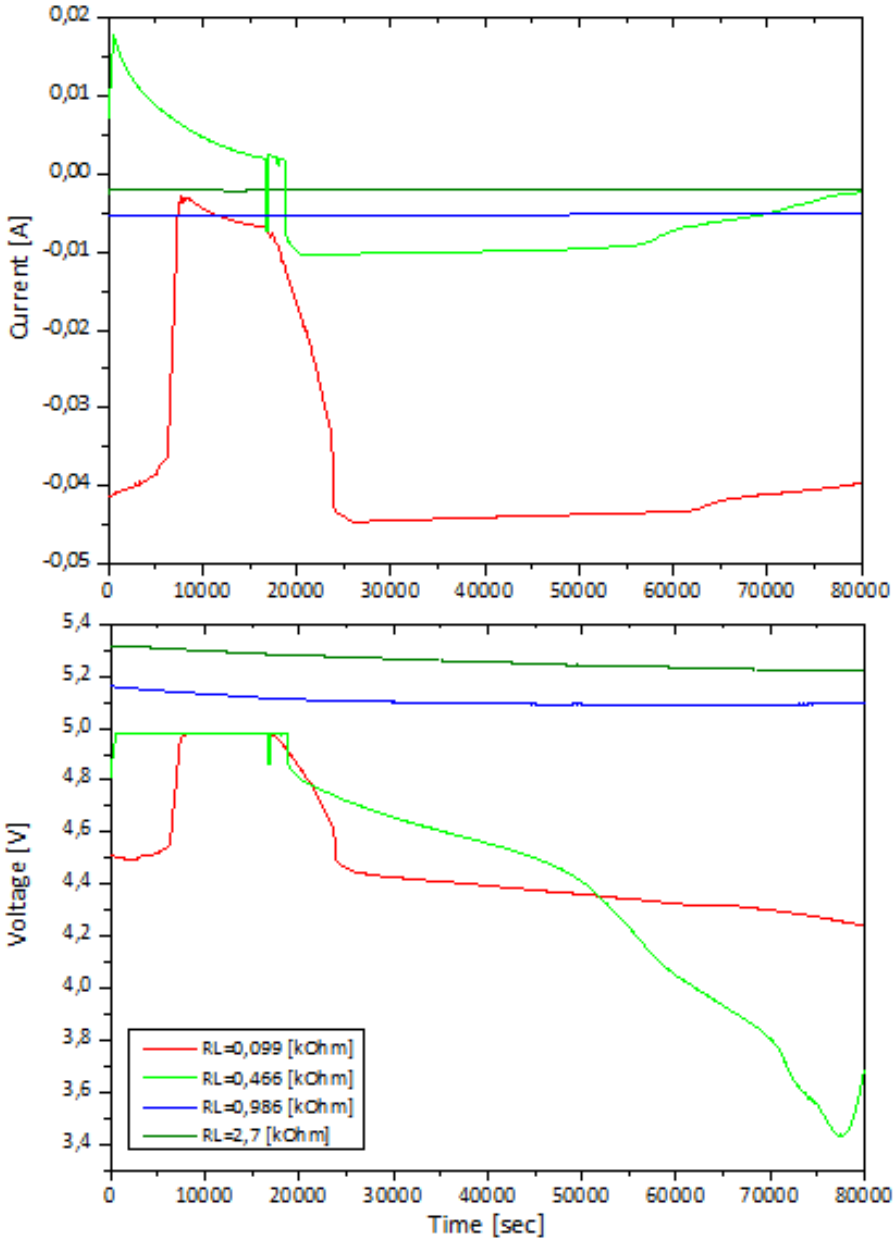

Figure 8.10. Voltage and current of the Ni-Cd 5V battery at different values of load (Source: Own Elaboration)

Then, finally when the circuit is tested by a RL = 0,099kΩ is observed that it is a too small resistance to allow the charge of the battery. It is true that the voltage in terminals of the battery manages to acquire the 5 V, but this does not mean that it allows the recharge of the battery because it is possible to observe in the curve of current across the battery that current will not acquire positive values. This means that the voltage increases due to the generation produced by the cell regulated by the voltage regulator, but the battery at all time works as generator because this resistance presents an easier path for the current.

If there compares the electrical circuit of 8.2 section with the present circuit with the same load RL =0,466 kΩ, the unique physical difference is the technology on which there is based the battery and the presence of the regulator.

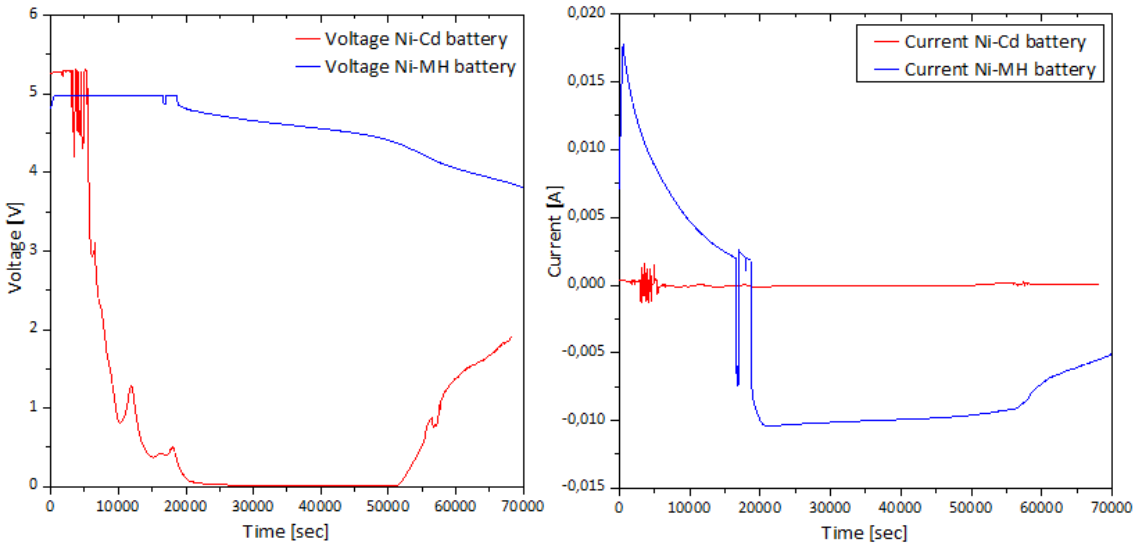

Figure 8.11. Comparison between circuit in section 8.2 and 8.3. (Source: Own Elaboration)

The differences between both circuits are:

- The battery of Ni-Cd experiences a small overload whereas Ni-MH's battery acquires a maximum voltage value in terminals of 5V, due to the presence of the voltage regulator.
- Ni-MH's battery does not present almost variation of the voltage in the period of charge, whereas the battery of Ni-Cd does not even present a charge-discharge ongoing reflected both in the sense of the current and in the voltage in terminals of the battery.
- Ni-MH's battery presents major linearity in the discharge period and also major period of discharge. Nevertheless, the charge-discharge cycle of the battery of Ni-Cd is taking less than 1 hour, fact that makes think that the battery is not working.

An improvement is experienced with regard to the previous circuit, though the voltage and the current supplied by the battery are not sufficient. For this reason, the following section appears.

8.4. Alkaline Non-rechargeable 9V Battery

In the previous section the voltage and the current supplied finally to the load are not sufficient to make runs the platform ArduinoUNO, and which is more important, make run the pins of reading. Knowing that the working voltage of Arduino Uno's is between 7 - 12V and that the cell of Polycrystalline Silicon can supply more than 7 V from 14:00 until 18:00 approximately, one decides in this paragraph to change it by the cell of Amorphous Silicon. Not only for this reason, but also because this new cell reaches major values of voltage, which allows to regulate the input voltage to higher output voltage.

Beside changing the cell, also the battery changes for the alkaline one of 9V not rechargeable. Once changed these components, the circuit needs a change also of the regulator because the previous one was turning to 5V and now in necessary a regulation to 9V approximately, that is capable of making the platform Arduino work when the photovoltaic cell cannot make it.

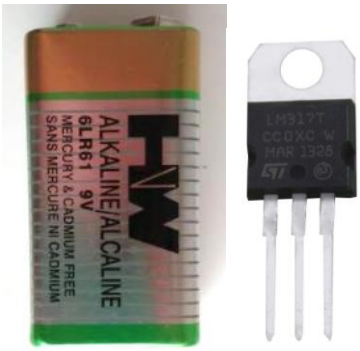

Figure 8.12. Alkaline 9V battery and LM317 regulator. (Source: Own Elaboration)

Then, the circuit is basically the same as the previous one, but now is like the circuit that follows:

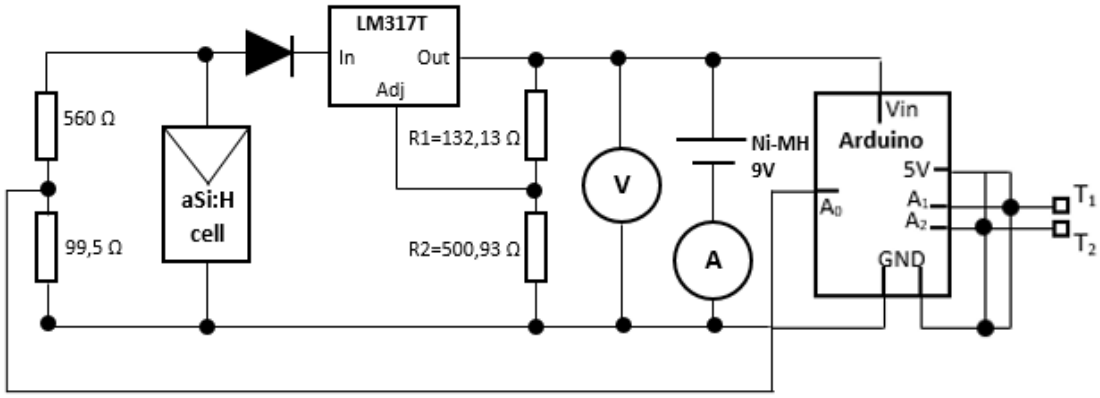

Figure 8.13. Tested circuit with Ni-MH 9V battery with LM317T regulator and ArduinoUNO system of measure. (Source: Own Elaboration)

To calculate the output voltage there is applied the following formula provided by the data sheet of the attached annex:

$$V_{out} = V_{REF} \cdot \left(1 + \frac{R_2}{R_1}\right) + I_{ADJ} \cdot R_2 \qquad \textbf{(Eq. 8.1)}$$

Where $V_{REF} = 1{,}25V$ in the voltage between the output of the regulator and the adjust pin, and I_{ADJ} is:

$$I_{ADJ} = \frac{V_{REF}}{R_1} \qquad \textbf{(Eq. 8.2)}$$

Then, the following expression allows to calculate the value of R2 in function of $R_1 = 132{,}13\Omega$ and the output voltage needed $V_{out} = 10{,}75V$:

$$R_2 = \frac{R_1 \cdot (V_{out} - 1{,}25)}{2 \cdot 1{,}25} = 500{,}51\ \Omega \qquad \textbf{(Eq. 8.3)}$$

Nevertheless, the results show a regulation of voltage almost 3V below the expected value.

The measurement of the voltage is monitored by the software VEEPro in terminals of the battery and the current across this one, and as it is observed also in the electrical circuit, across the ArduinoUNO platform

both temperatures measure up set already named in previous paragraphs and the voltage in points of the photovoltaic cell.

During two days of test the sense of the current across the battery indicates a continuous discharge until reaching a complete discharge. The values that the current assumes in the first 9 hours of test indicates the supply and Arduino Uno's functioning. This fact also is corroborated by the representation of the curve of working voltage of the cell, which already has been observed previously.

The curiosity of the representation of the current is the variation of the current supplied by the battery when Arduino is running. As seen in the paragraph in which the current consumed by Arduino is analysed, this one changes depending on the periods of "delay" and the periods in which it realizes the measure. This fact meets reflected in the fluctuation in the current.

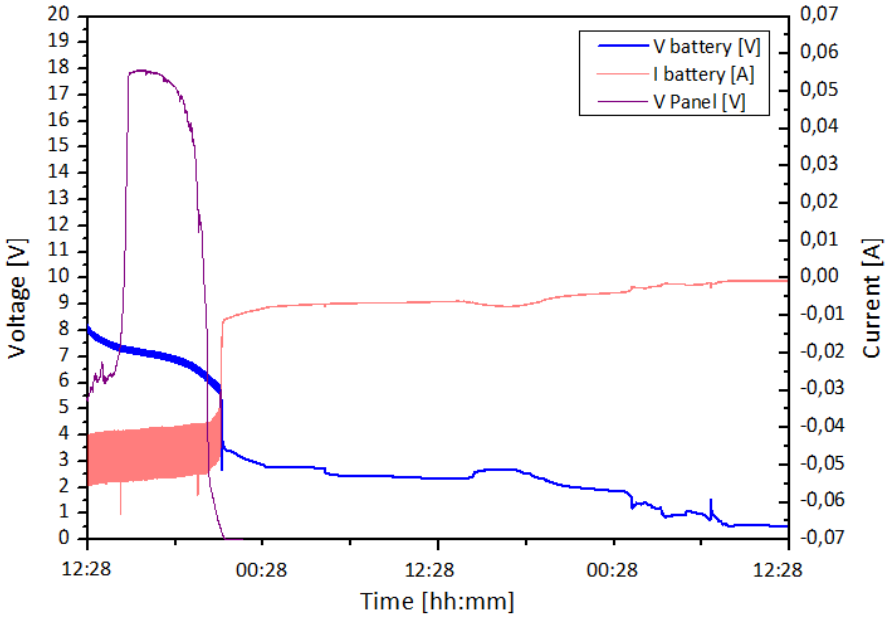

Figure 8.14. Results of circuit of Fig.8.13. Representation of Fluke45 and Arduino measurements of an autonomous embedded system of measurement. (Source: Own Elaboration)

Another important aspect, is the below observed influence of the generation of the cell on the discharge of the battery. To the beginning, the voltage of work of the cell is minor that the voltage of the battery provoking the fast discharge of the battery, since ArduinoUNO is supplied only by this one. Later, the discharge of the battery presents a slope less inclined while the voltage that contributes the cell is higher enough to that of the battery.

At 21:30h approximately of the first day of measurement, a great discharge of the battery is appreciated due to the fact that the supplied energy by the cell tends to zero with a completely vertical slope, making discharge the battery of 6V to 3,5V. At the same time, supplying to the platform a low voltage to 6V, this one stops working for the rest of the measurement and finally the battery is discharged completely in the following 39 hours.

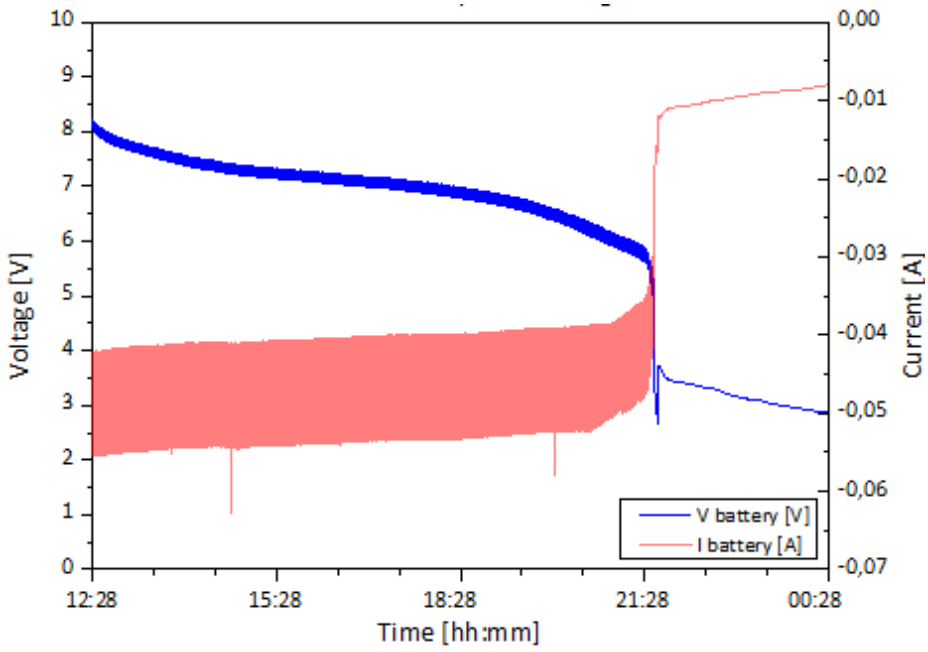

Figure 8.15. Extension of representation in Fig.8.14. (Source: Own Elaboration)

After Arduino stops working, the battery presents a discharge approximately linear, due to the presence of the voltage regulator.

Another indication that shows Fig. that the platform of measure stops working it is the information written by this one of temperature. The components most sensitive to a supplied insufficient energy are the pins of Arduino's reader. When the reading of these pins become meaningless, it is a clear sign of that the energy supplied the system is not sufficient.

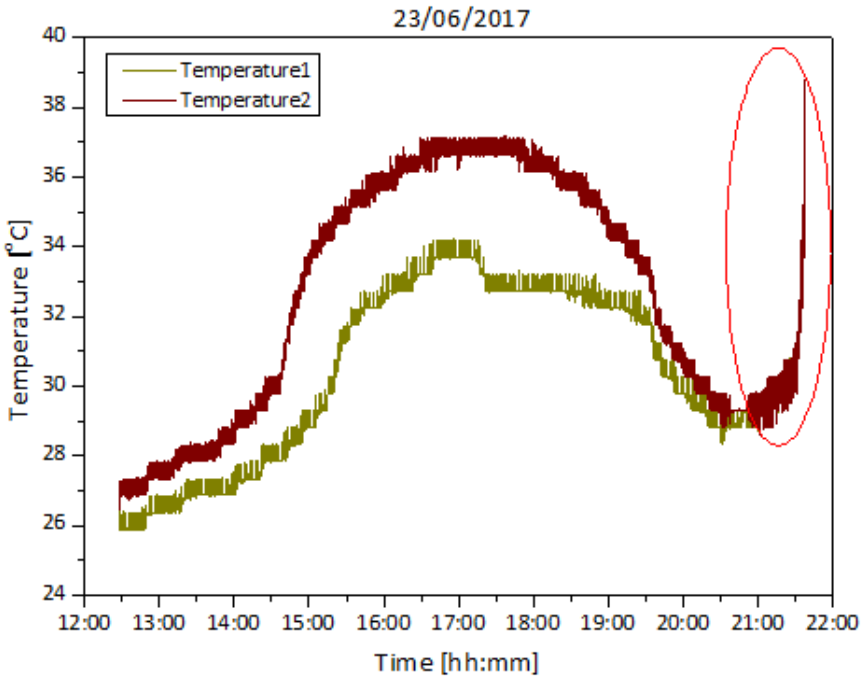

Figure 8.16. Representation of room temperatures 23/06/2017 in Ni-MH 9V non-recharge measurement (Source: Own Elaboration)

8.5. Ni-MH Rechargeable 10V Battery

Finally, one tries to prove the same previous circuit with the same procedure but increasing the value of the battery until 10V, doubling the voltage of 8.3 Section.

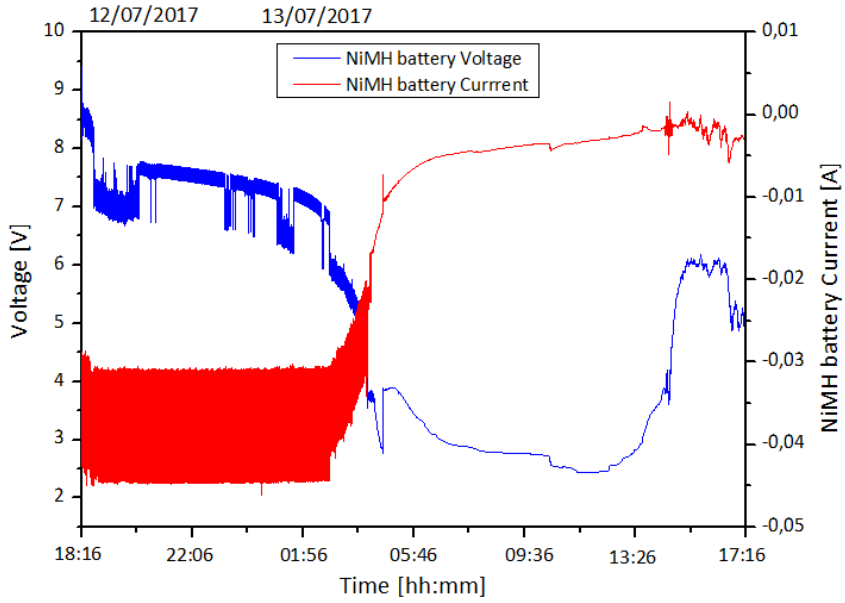

Figure 8.17. Representation of voltage and current of Ni-MH 10V rechargeable measurement by Fluke45. (Source: Own Elaboration)

In Fig.8.18 is shown the data registered by Arduino platform only supplied by aSi:H solar cell and a Ni-MH battery of 10V. As can be seen, Arduino system can only read over 5 hours and 30 minutes. The measurements of the platform seem valid if it is compared with the typical shape analysed in the first experimental section of the thesis. Also, can be notice the variation of the room temperature at the same time as voltage do it.

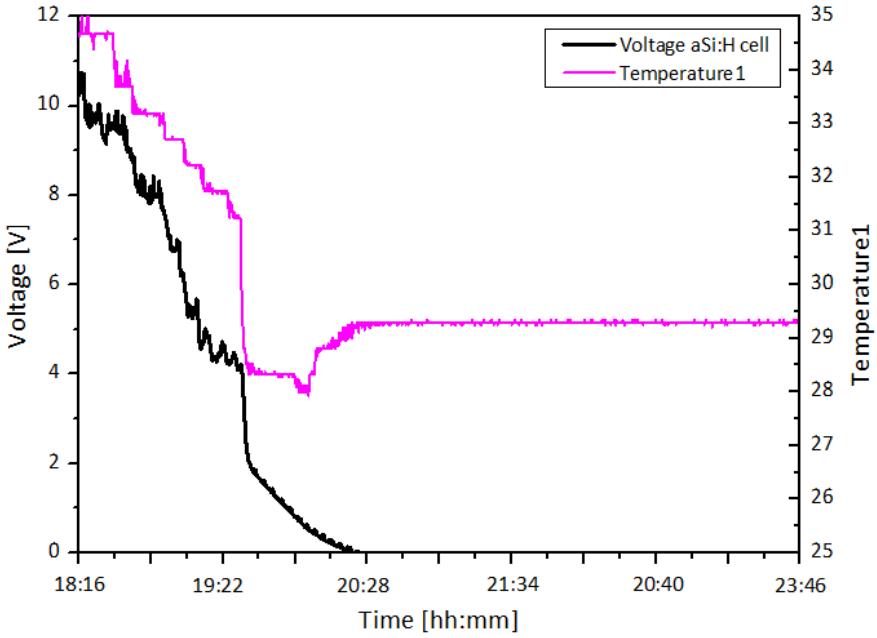

Figure 8.18. Representation of aSi:H solar cell voltage and room temperature of Ni-MH 10V rechargeable circuit measured by Arduino. (Source: Own Elaboration)

As can be seen in Fig.8.19, the registered data by Fluke45 show the discharge of the battery while is giving energy to the Arduino platform. It is notice because of the value and fluctuation of the current given. As seen in section 7, Arduino requires different current depending of the part of program it is executing. Moreover, also can be seen in Fig.8.20 some peaks at 0,03 A that reflect the shorter periods of delay and longer periods at 0,043 A corresponding with the execution and measure done by the program.

That is why the battery discharge while the flux of current decreases until zero. Then, the next day can be appreciated the new growing of voltage in terminals of the battery but it is not sufficient to recharge it either to restart the Arduino's measures.

In figure 8.20, can be observed the fluctuation due to the written program in Arduino system. It also makes vary the voltage in terminals of the battery.

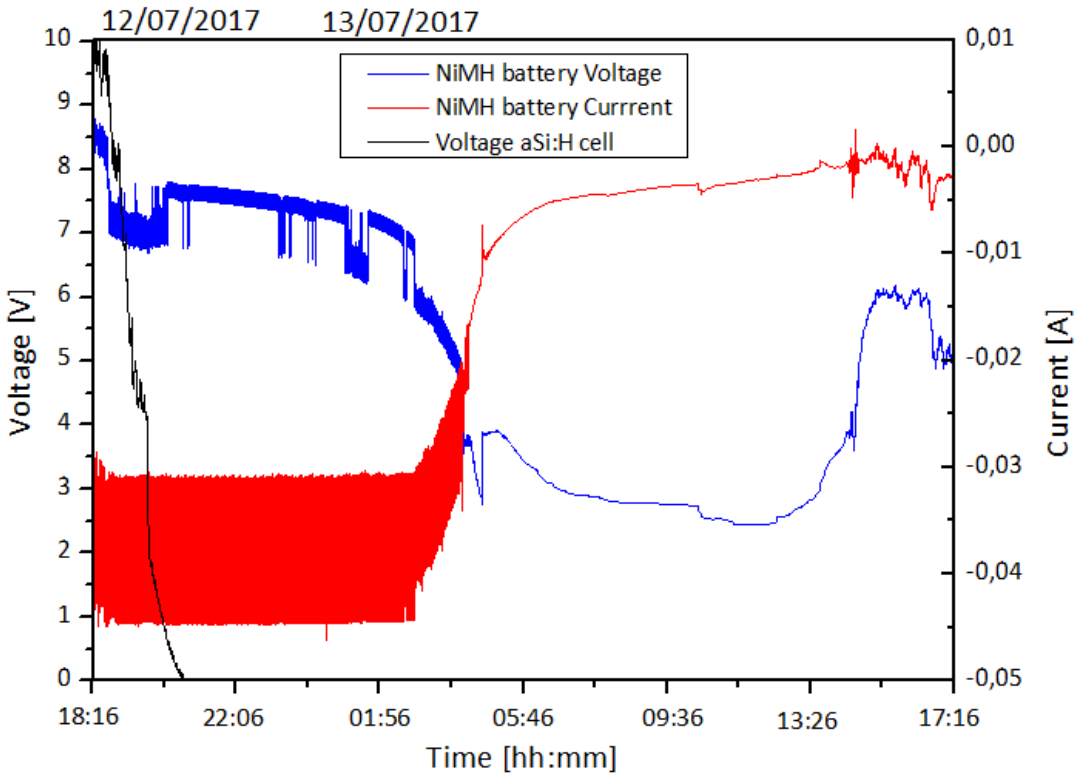

Figure 8.19. Representation Fluke45 measures of the voltage and current of Ni-MH 10V rechargeable battery supplied by the aSi:H solar cell. (Source: Own Elaboration)

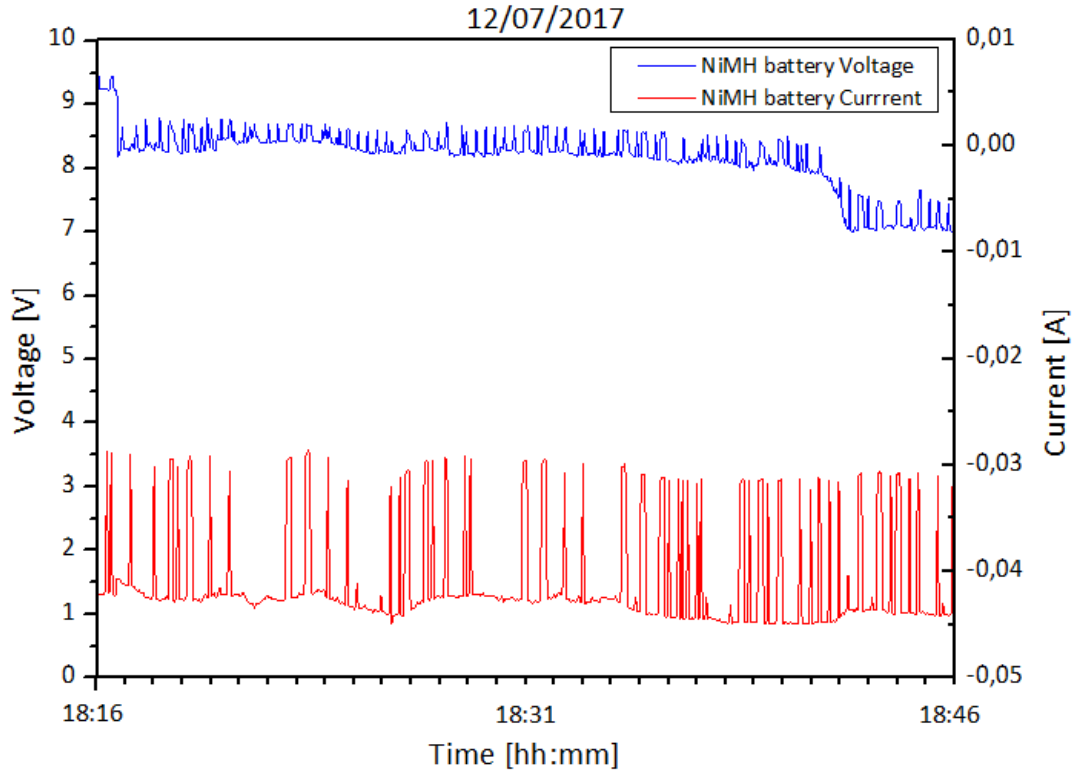

Figure 8.20. Zoom in figure 8.19 (Source: Own Elaboration)

Conclusions

At the end of this thesis there are some important conclusions that can be extracted from the analysis and execution of every designed circuit along this period.

First of all, the importance of the location and orientation of the solar cell array is well understood, as well as the inclination of it for a major capture of the solar radiation over the time. Also, pollution and clouds influence strongly on solar cell performance are really determining the energy production.

Moreover, the value of the bandgap decides the range of irradiance wavelength that solar cells can absorb, so, the more is the bandgap value the more is the range wavelength range of irradiance that solar cell can absorb. The bandgap of Amorphous Silicon solar cell has a bigger value 1,7 eV compared with the 1,1 eV of Polycrystalline Silicon but as seen in the representation of Sunlight spectrum this difference in not really important in this case, because with also 1,1 eV bandgap can absorb the majority of the more relevant wavelengths. Another important aspect is the "filter" effect of irradiance absorption by chemical elements in the solar atmosphere.

Comparing the main theoretical and experimental measures of electrical characteristics of both solar cells, it is strongly notice the importance of extrapolate the experimental data to the STC in order to do a better comparison between them, because as can be seen in the results in the thesis, the FF theoretical value differs from the experimental ones. However, can be observed that the most efficient solar cell between both versions, is the Polycrystalline Silicon solar cell since both generate the same current but the size of Amorphous Silicon cell is more than twice pc-Si cell size. Although, is the Amorphous Silicon cell which fits better charging the battery and also supplying power to Arduino system because of working voltage cell. In addition, for a same I_M's value, the V_M's values of the Amorphous Silicon cell are three times the $V_{M,}$'s values of polycrystalline Silicon cell. V_{oc}'s values also tripled, therefore the area under the I-V curve is major for the cell of Amorphous Silicon. Moreover, it is important that dark current is much lower in case of aSi:H solar cell.

After the research carried out to obtain the supply of an autonomous embedded system of measure for the characterization of low-power solar cells, the main conclusion is that the selection and of each component of the autonomous circuit needs to be studied in order to reduce losses in midstream components of the circuit and also guarantee the energy necessary to the correct operation of each component.

Between both technologies of batteries, it might be concluded with the Ni-MH technology because it is a much clean internal system than Ni-Cd and also shows a more stable operation.

With the selected elements that form the final circuit is possible the monitoring of data testing through the supply of Arduino system over a morning, but the monitoring has not been achieved neither the

recharge of the 10V battery after a complete discharge. For that reason, and since the project is limited in time, proposals for improving this project in future could be to change ArduinoUNO for any other Arduino as ArduinoNANO because of his lower consume, also to change the Amorphous Silicon solar for a bigger Polycrystalline Silicon solar cell, to calculate carefully the divider of voltage for the voltage regulator LM2953IN and to embed a Ni-MH battery because it is a much clean internal system than Ni-Cd and also shows a more stable operation. Also, could be interesting to create a system which allows the concentration of the incident radiation on the solar cells.

Finally, another very important conclusion that I could have extracted after the investigation of these 6 months is that any type of work of investigation needs of an important previous period of preparation. Whereas it is true that in this type projects can exist erroneous hypotheses, a previous preparation is important though it is erroneous, to be able to save time and extract a few good conclusions on the objectives.

Bibliography

[1] K. Properties and S. Radiation, "Key Properties of Solar Radiation," in *Photovoltaics:System Design and Practice*, 2012, p. Page 27-77.

[2] J. de la Hoz, "Dossier de la Analítica Antiaging." Barcelona, pp. 4–8.

[3] "Solar Orbit," *Green Rhino Energy website*, 2013. [Online]. Available: http://www.greenrhinoenergy.com/solar/radiation/solarorbit.php. [Accessed: 16-Jul-2017].

[4] G. González, J. W. Richards, and J. W. Richards, *El planeta privilegiado : cómo nuestro hogar en el cosmos está diseñado para el descubrimiento*. Palabra, 2006.

[5] E. A. Gibson and A. Hagfeldt, "Solar Energy Materials," in *Energy Materials*, 2011, pp. 95–243.

[6] L. Partain and L. Fraas, "Solar Cell electricity market history, public policy, projected future, and estimated costs," in *Solar Cells and their Applications: Second Edition*, 2007, pp. 17–42.

[7] "Energía solar: ventajas e inconvenientes." [Online]. Available: http://www.energiasrenovablesinfo.com/solar/energia-solar-ventajas-inconvenientes/. [Accessed: 16-Jul-2017].

[8] A. L. Fahrenbruch and R. H. Bube, "Fundamentals of Solar Cells," in *Designing Indoor Solar Products*, 1983, pp. 161–244.

[9] "Definición de conductividad - Qué es, Significado y Concepto." [Online]. Available: http://definicion.de/conductividad/. [Accessed: 16-Jul-2017].

[10] H. W. Goetzberger, A.; Hebling, C.; Schock, "Photovoltaic materials. History, status and outlook," *Mater. Sci. Eng. R*, vol. 40, no. 1, pp. 1–46, 2003.

[11] J. Pérez Porto and M. Merino, "Definición de silicio - Qué es, Significado y Concepto," *2010*, 2012. [Online]. Available: http://definicion.de/silicio/. [Accessed: 17-Jul-2017].

[12] "Russell Ohl - ETHW," 2016. [Online]. Available: http://ethw.org/Russell_Ohl. [Accessed: 17-Jul-2017].

[13] Alejandro, "Historia: La crisis del petróleo de 1973 | Blog de www.empleospetroleros.com," *Historia:La crisis del petróleo de 1973*, 2012. [Online]. Available: https://empleospetroleros.org/2012/11/15/historia-la-crisis-del-petroleo-de-1973/. [Accessed: 17-Jul-2017].

[14] Y. S. Tsuo, T. H. Wang, and T. F. Ciszek, "Crystalline-Silicon Solar Cells for the 21st Century," in *The Electrochemical Society Annual Meeting*, 1999, no. May, pp. 1–8.

[15] X. Deng and E. A. A. Schiff, "Amorphous silicon based solar cells," in *Handbook of Photovoltaic Science and Engineering*, 2003, pp. 505–565.

[16] Semiconductor National, "Lm35," *Data Sheet*, no. November, p. 13, 2000.

Index of Figures

Annex A

A1. ArduinoUNO Programme

```
#include <RTClib.h>
#include <Wire.h>
#include <SD.h>

RTC_DS1307 rtc;
File dataFile1;

char daysOfTheWeek[7][12] = {"Sunday", "Monday", "Tuesday", "Wednesday", "Thursday", "Friday", "Saturday"};
int VoltagePin = A0;
int TemperaturePin1 = A1;
int TemperaturePin2 = A2;


float VoltagePinValue = 0;
float TemperaturePin1Value = 0;
float TemperaturePin2Value = 0;

float VoltageValue = 0;
float TemperatureValue1 = 0;
float TemperatureValue2 = 0;


const int chipSelect = 9;
void setup() {

  Serial.begin(57600);
  if (! rtc.begin()) {
    Serial.println("Couldn't find RTC");
    while (1);
  }

  if (! rtc.isrunning()) {
    Serial.println("RTC is NOT running!");
    // following line sets the RTC to the date & time this sketch was compiled
    //rtc.adjust(DateTime(__DATE__, __TIME__));
    // This line sets the RTC with an explicit date & time, for example to set
    //January 21, 2014 at 3am you would call:
    // rtc.adjust(DateTime(2017, 3, 30, 17, 14, 0));
  }

   Serial.print("Initializing SD card...");

  if (!SD.begin(chipSelect)) {
    Serial.println("Couldn't find SD Card ");
    return;
  }
  Serial.println("SD Card Initialized.");
```

```
  // put your setup code here, to run once:
dataFile1 = SD.open("MPS.txt", FILE_WRITE);
  if (dataFile1){
  dataFile1.println(F("      Time                                    Voltage Value[V]                Temperature1       Temperature2"));
  dataFile1.println(F("-------------------------------------------------------------------------------------------------------------------------------"));
    dataFile1.println();

  dataFile1.close();
  }

}

void loop() {

// RTC code ____________________________________________________________
   DateTime now = rtc.now();

     DateTime future (now + TimeSpan(0,1,0,0));
File dataFile1 = SD.open("MPS.txt", FILE_WRITE);


     dataFile1.print(now.day(), DEC);
     dataFile1.print('/');
     dataFile1.print(now.month(), DEC);
     dataFile1.print('/');
     dataFile1.print(now.year(), DEC);
     dataFile1.print(" (");
     dataFile1.print(daysOfTheWeek[now.dayOfTheWeek()]);
     dataFile1.print(") ");
     dataFile1.print(future.hour(), DEC);
     dataFile1.print(':');
     dataFile1.print(now.minute(), DEC);
     dataFile1.print(':');
     dataFile1.print(now.second(), DEC);
     dataFile1.print("                        ");


     Serial.print(now.year(), DEC);
     Serial.print('/');
     Serial.print(now.month(), DEC);
     Serial.print('/');
     Serial.print(now.day(), DEC);
     Serial.print(" (");
     Serial.print(daysOfTheWeek[now.dayOfTheWeek()]);
     Serial.print(") ");
     Serial.print(future.hour(), DEC);
     Serial.print(':');
     Serial.print(now.minute(), DEC);
     Serial.print(':');
     Serial.print(now.second(), DEC);
     Serial.println();

 //  Voltage code_____________________________________________________

float sum1=0;
float average_VR2=0;
float V_Out=0.0;
int i=0;
float sampels=10;
float R2=99.5;
float R1=560;
for(i=0;i<sampels;i++)
```

```
 //  Voltage code_____________________________________________________________

float sum1=0;
float average_VR2=0;
float V_Out=0.0;
int i=0;
float sampels=10;
float R2=99.5;
float R1=560;
for(i=0;i<sampels;i++)
{
  analogRead(VoltagePin);
  delay(100);
VoltagePinValue = analogRead(VoltagePin);
VoltageValue = (VoltagePinValue/1023.000)*5.000;
sum1=sum1 + VoltageValue;
delay(200); //delay between two values
}
average_VR2= (sum1/sampels);
V_Out=average_VR2*(R1+R2)/R2;
sum1=0;

Serial.println(V_Out);
dataFile1.print(V_Out);
//_____________________________________________________________________________


float sum2=0.00;
float average_Temp=0.00;
float celsius;
for(i=0;i<sampels;i++)
{
  analogRead(TemperaturePin1);
  delay(100);
TemperaturePin1Value = analogRead(TemperaturePin1);
TemperatureValue1 = ( TemperaturePin1Value/1024.00)*5000.00; // value of temperature directly in mV
celsius =TemperatureValue1/10.00; // Value of temperature in Celsius degrees
sum2=sum2 + celsius;
delay(200); //ritardo tra due campionature successive
}
average_Temp= (sum2/sampels); //calcolo del valore medio di n sampels
sum2=0; // riazzeramento della variabile somma
     dataFile1.print("                      ");
     dataFile1.print(average_Temp);

Serial.print(average_Temp);Serial.println(" C");

  dataFile1.print("       ");
```

```
float sum3=0.00;
float average_Temp2=0.00;
float celsius2;
for(i=0;i<sampels;i++)
{
analogRead(TemperaturePin2);
  delay(100);
TemperaturePin2Value = analogRead(TemperaturePin2);
celsius2 = ( TemperaturePin2Value/1024.00)*500.00; // Value of temperature in Celsius degrees
sum3=sum3 + celsius2;
delay(200); //ritardo tra due campionature successive
}
average_Temp2= (sum3/sampels); //calcolo del valore medio di n sampels
sum3=0; // riazzeramento della variabile somma
     dataFile1.print("                        ");
     dataFile1.print(average_Temp2);

Serial.print(average_Temp2);Serial.println(" C");

  dataFile1.println();
```

A2. Images of each implemented circuit

- **Section 5**

- **Section 6**

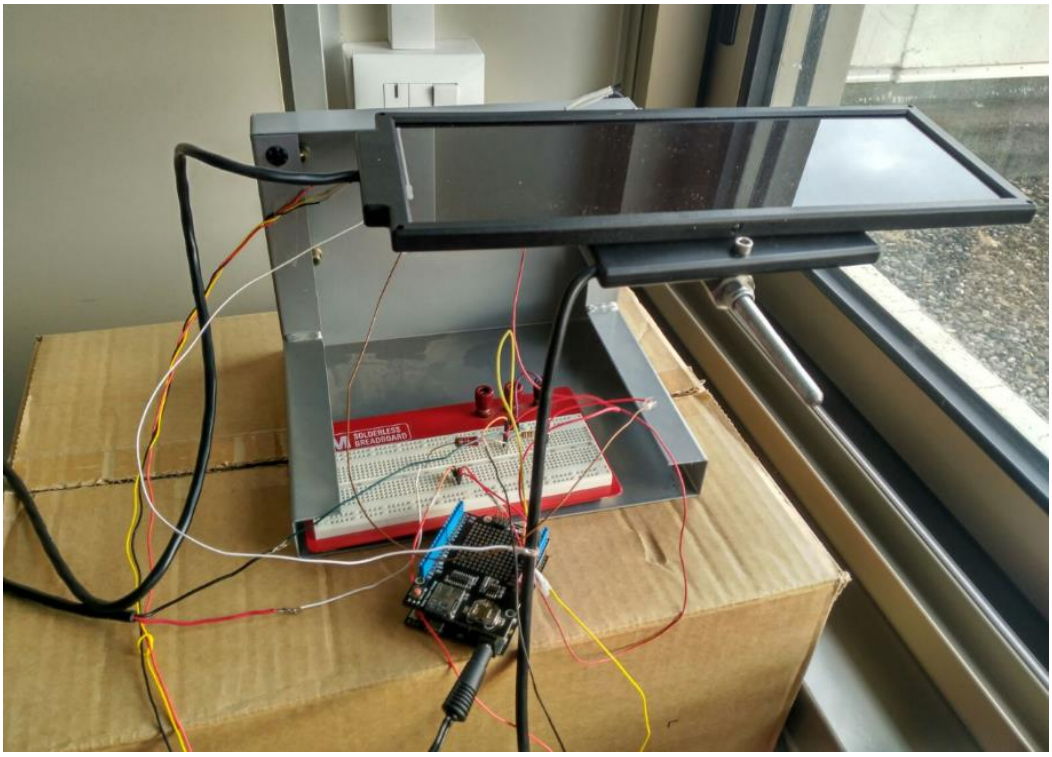

- **Section 7**

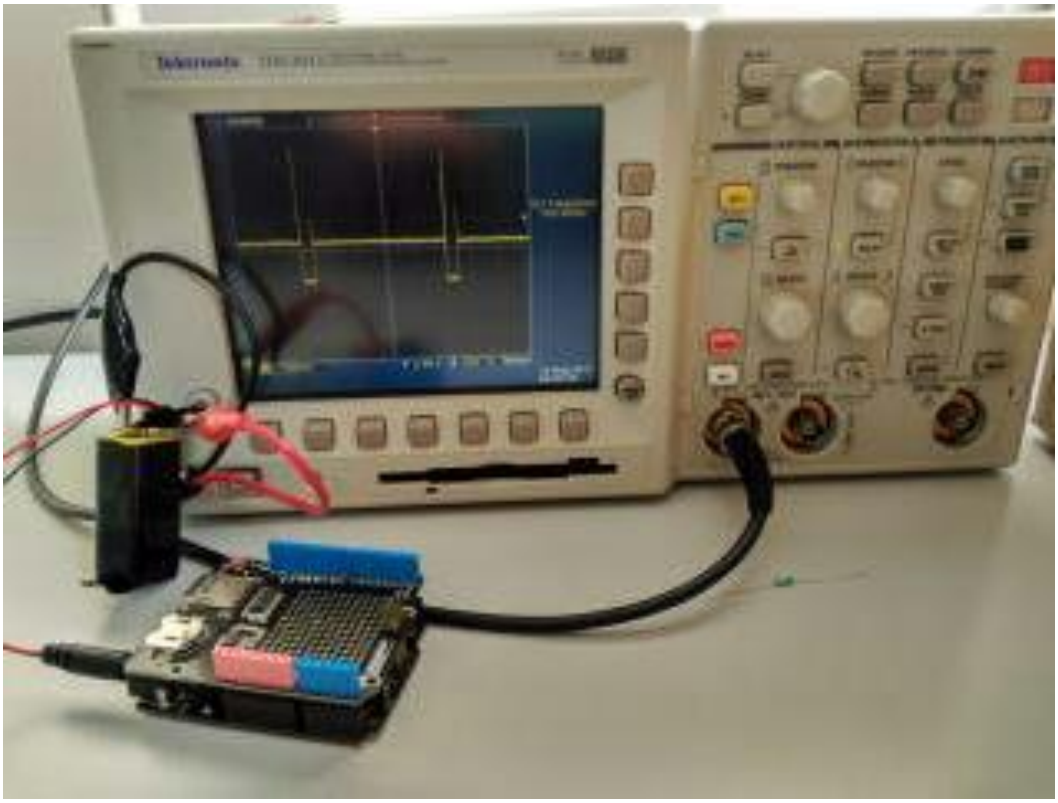

- **Section 8**

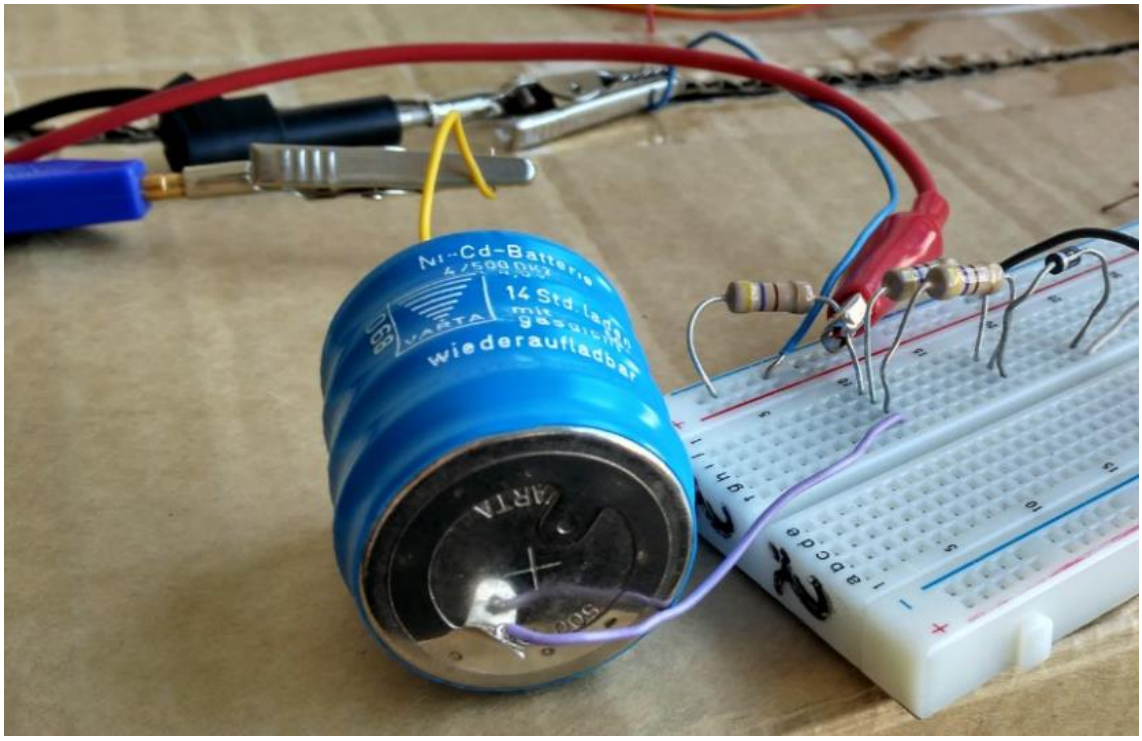

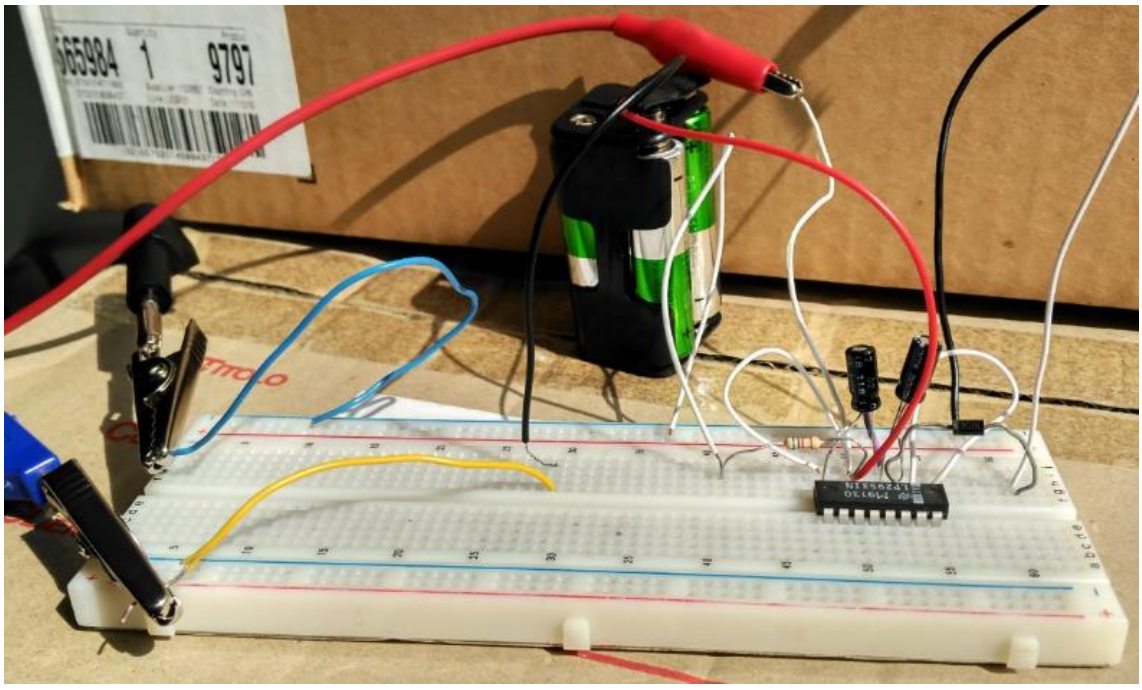

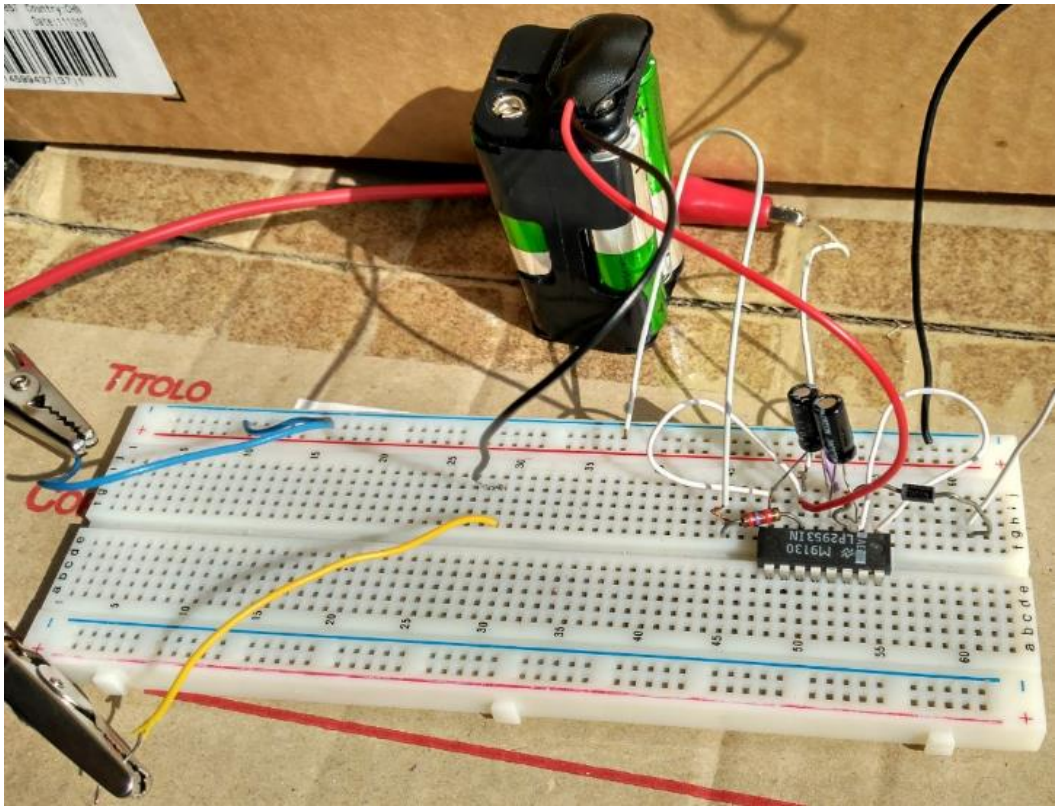
TITOLO
M9130
LP2953N

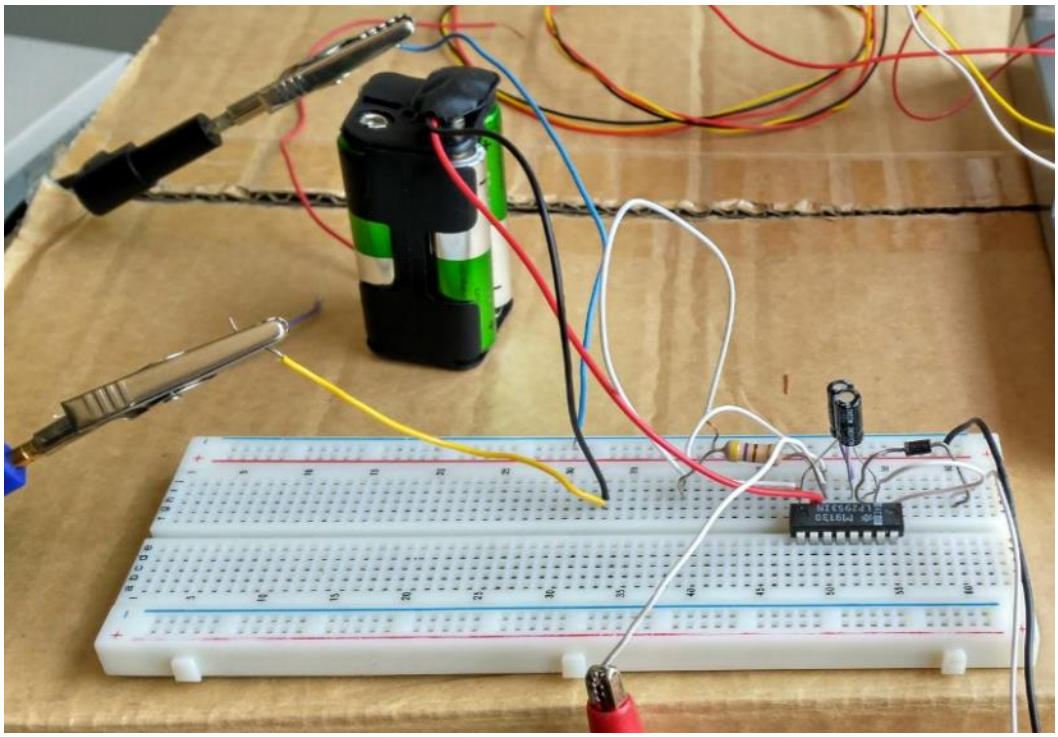

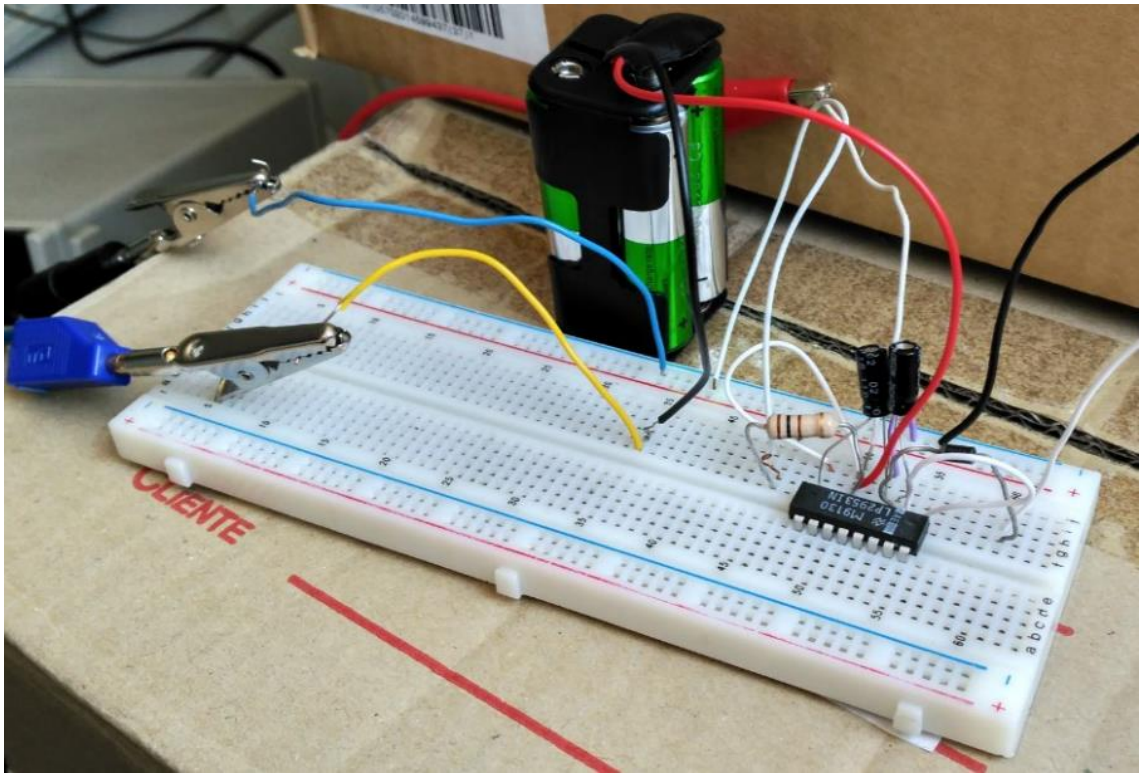
OLIENTE

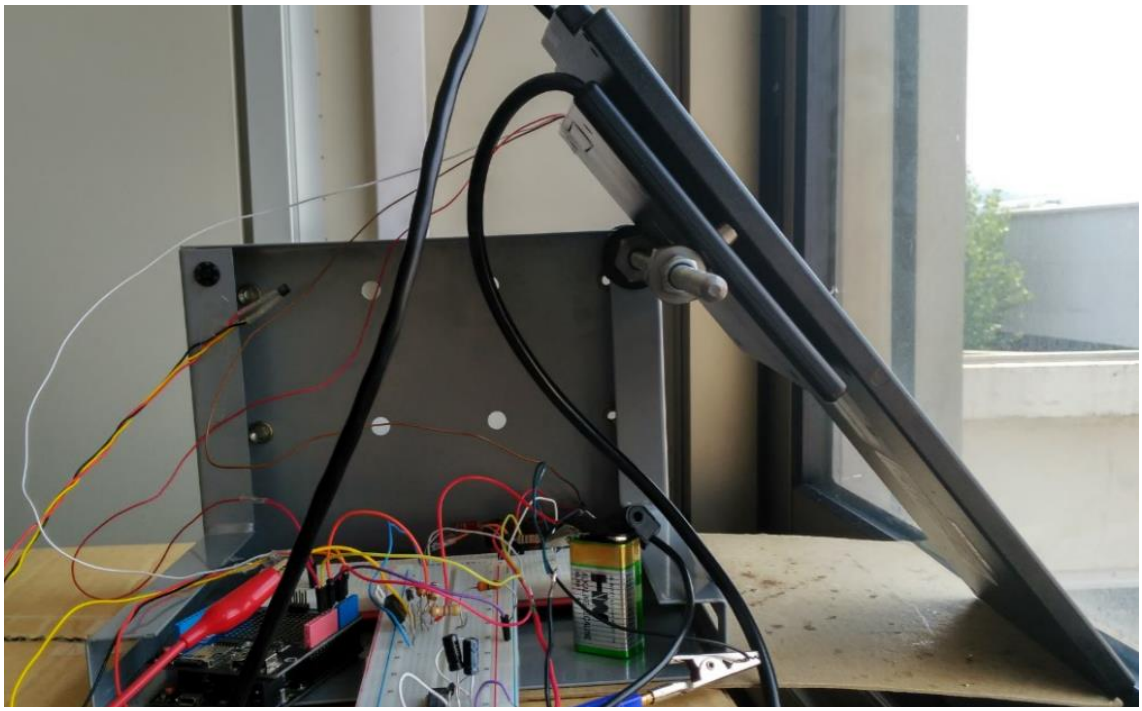

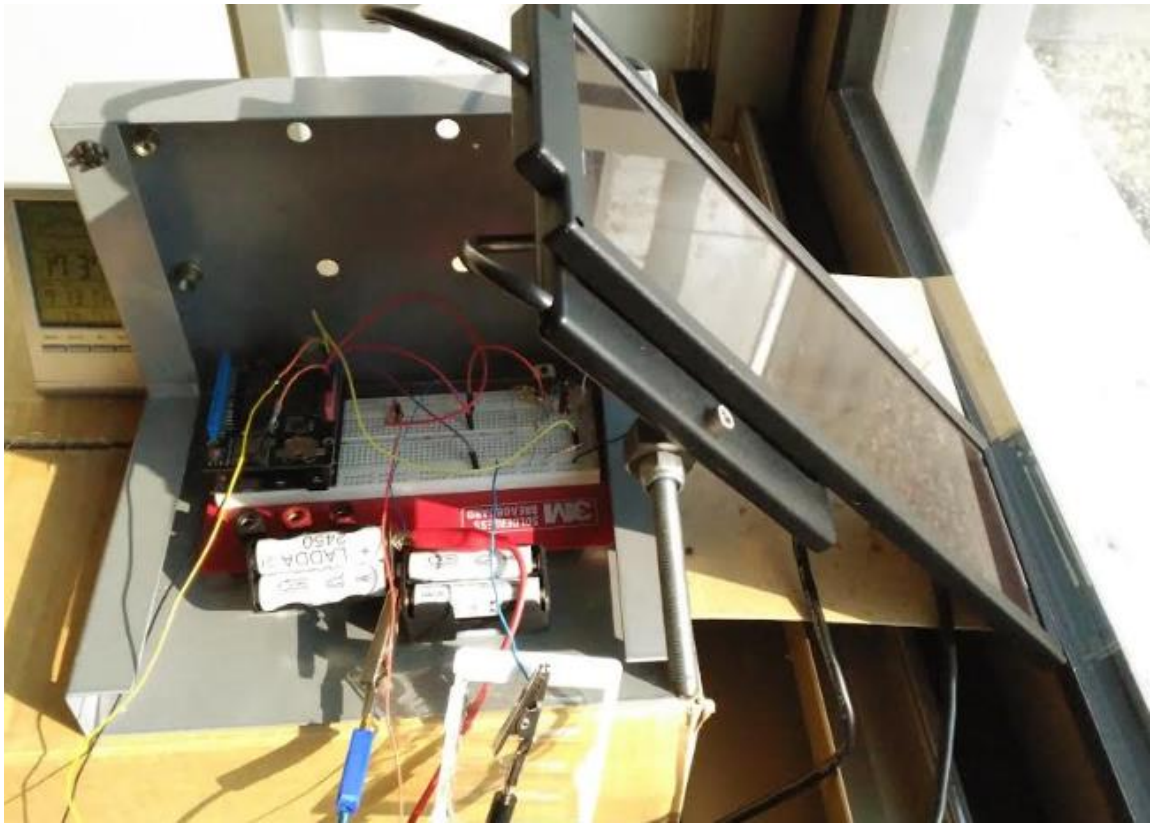

A3. Data Sheets

The following are typical configurations for absorbance, transmission, irradiance, and reflection experiments.

1.4 Measurement Setup

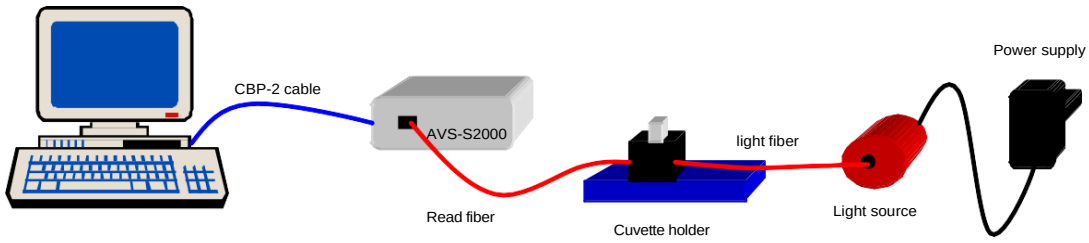

Absorbance/Transmission Setup

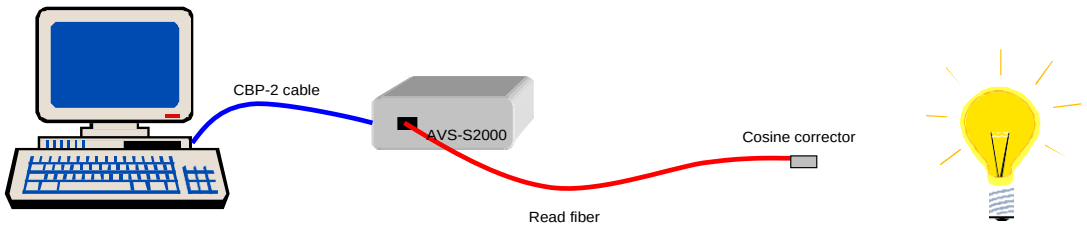

Irradiance Setup

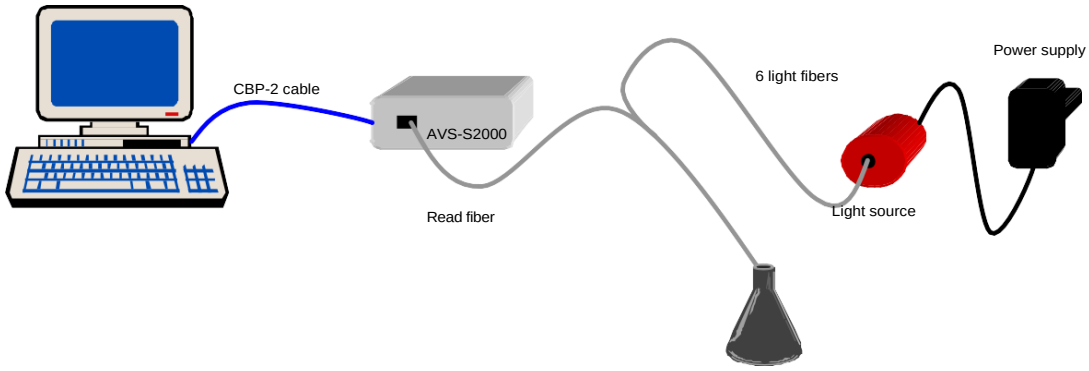

Reflection / Dip-probe Setup

AVS-PC-2000 Plug-in spectrometer

The AVS-PC2000 plug-in spectrometer is a combination of the AVS-S2000 and ADC1000. Most technical data can be found in either chapter 2.1 AVS-S2000 or in chapter 3.1 ADC-1000.
The table below gives the H1 header 1 connection pin outs, the J2 (D-sub-15) connector pin outs are given under 2.1.2.

H1 Header Block connecting Master to other Slaves

Pin	Description
1	Analog Channel 1 (slave1)
2	Analog Channel 2
3	Analog Channel 3
4	Analog Channel 4
5	Analog Channel 5
6	Analog Channel 6
7	Analog Channel 7
8	GND
9	GND
10	S0
11	Reserved
12	Multiple Strobe
13	Single Strobe
14	Reserved
15	F read (ROG)
16	F clock

2.3.2 AVS-USB2000

Absolute Maximum Ratings

Vcc	8,0 VDC
Voltage on any pin	7,0 VDC

Physical Specifications

Physical dimensions (no enclosure)	89 x 64 x 34 mm LWH
Weight	200 g (without cable), 270 grams with cable

Power

Power requirement	100 mA at +5 VDC
Supply voltage	3,9 – 8,0 V

Spectrometer

Design	asymmetric crossed Czerny-Turner
Focal length (input)	42 mm
Focal length (output)	68 mm
Input fiber connector	SMA 905
Gratings	14 different gratings
Optional Entrance slit	5, 10, 25, 50, 100, or 200 µm slits. (In the absence of a slit, the fiber acts as the entrance slit.)
Detector	Sony ILX511 CCD
Optional Filters	2nd order rejection, long pass (optional)
Optional Collection lens	Cylindrical lens improves light-collection efficiency by ~5x
Optional Sorting coatings	Blocks 2nd and 3rd order effects for grating #1,#2 only
Optional UV detector upgrade	Detector upgrade for enhanced sensitivity in UV < 360nm

Spectroscopic

Integration time	3 – 60 seconds
Dynamic range	2 x 10^{8}
Signal-to-Noise	250:1 single acquisition
Readout noise single dark spectrum)	(3.5 counts RMS, 20 counts peak-to-peak
Resolution (FWHM)	0.3 – 10.0 nm varies by configuration
Stray light	<0,05% at 600 nm; <0,10% at 435 nm

Environmental Conditions

Temperature
-30°C to +70°C Storage; -10°C to +50°C Operation

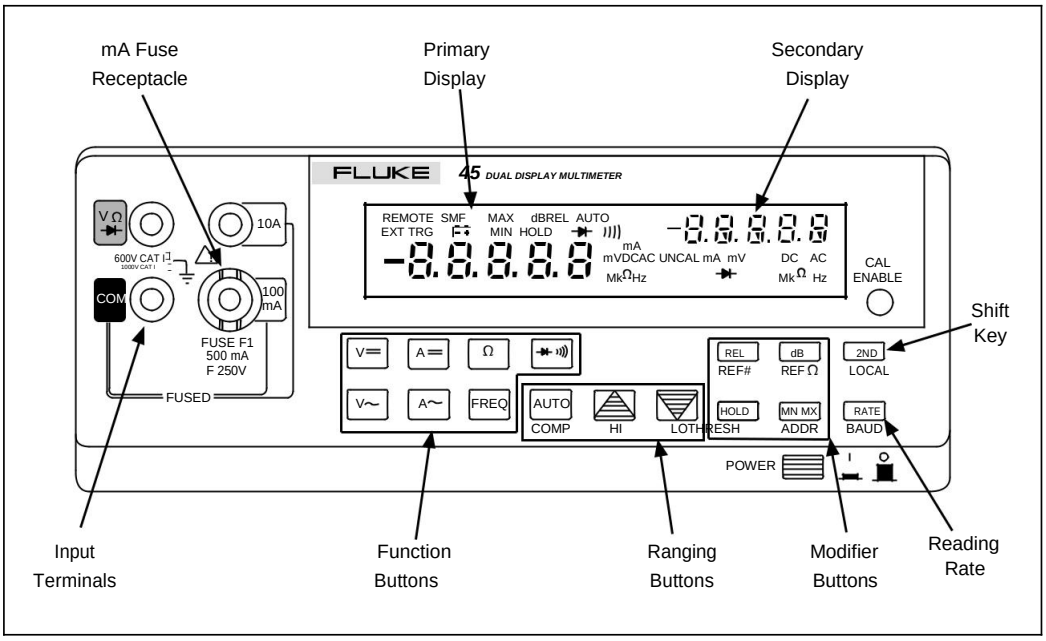

aam01f.eps

Figure 2-1. Front Panel

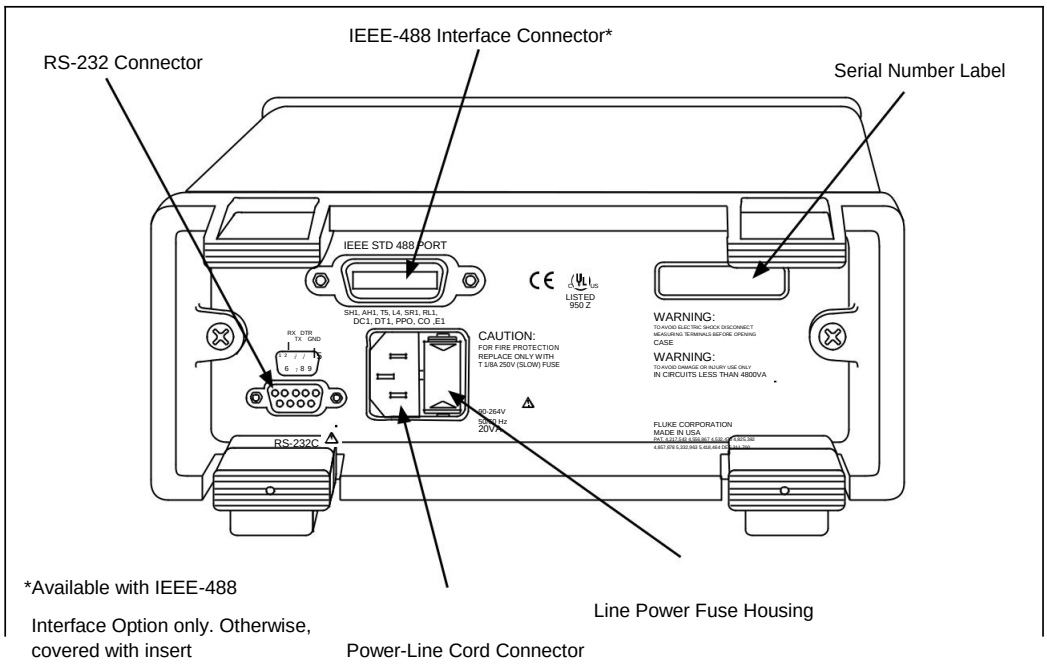

aam02f.eps

Figure 2-2. Rear Panel

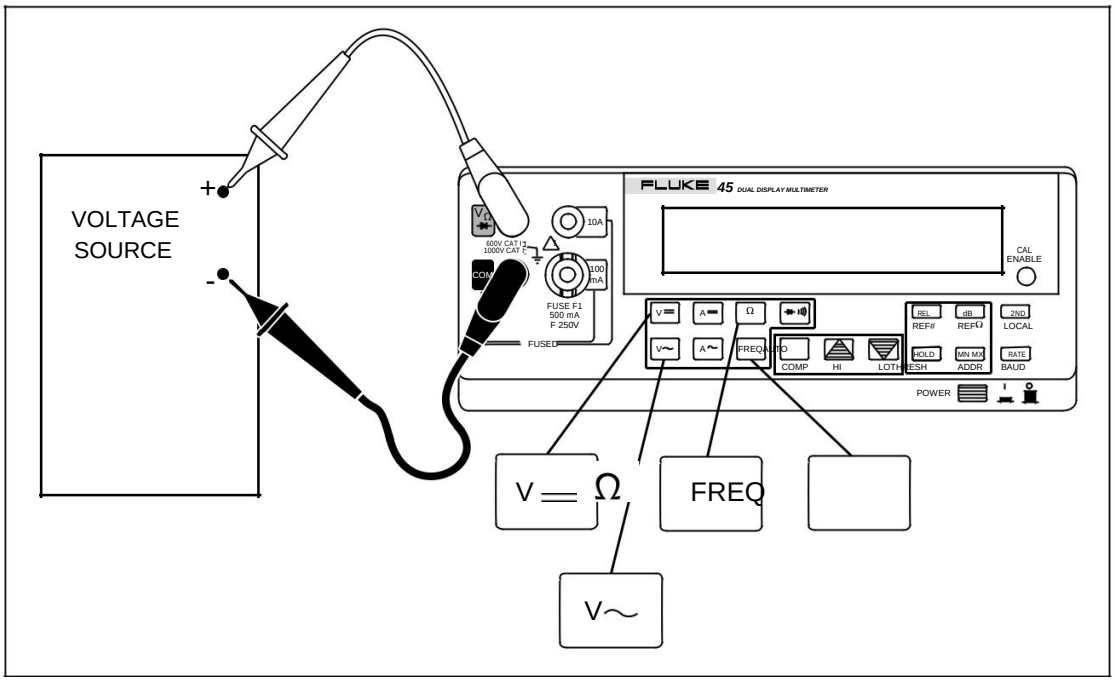

aam05f.eps

Figure 2-5. Measuring Voltage, Resistance, or Frequency

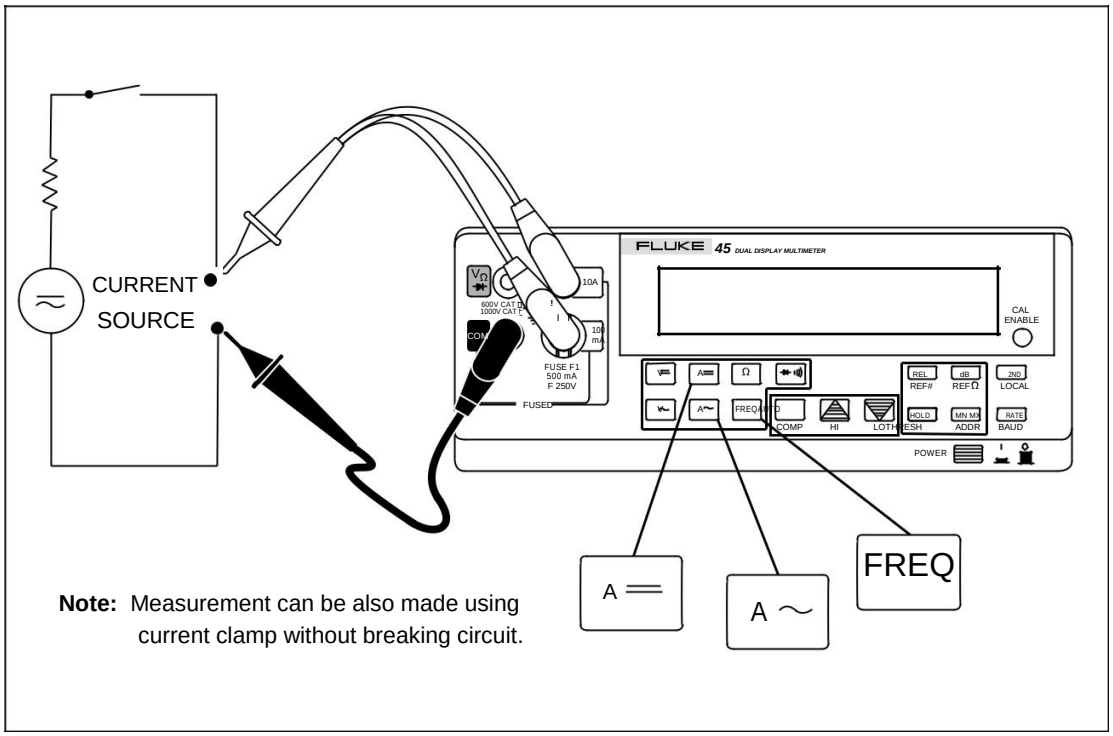

aam06f.eps

Figure 2-6. Measuring Current or Frequency

Neither function modifiers (REL, dB, HOLD, and MN MX) nor the manual range mode can be selected in the secondary display. Measurement ranges in the secondary display are always selected through autoranging.

Input Terminals

The input terminals, shown in Figure 3-4, are located on the left of the front panel.

The meter is protected against overloads up to the limits shown in Table 3-1. Exceeding these limits poses a hazard to both the meter and operator.

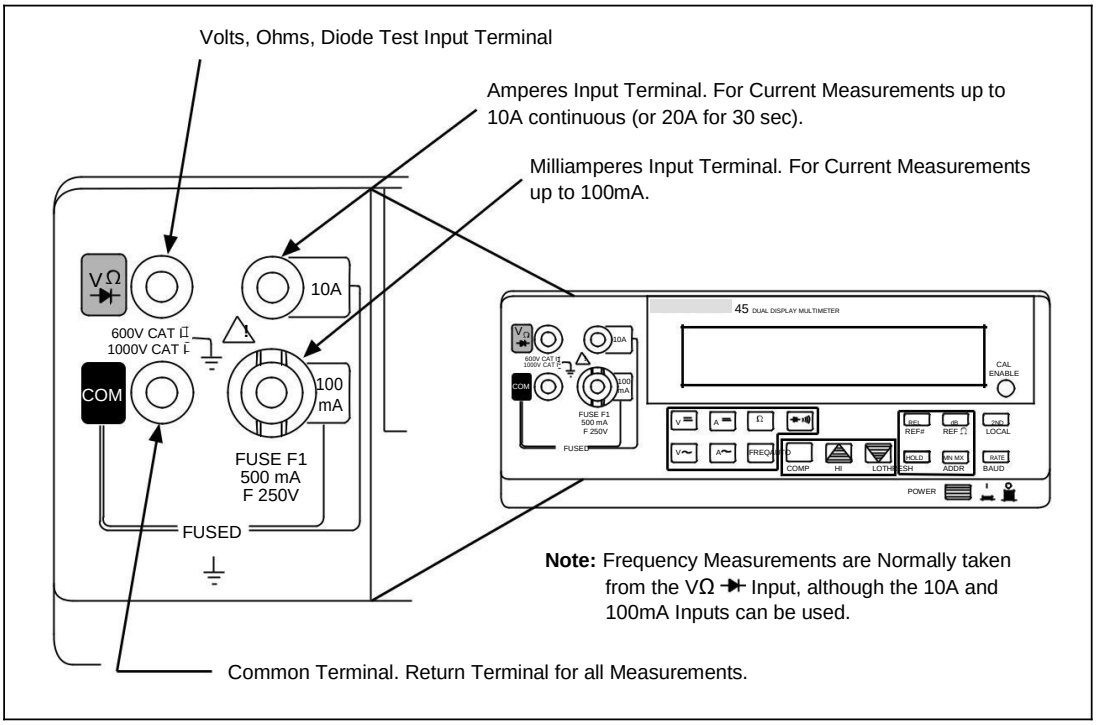

aam12f.eps

Figure 3-4. Input Terminals

LM217, LM317

1.2 V to 37 V adjustable voltage regulators

Datasheet - production data

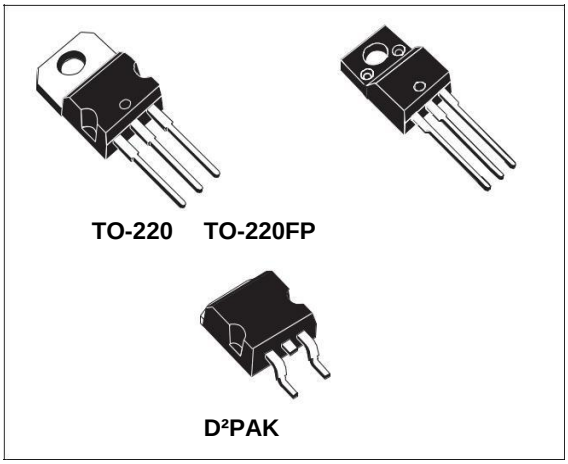

Description

The LM217, LM317 are monolithic integrated circuits in TO-220, TO-220FP and D²PAK packages intended for use as positive adjustable voltage regulators. They are designed to supply more than 1.5 A of load current with an output voltage adjustable over a 1.2 to 37 V range. The nominal output voltage is selected by means of a resistive divider, making the device exceptionally easy to use and eliminating the stocking of many fixed regulators.

Features

- Output voltage range: 1.2 to 37 V
- Output current in excess of 1.5 A
- 0.1 % line and load regulation
- Floating operation for high voltages
- Complete series of protections: current limiting, thermal shutdown and SOA control

Table 1. Device summary

Order codes			
TO-220 (single gauge)	**TO-220 (double gauge)**	**D²PAK (tape and reel)**	**TO-220FP**
LM217T	LM217T-DG	LM217D2T-TR	
LM317T	LM317T-DG	LM317D2T-TR	LM317P
LM317BT			

1 Pin configuration

Figure 1. Pin connections (top view)

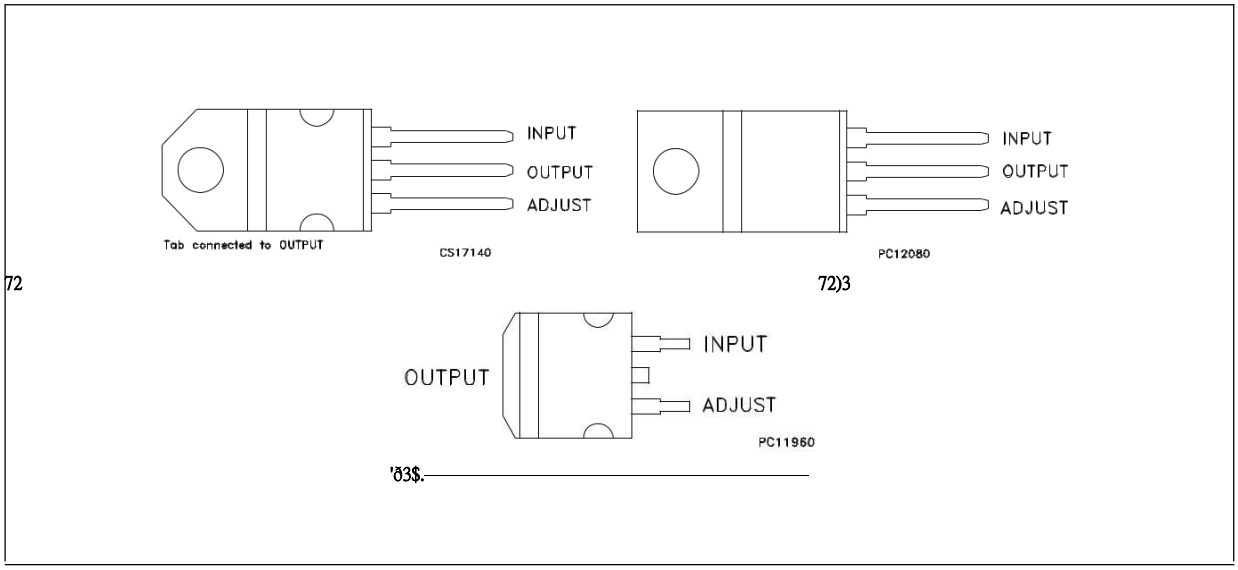

2 Maximum ratings

Table 2. Absolute maximum ratings

Symbol	Parameter		Value	Unit
$V_I - V_O$	Input-reference differential voltage		40	V
I_O	Output current		Internally limited	A
T_{OP}	Operating junction temperature for:	LM217	- 25 to 150	°C
		LM317	0 to 125	
		LM317B	-40 to 125	
P_D	Power dissipation		Internally limited	
T_{STG}	Storage temperature		- 65 to 150	°C

Note: Absolute maximum ratings are those values beyond which damage to the device may occur.
Functional operation under these condition is not implied.

Table 3. Thermal data

Symbol	Parameter	D²PAK	TO-220	TO-220FP	Unit
R_{thJC}	Thermal resistance junction-case	3	5	5	°C/W
R_{thJA}	Thermal resistance junction-ambient	62.5	50	60	°C/W

4 Electrical characteristics

V_I - V_O = 5 V, I_O = 500 mA, I_{MAX} = 1.5 A and P_{MAX} = 20 W, T_J = - 55 to 150 °C, unless otherwise specified.

Table 4. Electrical characteristics for LM217

Symbol	Parameter	Test conditions		Min.	Typ.	Max.	Unit
V_O	Line regulation	V_I - V_O = 3 to 40 V	T_J = 25°C		0.01	0.02	%/V
					0.02	0.05	
V_O	Load regulation	V_O ≤5 V I_O = 10 mA to I_{MAX}	T_J = 25°C		5	15	mV
					20	50	
		V_O ≥5 V, I_O = 10 mA to I_{MAX}	T_J = 25°C		0.1	0.3	%
					0.3	1	
I_{ADJ}	Adjustment pin current				50	100	µA
I_{ADJ}	Adjustment pin current	V_I - V_O = 2.5 to 40V I_O = 10 mA to I_{MAX}			0.2	5	µA
V_{REF}	Reference voltage	V_I - V_O = 2.5 to 40V I_O= 10 mA to I_{MAX} $P_D \geq P_{MAX}$		1.2	1.25	1.3	V
V_O/V_O	Output voltage temperature stability				1		%
$I_{O(min)}$	Minimum load current	V_I - V_O = 40 V			3.5	5	mA
$I_{O(max)}$	Maximum load current	V_I - V_O ≤ 15 V, P_D < P_{MAX}		1.5	2.2		A
		V_I - V_O = 40 V, P_D < P_{MAX}, T_J = 25°C			0.4		
eN	Output noise voltage (percentage of V_O)	B = 10Hz to 100kHz, T_J = 25°C			0.003		%
SVR	Supply voltage rejection (1)	T_J = 25°C, f = 120Hz	C_{ADJ}=0		65		dB
			C_{ADJ}=10µF	66	80		

1. C_{ADJ} is connected between adjust pin and ground.

$V_I - V_O$ = 5 V, I_O = 500 mA, I_{MAX} = 1.5 A and P_{MAX} = 20 W, T_J = 0 to 125 °C, unless otherwise specified.

Table 5. Electrical characteristics for LM317

Symbol	Parameter	Test conditions		Min.	Typ.	Max.	Unit
V_O	Line regulation	$V_I - V_O$ = 3 to 40 V	T_J = 25°C		0.01	0.04	%/V
					0.02	0.07	
V_O	Load regulation	$V_O \leq 5$ V I_O = 10 mA to I_{MAX}	T_J = 25°C		5	25	mV
					20	70	
		$V_O \geq 5$ V, I_O = 10 mA to I_{MAX}	T_J = 25°C		0.1	0.5	%
					0.3	1.5	
I_{ADJ}	Adjustment pin current				50	100	µA
I_{ADJ}	Adjustment pin current	$V_I - V_O$ = 2.5 to 40V, I_O = 10 mA to 500mA			0.2	5	µA
V_{REF}	Reference voltage (between pin 3 and pin 1)	$V_I - V_O$ = 2.5 to 40V I_O = 10 mA to 500mA $P_D \leq P_{MAX}$		1.2	1.25	1.3	V
V_O/V_O	Output voltage temperature stability				1		%
$I_{O(min)}$	Minimum load current	$V_I - V_O$ = 40 V			3.5	10	mA
$I_{O(max)}$	Maximum load current	$V_I - V_O \leq 15$ V, $P_D < P_{MAX}$		1.5	2.2		A
		$V_I - V_O$ = 40 V, $P_D < P_{MAX}$, T_J = 25°C			0.4		
eN	Output noise voltage (percentage of V_O)	B = 10Hz to 100kHz, T_J = 25°C			0.003		%
SVR	Supply voltage rejection (1)	T_J = 25°C, f = 120Hz	C_{ADJ}=0		65		dB
			C_{ADJ}=10µF	66	80		

1. C_{ADJ} is connected between adjust pin and ground.

V_I - V_O = 5 V, I_O = 500 mA, I_{MAX} = 1.5 A and P_{MAX} = 20 W, T_J = - 40 to 125 °C, unless otherwise specified.

Table 6. Electrical characteristics for LM317B

Symbol	Parameter	Test conditions		Min.	Typ.	Max.	Unit
V_O	Line regulation	V_I - V_O = 3 to 40 V	T_J = 25°C		0.01	0.04	%/V
					0.02	0.07	
V_O	Load regulation	V_O ≤ 5 V I_O = 10 mA to I_{MAX}	T_J = 25°C		5	25	mV
					20	70	
		V_O ≥5 V, I_O = 10 mA to I_{MAX}	T_J = 25°C		0.1	0.5	%
					0.3	1.5	
I_{ADJ}	Adjustment pin current				50	100	µA
I_{ADJ}	Adjustment pin current	V_I - V_O = 2.5 to 40V, I_O = 10 mA to 500mA			0.2	5	µA
V_{REF}	Reference voltage (between pin 3 and pin 1)	V_I - V_O = 2.5 to 40V I_O = 10 mA to 500mA $P_D \leq P_{MAX}$		1.2	1.25	1.3	V
V_O/V_O	Output voltage temperature stability				1		%
$I_{O(min)}$	Minimum load current	V_I - V_O = 40 V			3.5	10	mA
$I_{O(max)}$	Maximum load current	V_I - V_O ≤ 15 V, P_D < P_{MAX}		1.5	2.2		A
		V_I - V_O = 40 V, P_D < P_{MAX}, T_J = 25°C			0.4		
eN	Output noise voltage (percentage of V_O)	B = 10Hz to 100kHz, T_J = 25°C			0.003		%
SVR	Supply voltage rejection (1)	T_J = 25°C, f = 120Hz	C_{ADJ}=0		65		dB
			C_{ADJ}=10µF	66	80		

1. C_{ADJ} is connected between adjust pin and ground.

5 Typical characteristics

Figure 3. Output current vs. input-output differential voltage

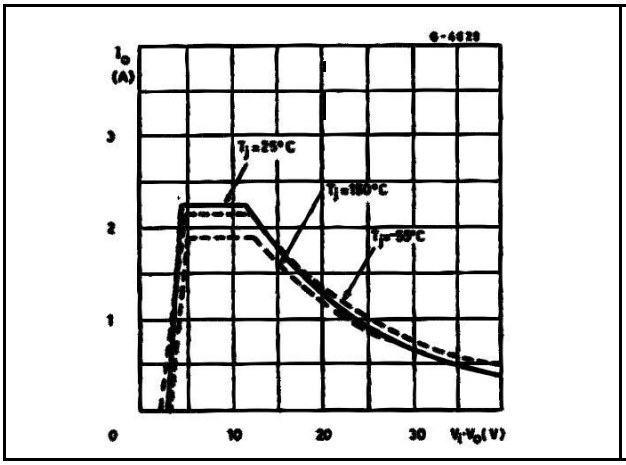

Figure 4. Dropout voltage vs. junction temperature

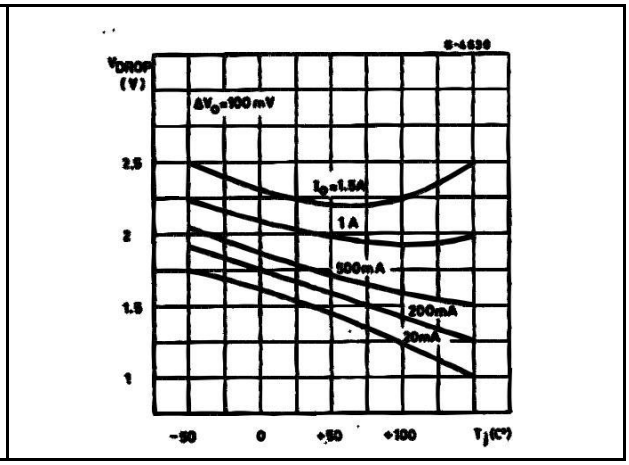

Figure 5. Reference voltage vs. junction

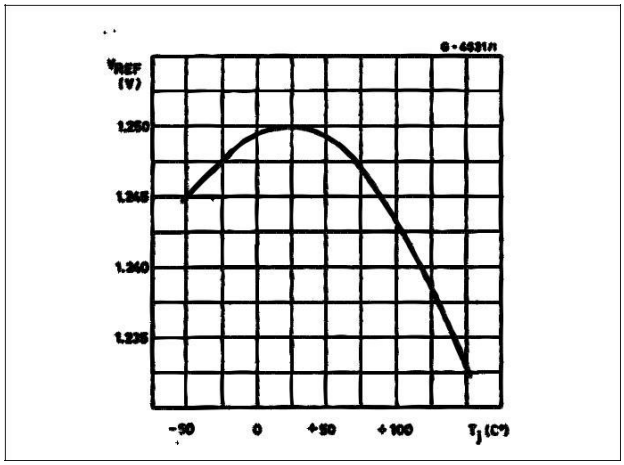

Figure 6. Basic adjustable regulator

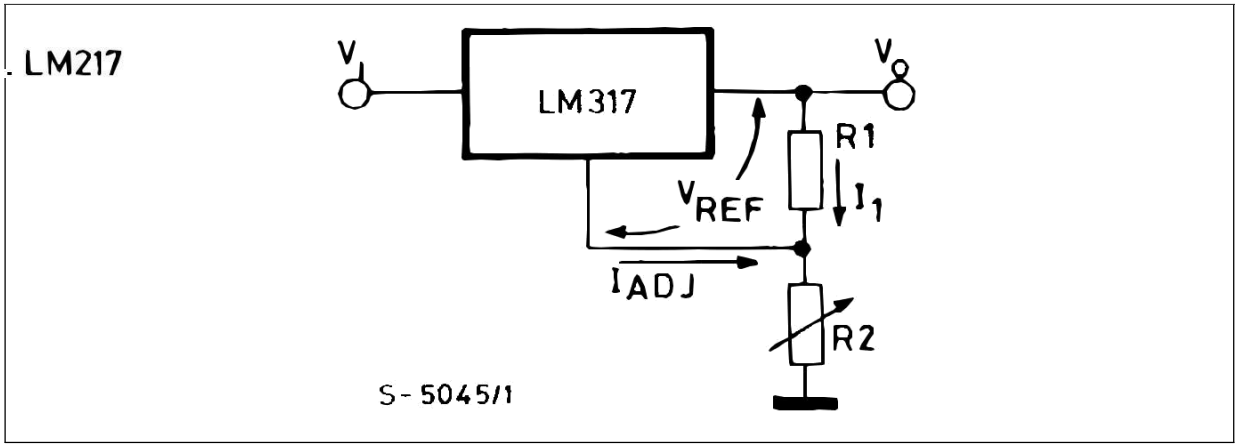

March 2005

National Semiconductor

LP2952/LP2952A/LP2953/LP2953A
Adjustable Micropower Low-Dropout Voltage Regulators

General Description

The LP2952 and LP2953 are micropower voltage regulators with very low quiescent current (130 µA typical at 1 mA load) and very low dropout voltage (typ. 60 mV at light load and 470 mV at 250 mA load current). They are ideally suited for battery-powered systems. Furthermore, the quiescent cur-rent increases only slightly at dropout, which prolongs bat-tery life.

The LP2952 and LP2953 retain all the desirable character-istics of the LP2951, but offer increased output current, additional features, and an improved shutdown function.

The internal crowbar pulls the output down quickly when the shutdown is activated.

The error flag goes low if the output voltage drops out of regulation.

Reverse battery protection is provided.

The internal voltage reference is made available for external use, providing a low-T.C. reference with very good line and load regulation.

The parts are available in DIP and surface mount packages.

Features

V Output voltage adjusts from 1.23V to 29V
n Guaranteed 250 mA output current
n Extremely low quiescent current
n Low dropout voltage
n Extremely tight line and load regulation
n Very low temperature coefficient
n Current and thermal limiting
n Reverse battery protection
n 50 mA (typical) output pulldown crowbar
n 5V and 3.3V versions available

LP2953 Versions Only

V Auxiliary comparator included with CMOS/TTL compatible output levels. Can be used for fault detection, low input line detection, etc.

Applications

V High-efficiency linear regulator
* Regulator with under-voltage shutdown n
Low dropout battery-powered regulator
n Snap-ON/Snap-OFF regulator

Block Diagrams

LP2952

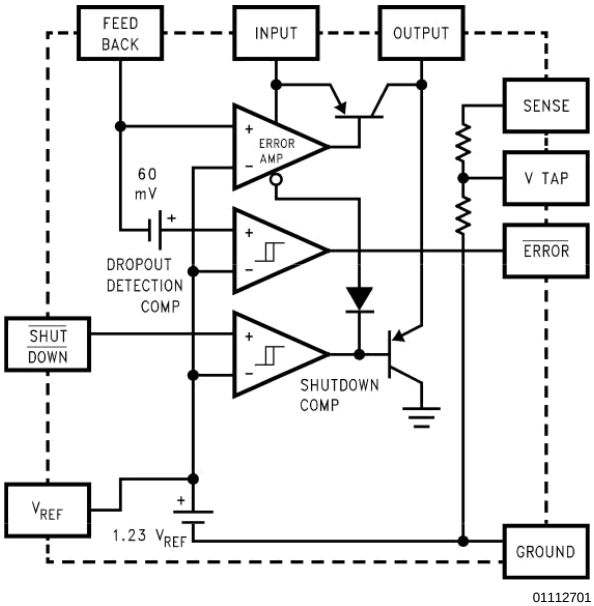

01112701

LP2953

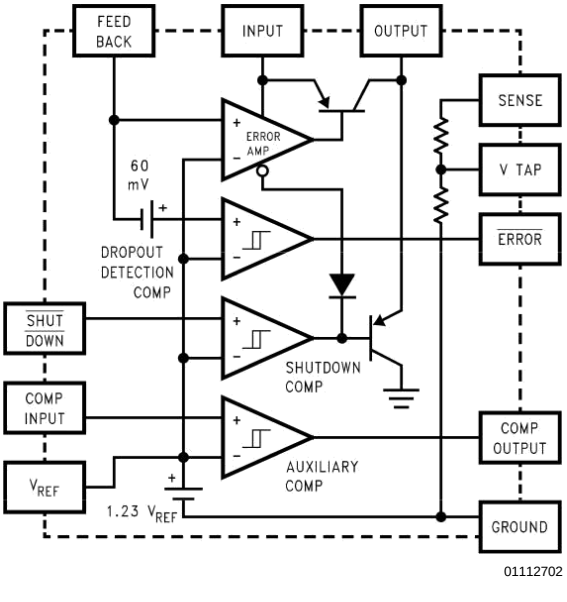

01112702

Pinout Drawings

LP2952
14-Pin DIP

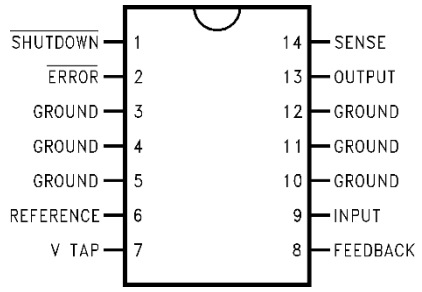

01112711

LP2953
16-Pin DIP

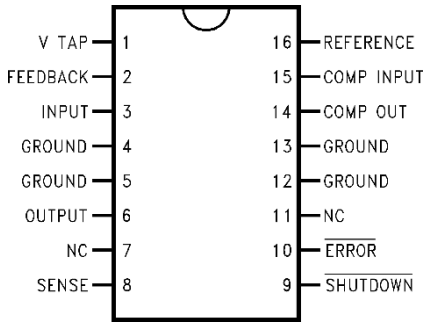

01112713

LP2952
16-Pin SO

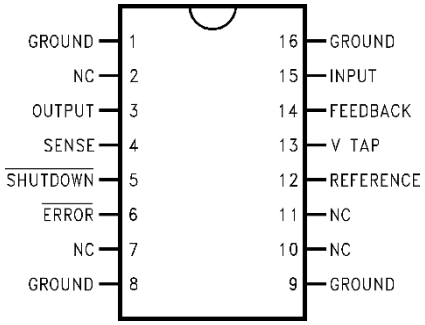

01112712

LP2953
16-Pin SO

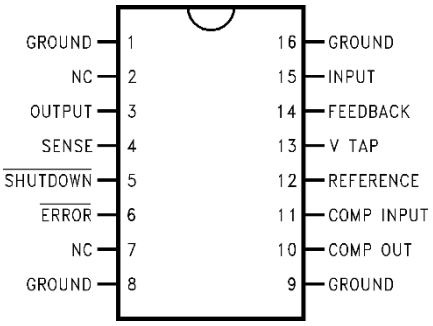

01112714

Ordering Information

LP2952

Order Number	Temp. Range (T_J) ûC	Package	NSC Drawing Number
LP2952IN, LP2952AIN, LP2952IN-3.3, LP2952AIN-3.3	−40 to +125	14-Pin Molded DIP	N14A
LP2952IM, LP2952AIM, LP2952IM-3.3, LP2952AIM-3.3	−40 to +125	16-Pin Surface Mount	M16A

LP2953

Order Number	Temp. Range (T_J) ûC	Package	NSC Drawing Number
LP2953IN, LP2953AIN, LP2953IN-3.3, LP2953AIN-3.3	−40 to +125	16-Pin Molded DIP	N16A
LP2953IM, LP2953AIM, LP2953IM-3.3, LP2953AIM-3.3	−40 to +125	16-Pin Surface Mount	M16A
LP2953AMJ/883 5962-9233601MEA LP2953AMJ-QMLV 5962-9233601VEA	−55 to +150	16-Pin Ceramic DIP	J16A
LP2953AMWG/883 5962-9233601QXA LP2953AMWG-QMLV 5962-9233601VXA	−55 to +150	16-Pin Ceramic Surface Mount	WG16A

Absolute Maximum Ratings (Note 1)

If Military/Aerospace specified devices are required, please contact the National Semiconductor Sales Office/ Distributors for availability and specifications.

Storage Temperature Range	−65˚C ≤ T_A ≤ +150˚C
Operating Temperature Range	
LP2952I, LP2953I, LP2952AI, LP2953AI, LP2952I-3.3, LP2953I-3.3, LP2952AI-3.3, LP2953AI-3.3	−40˚C ≤ T_J ≤ +125˚C
LP2953AM	−55˚C ≤ T_A ≤ +125˚C
Lead Temp. (Soldering, 5 seconds)	260˚C
Power Dissipation (Note 2)	Internally Limited
Maximum Junction Temperature	
LP2952I, LP2953I, LP2952AI, LP2953AI, LP2952I-3.3, LP2953I-3.3, LP2952AI-3.3, LP2953AI-3.3	+125˚C
LP2953AM	+150˚C
Input Supply Voltage	−20V to +30V
Feedback Input Voltage (Note 3)	−0.3V to +5V
Comparator Input Voltage (Note 4)	−0.3V to +30V
Shutdown Input Voltage (Note 4)	−0.3V to +30V
Comparator Output Voltage (Note 4)	−0.3V to +30V
ESD Rating (Note 15)	2 kV

3A

Electrical Characteristics

Limits in standard typeface are for T_J = 25˚C, **bold typeface** applies over the full operating temperature range. Limits are guaranteed by production testing or correlation techniques using standard Statistical Quality Control (SQC) methods. Unless otherwise specified: $V_{IN} = V_O(NOM) + 1V$, I_L = 1 mA, C_L = 2.2 µF for 5V parts and 4.7µF for 3.3V parts. Feedback pin is tied to V Tap pin, Output pin is tied to Output Sense pin.

3.3V Versions

Symbol	Parameter	Conditions	Typical	LP2952AI-3.3, LP2953AI-3.3		LP2952I-3.3, LP2953I-3.3		Units
				Min	Max	Min	Max	
V_O	Output Voltage		3.3	3.284 **3.260**	3.317 **3.340**	3.267 **3.234**	3.333 **3.366**	V
		1 mA ≤ I_L ≤ 250 mA	3.3	**3.254**	**3.346**	**3.221**	**3.379**	

5V Versions

Symbol	Parameter	Conditions	Typical	LP2952AI, LP2953AI, LP2953AM (Note 17)		LP2952I, LP2953I		Units
				Min	Max	Min	Max	
V_O	Output Voltage		5.0	4.975 **4.940**	5.025 **5.060**	4.950 **4.900**	5.050 **5.100**	V
		1 mA ≤ I_L ≤ 250 mA	5.0	**4.930**	**5.070**	**4.880**	**5.120**	

All Voltage Options

Electrical Characteristics

Limits in standard typeface are for T_J = 25˚C, **bold typeface** applies over the full operating temperature range. Limits are guaranteed by production testing or correlation techniques using standard Statistical Quality Control (SQC) methods. Unless otherwise specified: $V_{IN} = V_O(NOM) + 1V$, I_L = 1 mA, C_L = 2.2 µF for 5V parts and 4.7µF for 3.3V parts. Feedback pin is tied to V Tap pin, Output pin is tied to Output Sense pin.

Symbol	Parameter	Conditions	Typical	LP2952AI, LP2953AI, LP2952AI-3.3, LP2953AI-3.3, LP2953AM (Notes 16, 17)		LP2952I, LP2953I, LP2952I-3.3, LP2953I-3.3		Units
				Min	Max	Min	Max	
REGULATOR								
$\frac{\Delta V_O}{\Delta T}$	Output Voltage Temp. Coefficient	(Note 5)	**20**		**100**		**150**	ppm/˚C
$\frac{\Delta V_O}{V_O}$	Output Voltage Line Regulation	$V_{IN} = V_O(NOM) + 1V$ to 30V	0.03		0.1 **0.2**		0.2 **0.4**	%

All Voltage Options (Continued)

Electrical Characteristics (Continued)

Limits in standard typeface are for T_J = 25˚C, **bold typeface** applies over the full operating temperature range. Limits are guaranteed by production testing or correlation techniques using standard Statistical Quality Control (SQC) methods. Unless otherwise specified: $V_{IN} = V_O(NOM) + 1V$, I_L = 1 mA, C_L = 2.2 µF for 5V parts and 4.7µF for 3.3V parts. Feedback pin is tied to V Tap pin, Output pin is tied to Output Sense pin.

Symbol	Parameter	Conditions	Typical	LP2952AI, LP2953AI, LP2952AI-3.3, LP2953AI-3.3, LP2953AM (Notes 16, 17)		LP2952I, LP2953I, LP2952I-3.3, LP2953I-3.3		Units
				Min	Max	Min	Max	
	Output Voltage Load Regulation (Note 6)	I_L = 1 mA to 250 mA	0.04		0.16		0.20	%
		I_L = 0.1 mA to 1 mA			**0.20**		**0.30**	
$V_{IN}–V_O$	Dropout Voltage (Note 7)	I_L = 1 mA	60		100		100	mV
					150		**150**	
		I_L = 50 mA	240		300		300	
					420		**420**	
		I_L = 100 mA	310		400		400	
					520		**520**	
		I_L = 250 mA	470		600		600	
					800		**800**	
I_{GND}	Ground Pin Current (Note 8)	I_L = 1 mA	130		170		170	µA
					200		**200**	
		I_L = 50 mA	1.1		2		2	mA
					2.5		**2.5**	
		I_L = 100 mA	4.5		6		6	
					8		**8**	
		I_L = 250 mA	21		28		28	
					33		**33**	
I_{GND}	Ground Pin Current at Dropout	$V_{IN} = V_O(NOM) - 0.5V$ I_L = 100 µA	165		210		210	µA
					240		**240**	
I_{GND}	Ground Pin Current at Shutdown (Note 8)	$V_{SHUTDOWN} \geq 1.1V$	105		140		140	µA
I_{LIMIT}	Current Limit	V_{OUT} = 0	380		500		500	mA
					530		**530**	
	Thermal Regulation	(Note 10)	0.05		0.2		0.2	%/W
e_n	Output Noise Voltage (10 Hz to 100 kHz)	C_L = 4.7 µF	400					µV RMS
		C_L = 33 µF	260					
	I_L = 100 mA	C_L = 33 µF (Note 11)	80					
V_{REF}	Reference Voltage	(Note 12)	1.230	1.215	1.245	1.205	1.255	V
				1.205	**1.255**	**1.190**	**1.270**	
	Reference Voltage Line Regulation	V_{IN} = 2.5V to $V_O(NOM)$ + 1V	0.03		0.1		0.2	%
		$V_{IN} = V_O(NOM) + 1V$ to 30V (Note 13)			**0.2**		**0.4**	
	Reference Voltage Load Regulation	I_{REF} = 0 to 200 µA	0.25		0.4		0.8	%
					0.6		**1.0**	
	Reference Voltage	(Note 5)	**20**					ppm/˚C

Temp. Coefficient								

All Voltage Options (Continued)

Electrical Characteristics (Continued)

Limits in standard typeface are for T_J = 25˚C, **bold typeface** applies over the full operating temperature range. Limits are guar-anteed by production testing or correlation techniques using standard Statistical Quality Control (SQC) methods. Unless other-wise specified: $V_{IN} = V_O(NOM) + 1V$, I_L = 1 mA, C_L = 2.2 µF for 5V parts and 4.7µF for 3.3V parts. Feedback pin is tied to V Tap pin, Output pin is tied to Output Sense pin.

Symbol	Parameter	Conditions	Typical	LP2952AI, LP2953AI, LP2952AI-3.3, LP2953AI-3.3, LP2953AM (Notes 16, 17)		LP2952I, LP2953I, LP2952I-3.3, LP2953I-3.3		Units
				Min	Max	Min	Max	
I_B(FB)	Feedback Pin Bias Current		20		40 **60**		40 **60**	nA
I_O(SINK)	Output "OFF" Pulldown Current	(Note 9)		30 **20**		30 **20**		mA
DROPOUT DETECTION COMPARATOR								
I_{OH}	Output "HIGH" Leakage	V_{OH} = 30V	0.01		1 **2**		1 **2**	µA
V_{OL}	Output "LOW" Voltage	$V_{IN} = V_O(NOM) - 0.5V$ I_O(COMP) = 400 µA	150		250 **400**		250 **400**	mV
V_{THR} (MAX)	Upper Threshold Voltage	(Note 14)	−60	−80 **−95**	−35 **−25**	−80 **−95**	−35 **−25**	mV
V_{THR} (MIN)	Lower Threshold Voltage	(Note 14)	−85	−110 **−160**	−55 **−40**	−110 **−160**	−55 **−40**	mV
HYST	Hysteresis	(Note 14)	15					mV
$\overline{\text{SHUTDOWN}}$ **INPUT** (Note 15)								
V_{OS}	Input Offset Voltage	(Referred to V_{REF})	±3	−7.5 **−10**	7.5 **10**	−7.5 **−10**	7.5 **10**	mV
HYST	Hysteresis		6					mV
I_B	Input Bias Current	V_{IN}(S/D) = 0V to 5V	10	−30 **−50**	30 **50**	−30 **−50**	−30 **50**	nA

			LP2953AM	10	−30 **−75**	30 **75**			
AUXILIARY COMPARATOR (LP2953 Only)									
V_{OS}	Input Offset Voltage	(Referred to V_{REF})		±3	−7.5 **−10**	7.5 **10**	−7.5 **−10**	7.5 **10**	mV
			LP2953AM	±3	−7.5 **−12**	7.5 **12**			
HYST	Hysteresis			6					mV
I_B	Input Bias Current	V_{IN}(COMP) = 0V to 5V		10	−30 **−50**	30 **50**	−30 **−50**	30 **50**	nA
			LP2953AM	10	−30 **−75**	30 **75**			
I_{OH}	Output “HIGH” Leakage	V_{OH} = 30V V_{IN}(COMP) = 1.3V		0.01		1 **2**		1 **2**	µA
			LP2953AM	0.01		1 **2.2**			
V_{OL}	Output “LOW” Voltage	V_{IN}(COMP) = 1.1V I_O(COMP) = 400 µA		150		250 **400**		250 **400**	mV
			LP2953AM	150		250 **420**			

Application Hints (Continued)

SHUTDOWN INPUT

A logic-level signal will shut off the regulator output when a "LOW" (<1.2V) is applied to the Shutdown input.

To prevent possible mis-operation, the Shutdown input must be actively terminated. If the input is driven from open-collector logic, a pull-up resistor (20 kΩ to 100 kΩ recom-mended) should be connected from the Shutdown input to the regulator input.

If the Shutdown input is driven from a source that actively pulls high and low (like an op-amp), the pull-up resistor is not required, but may be used.

If the shutdown function is not to be used, the cost of the pull-up resistor can be saved by simply tying the Shutdown input directly to the regulator input.

IMPORTANT: Since the Absolute Maximum Ratings state that the Shutdown input can not go more than 0.3V below ground, the reverse-battery protection feature which protects the regulator input is sacrificed if the Shutdown input is tied directly to the regulator input.

If reverse-battery protection is required in an application, *the pull-up resistor between the Shutdown input and the regula-tor input must be used.*

Typical Applications

Basic 5V Regulator

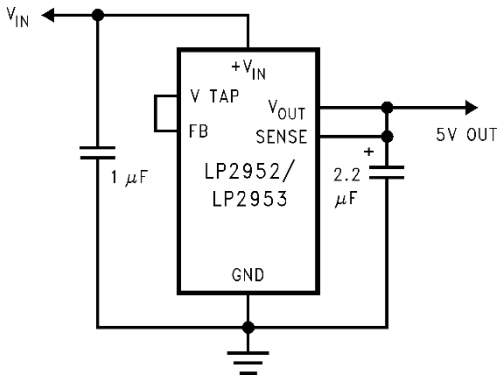

01112715

5V Current Limiter with Load Fault Indicator

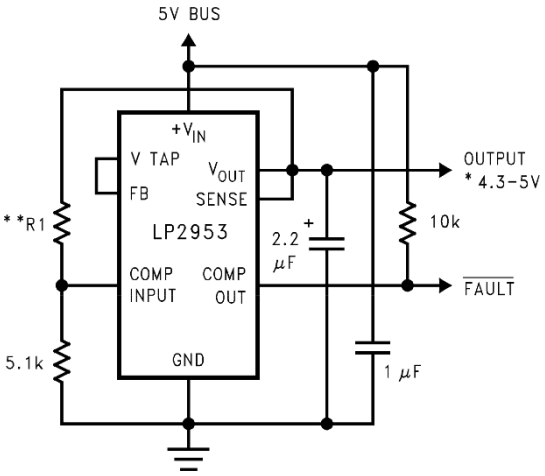

01112716

** Output voltage equals $+V_{IN}$ minum dropout voltage, which varies with output current. Current limits at a maximum of 380 mA (typical).

** Select R1 so that the comparator input voltage is 1.23V at the output voltage which corresponds to the desired fault current value.

Low T.C. Current Sink

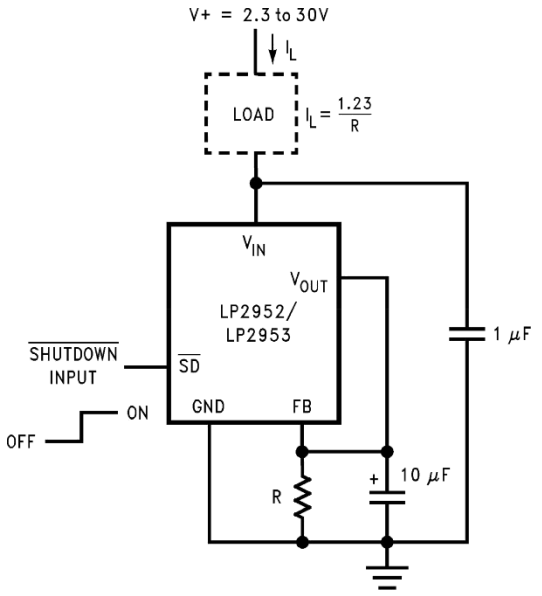


UNIVERSITÀ
DEGLI STUDI
DI SALERNO